THE ROLE OF CERAMIDES IN CIGARETTE

SMOKE-INDUCED ALVEOLAR CELL DEATH

Krzysztof Kamocki

Submitted to the faculty of the University Graduate School
in partial fulfillment of the requirements
for the degree
Doctor of Philosophy
in the Department of Biochemistry and Molecular Biology
Indiana University

November 2012

Accepted by the Faculty of Indiana University, in partial
fulfillment of the requirements for the degree of Doctor of Philosophy.

_____

Irina Petrache, M.D., Chair

_____

Susan Gunst, Ph.D.

Doctoral Committee

_____

Laurence Quilliam, Ph.D.

August, 22nd, 2012

_____

Simon Atkinson, Ph.D.

Dedication

I dedicate my thesis to my wife, Malgorzata Maria Kamocka.

Acknowledgements

I would like to thank Dr. Irina Petrache for being my mentor during my graduate program. Dr. Petrache is not only an exceptional scientist, but also an excellent teacher. Thank you for your advice and guidelines during my scientific journey. Thank you for support and for teaching me how to think critically, for teaching me all of the aspects, which are important for a successful scientist. Thank you for your investment in me, both in funding and time you spent. In your laboratory I had an opportunity not only to learn how to design, perform experiments, and analyzed data, but also I was feeling unrestrained due to freedom for scientific exploration you offered.

I would also like to thank the other members of my research committee: Dr. Susan Gunst, Dr. Lawrence Quilliam, and Dr. Simon Atkinson. Thank you all for your time, advice, constructive criticism and support. Your guidance during my graduate study was extremely helpful.

In addition, I would like to thank all members in Dr. Petrache's lab, both present and former. Scientific work demands a lot of cooperation between many lab members and I had an opportunity to be a part of the great lab team.

Abstract

Krzysztof Kamocki

THE ROLE OF CERAMIDES IN CIGARETTE SMOKE-INDUCED ALVEOLAR
CELL DEATH

The complex pathogenesis of emphysema involves disappearance of

alveolar structures, in part attributed to alveolar cell apoptosis. The mechanism

by which cigarette smoke (CS) induces alveolar cell apoptosis is not known. We

hypothesized that ceramides are induced by CS *via* specific enzymatic pathways

that can be manipulated to reduce lung cell apoptosis. CS increased ceramides

in the whole lung and in cultured primary structural lung cells. Exposure to CS

activated within minutes the acid sphingomyelinase, and within weeks the *de*

novo- ceramide synthesis pathways. Pharmacological inhibition of acid

sphingomyelinase significantly attenuated CS-induced apoptosis. To understand

the mechanisms by which ceramides induce apoptosis, we investigated the cell

types affected and the involvement of RTP801, a CS-induced pro-apoptotic and

pro-inflammatory protein. Direct lung augmentation of ceramide caused

apoptosis of both endothelial and epithelial type II cells. Ceramide upregulated

RTP801 and the transgenic loss of RTP801 inhibited only epithelial, but not

endothelial cell apoptosis induced by ceramide. In conclusion, CS induces acid

sphingomyelinase-mediated ceramide upregulation and apoptosis in a cell-

specific manner, which in epithelial cells involves induction of stress response

proteins that may further amplify lung injury. Molecular targeting of amplification

pathways may provide therapeutic opportunities to halt emphysema progression.

Irina Petrache, M.D., Chair

Table of Contents

List of Schematics

List of Figures

List of Abbreviations

ATF-2   Activating transcription factor 1

Apaf-1   Apoptotic protease activating factor

BAK   BCL2 antagonist killer 1

BAL   Bronchoalveolar lavage

BAX   Bcl-2 associated X protein

Blc-2   B-cell lymphoma protein 2

CAD   Caspase-activated DNAse

CaN   Calcineurin

CAPK/KSR   Ceramide activated protein kinase/kinase suppressor of Ras

Caspase-3   Cysteinyl aspartic acid-protease-3

Caspase-7   Cysteinyl aspartic acid-protease-7

Caspase-8   Cysteinyl aspartic acid-protease-8

Caspase-9   Cysteinyl aspartic acid-protease-9

CDase   Ceramidase

Cdc-42   Cell division control protein 42 homolog

CD3	Cluster of differentiation 3 molecule
CD4	Cluster of differentiation 4 molecule
CD8	cluster of differentiation 8 molecule
Cer	Ceramide
CerS	Ceramide synthase
COPD	Chronic obstructive pulmonary disease
CS	Cigarette smoke
CSE	Cigarette smoke extract
CXCL10	Chemokine (C-X-C motif) ligand 10
CXCR3	Chemokine (C-X-C motif) receptor 3
C1P	Ceramide-1-phosphate
DAG	Diacylglycerol
DEGS	Dihydroceramide desaturase
DES	Desaturase
DHC	Dihydroceramide
DISC	Death inducing signaling complex

DTT	Dithiothreitol
EGFR	Epidermal growth factor receptor
FADD	Fas-associated death domain
FAN	Factor associated with nSM activation
FasL	Fatty acid synthetase ligand
FasR	Fatty acid synthetase receptor
FBS	Fetal bovine serum
FB1	Fumonisin B1
FITC	Fluorescein isothiocyanate
GCase	Glucosyl ceramidase
GCS	Glucosyl ceramide synthase
GSH	Glutathion
HDL	High density lipoprotein
HLMVEC	Human lung micro-vascular endothelial cell
HtrA2/Omi	High-temperature requirement serine protease Omi protein A2

IAP	Inhibitors of apoptosis proteins
ICAM-1	Intercellular Adhesion Molecule 1
IHC	Immunohistochemistry
IL-1β	Interleukin-1 beta
IL-8	Interleukin-8
JNK	c-Jun N-terminal kinase
KDS	3-ketodihydrosphingosine
KO	Knockout
L-ASMase	Lysosomal acid sphingomyelinase
LASS	Longevity assurance genes
LCB1	Long chain base 1
LCB2	Long chain base 2
LCB3	Long chain base 3
LC-MS/MS	Liquid chromatography/tandem mass spectroscopy
LMPA	Low melting point agarose
LPS	Lipopolysaccharide

LTB4	Leukotriene B4
MAPK	Mitogen activated protein kinase
MAPP	(1S, 2R)-D-*erythro*-2-(N-Myristoylamino)-1-phenyl-1 propanol
MHC II	Major Histocompatability Complex II
MOMP	Mitochondrial Outer Membrane Permeabilization
MPT	Mitochondrial permeability transition
mRNA	Messenger ribonucleic acid
mTOR	Mammalian target of Rapamycin
MYR	Myriocin
NF-κB	Nuclear factor kappa B
NM	Nuclear membrane
NO	Nitric Oxide
Nrf2	Nuclear factor (erythroid-derived 2)-like 2
nSMase	Neutral sphingomyelinase

ORM	Orosomucoid
Ox-stress	Oxidative stress
PARP	Poly(ADP-ribose) polymerase
PAF	Platelet activating factor
PC	Phosphatidyl choline
PE	Phycoerythrin
PEG	Poly-ethylene glycol
PFTs	Pulmonary function tests
PKC	Protein kinase C
PLP	Pyridoxal 5V-phosphate
PM	Plasma membrane
POAS	(PLP)-dependent α-oxoamine synthases
PP2B	Protein phosphatase 2B
Rac1	Ras-related C3 botulinum toxin substrate 1
RIP	Receptor-interacting protein
ROS	Reactive oxygen species

RT-PCR	Quantitative reverse transcription polymerase chain reaction
sASMase	Secreted/soluble acid sphingomyelinase
siRNA	Short interfering ribonucleic acid
SK	Sphingosine kinase
Smac/DIABLO	Second mitochondrial activator of caspases/direct IAP
SM	Sphingomyelin
SMS1	Sphingomyelinase synthase 1
SMS2	Sphingomyelinase synthase 2
SOD	superoxide dismutase
SPPase	Sphingosine phosphate phosphatase
SPT	Serine-palmitoyl transferase
SPTLC	Serine-palmitoyl transferase long chain
S1P	Sphingosine-1-phoshate
TLC	Tram, Lag, CLN8
TNF-α	Tumor necrosis factor alfa

TNFR1	Tumor necrosis factor receptor 1
TORC 2	Target of rapamycine complex 2
TRADD	TNF receptor-associated death domain
TRAF 2	TNFR-associated factor 2
VEGF	Vascular endothelial growth factor
VEGFR	Vascular endothelial growth factor receptor
WT	Wild type
Ypk1	Yeast protein kinase 1

A. INTRODUCTION

1. COPD

The term chronic obstructive pulmonary disease (COPD) covers two diseases: chronic bronchitis and emphysema. Chronic bronchitis is characterized as a chronic cough for at least three months per year in two consecutive years, with increased production of mucus and sputum. Emphysema is defined as an abnormal, permanent enlargement of airspaces distal to the terminal bronchiole, through the destruction of their walls [1]. There are many risk factors responsible for the development of COPD, including tobacco smoke [2], indoor [3] and outdoor air pollutions [4], and genetic factors, like cystic fibrosis (CF) and α-1-antitrypsin deficiency [5] and diet [6]. The processes invoked in the pathogenesis of COPD include oxidative stress, inflammation, and matrix proteolysis [7], [8]. In addition extensive apoptosis of lung parenchyma leading to alveolar cell destruction is involved in the pathogenesis of emphysema [9]. Emphysema is a disease with a high mortality and no cure [10] and COPD is the 3rd leading cause of death in the US [11]. COPD is becoming an economic burden not only for the costs of diagnosis and management, but also for causing disability and early death. Only in 2005 the cost of COPD treatment was $38.8 billion [1].

1.1. Inflammation in COPD

CS is the major factor which causes an inflammatory reaction and many kinds of inflammatory cells, including neutrophils, macrophages, and T lymphocytes have been documented to be involved in the pathogenesis of COPD [12]. Recent data indicate an important role of T lymphocytes and their excessive biological activity correlates with COPD progression [13]. Specifically, the number of CD3+ and CD8+ T cells was found to be amplified in bronchi [14], parenchymal tissue, pulmonary arteries and small airways [15], and the quantity of T cells was inversely proportional to predicted $FEV_1\%$. In addition, both the number of CXCR3+ cells, CXCR3-ligand, and CXCL10 were elevated in the lungs of COPD patients. Neutrophils are also involved in pathogenesis of COPD *via* several mechanisms. CS causes rapid PMN recruitment to the lung [16]. Granulocyte adhesion and diapedesis are increased due to the over-expression of various adhesion molecules, such as ICAM-1 and E-selectin, on inflammatory cells and in pulmonary lung vasculature, respectively [17], [18]. Moreover, both neutrophils and macrophages discharge a multitude of cytokines and chemo-attractants, for example IL-8 and LTB4 [19, 20], thereby self-perpetuating inflammatory processes. Macrophages, which specialize in the clearance of detrimental particles from the lower respiratory system, are increased in number in COPD patients and they participate in delineation of specific inflammatory phenotypes during its course [21, 22]. Macrophages, as MHC II cell are also responsible for the engulfment and presentation of antigens to CD4+ T cells and modulating immune responses in the lungs [23].

1.1.2. Ceramides and inflammation

Inflammatory cytokines such as tumor necrosis factor-α (TNF-α) may play an important role in the generation of ceramides in vascular endothelial cells. TNF-α normally causes endothelial cell activation through transcription factors NF-κB and -Jun/ATF-2. Studies performed on human umbilical vein endothelial cells showed the significance of the adaptor protein TRAF-2 for activation of both NF-κB and JNK [24]. In addition, JNK activation occurs *via* small G proteins Rac-1 and/or cdc-42. Interestingly, TNF-α induces apoptosis when combined with protein synthesis inhibitor, cycloheximide (CHX) or ceramide. The apoptotic pathways seems to be dissimilar, because pathway induced with TNF-α + CHX is inhibited by the caspase inhibitors crmA or the peptide zVAD.fmk, whereas that induced by TNF-α + cer is blocked by the anti-apoptotic proteins Bcl-2, Bcl-XL or AI [24]. These data indicate a dual role of TNF-α, whereby it can act as a pro-apoptotic agent when associated with cytotoxicity or irradiation. The mechanism involved in this process includes TNF-α mediated induction of nSMase, augmentation of ceramides and apoptosis. The adaptor protein FAN plays a key role in the activation of nSMase, as TNF-α is not able to generate appropriate level of ceramides, when FAN is underexpressed [24].

Action of inflammatory cytokine IL-1β is also linked with ceramide synthesis in many tissues. In anterior hypothalamic (AH) neurons IL-1β inhibits neuronal signaling by rapidly increasing the phosphorylation of the tyrosine kinase Src and kinase suppressor of Ras (ceramide activated protein kinase)

3

(CAPK/KSR), leading to activation of the neutral sphingomyelinase and accumulation of ceramide [25].

The involvement of ceramide as a second messenger in inflammatory lung diseases has been shown for acute lung injury and emphysema. Ceramides play a pathologic role in acute lung injury induced by platelet-activating factor (PAF). PAF-dependent pulmonary edema develops either trough the activation of the cyclooxygenase pathway or activation of acid sphingomyelinase with the latter leading to accumulation of ceramides [26].

Acid sphingomyelinase also has a role in the formation of ceramides following injection of lipopolysaccharide (LPS) or TNF-α, into C57BL/6 mice, which was associated with apoptosis in endothelium of intestine, lung, fat and thymus. Interestingly, the apoptosis was inhibited in the endothelium by administration of TNF-binding protein, a protective factor against LPS-induced cell death. That ASMase knockout mice were protected against endothelial cell apoptosis suggested the importance of ceramides in programmed cell death [27].

Vascular endothelial growth factor (VEGF) family and its receptors are major mediators responsible for angiogenesis and vasculogenesis [28], [29]. Chronic blockade of VEGFR in rats with the inhibitor SU5416 causes alveolar cell apoptosis and emphysema [30], a finding recapitulated in VEGFloxP mice, after ablation of the VEGF gene following intra-tracheal administration of an adeno-associated cre recombinase virus (AAV/Cre) [31]. Ceramide, a second messenger lipid, was a critical mediator of alveolar destruction in emphysema caused by blockade of the vascular endothelial growth factor receptors in both

rats and mice [32]. Inhibition of enzymes controlling *de novo* ceramide synthesis prevented alveolar cell apoptosis, oxidative stress and emphysema. In a model of emphysema reproduced with intratracheal instillation of ceramide in naive mice, a feed-forward mechanism was observed, in that synthesis of ceramides was mediated by activation of secretory acid sphingomyelinase [32].

Furthermore, reduction of lung levels of very long ceramides after administration of a neutralizing ceramide antibody *in vivo* and the inability of acid sphingomyelinase–deficient fibroblasts to augment endogenous ceramide synthesis in response to exogenous ceramide also indicated a feed-forward mechanism of ceramide regulation mediated *via* the secretory acid sphingomyelinase [33].

1.2. Protease-antiprotease disequilibrium in emphysema

The concept of protease-antiprotease imbalance was the first mechanism involved in emphysema development. It has been shown, that emphysema develops when there is an overabundance of proteases with/or a decrease in antiproteases activity, which leads to destruction of the lung matrix. Neutrophils participate in the destruction of lung tissue in COPD *via* secretion of numerous proteases, such as elastase, proteinase-3, catepsins G and B [34-37] leading to lung tissue digestion. Macrophages can also participate in lung destruction. They synthesize and discharge many proteinases, including matrix metalloproteases (MMPs), cathepsin K, L and S [38], [23]. Interestingly, they are able to engulf and

5

store elastase from neutrophils for later release [39]. The antiproteases degrade or neutralize proteases, maintaining appropriate homeostatic balance, as illustrated by the action of α-1-antitrypsin, an inhibitor of neutrophil elastase [40] [41]. Low circulating levels of α-1-antitrypsin are associated with a panacinar type of emphysema development at an earlier age compared to usual emphysema [42].

1.3. Oxidative stress in emphysema

Oxidative stress can be characterized as disproportion between reactive oxygen species (ROS) production and capability of cells or tissues for neutralization of ROS *via* antioxidants [43]. In humans, oxidative stress has been implicated in the pathogenesis of many diseases, including cancer [44], Parkinson's and Alzheimer's diseases [43], atherosclerosis, myocardial infarction [45], and emphysema [7]. For the development of COPD and particularly emphysema, CS is considered the most important environmental factor. CS contains approximately 4,700 chemical compounds and one CS puff comprises 10^{15} ROS of whose alkyl and peroxyl types are the most common [46]. CS also comprises many chemical particles with high redox potential, responsible for indirect generation of superoxide anion, peoxynitrite, alkyl peroxynitrites and hydrogen peroxides [47]. Moreover, CS accumulates over time in the lungs of smokers in the form of tar, that constitutes a permanent source of ROS production, especially when antioxidant mechanisms, such as GSH, Nrf2, SOD

are depleted [48], [49]. In patients with COPD, the increased influx of inflammatory cells, such as neutrophils and macrophages is also a prolific ROS source. ROS, that include H_2O_2, superoxide peroxynitrite, are responsible for many pathological issues during the course of COPD, such as suppression of antiproteolytic enzymes, peroxidation of membrane lipids, extracellular matrix remodeling and direct injury of alveolar cells, including apoptosis [46]. The oxidative stress participates in the generation of ceramide and is responsible for ceramide-induced apoptosis in human lung epithelial cells [50]. It has been proposed that apoptosis can be a consequence of an imbalance between reactive oxygen species (ROS), and antioxidants production [51].

2. Sphingolipids

2.1. The role of sphingolipids in cell biology

Sphingolipids are a group of lipids which have as a backbone a sphingoid base, an amino alcohol to which various groups are attached. They were first discovered in extracts from brain in the 1870s. The reason they were named after the mythological Sphinx was because of their enigmatic structure. Sphingolipids, including ceramides are important components of cellular membranes and their composition impact plasma and other membrane functions and dynamics.

Ceramides are involved in signaling of a variety of cellular processes, such as apoptosis, growth arrest, and senescence [52-54] and they have been reported to be a second messenger of apoptosis of both lung endothelial and

epithelial cells *in vitro.* Overproduction and accumulation of ceramides are involved in the alterations of the lung parenchyma induced by CS, which culminate in the development of emphysema [55], [9]. Ceramide can be synthesized *via* several pathways, of which the most relevant are the *de novo* and sphingomyelinase pathways. Enzymes involved in the *de novo* ceramide synthesis can be activated by many environmental factors, including heat stress, oxidative stress and many others which collectively lead to overproduction of different ceramide species. An increase in ceramide production or paracrine action of instilled ceramides in experimental emphysema models leads to activation of death receptors and finally to caspase-3 activation. Petrache *et al.* previously identified ceramide as an upstream mediator of lung cell apoptosis in a murine model of emphysema which is induced by blockade of the vascular endothelial growth factor [32]. They then documented increased ceramide levels in response to smoking. However, the mechanism by which various environmental factors, including CS increases ceramide species in the lung is still not fully understood. Because in a simplified experimental model of emphysema development extensive lung apoptosis was dependent on increased in ceramides [32], I propose that ceramide may be an important mediator of cigarette smoke-induced lung cell death and hence emphysema. Since ceramides are actively regulated by both synthetic enzymes and various degradation pathways, they may be targeted for therapeutic purposes to reduce CS-induced lung cell apoptosis.

2.2. Overview of sphingolipids biochemistry

2.2.1. *De novo* pathway of ceramide synthesis

2.2.1.1. Serine palmitoyl transferase

Serine palmitoyl transferase (SPT) [EC 2.3.1.50] is responsible for the first committed step in the *de novo* ceramide synthesis pathway (Schematic 1) in all organisms studied to date [56]. Although its role is to combine serine and palmitoyl-CoA into 3-ketodihydrosphingosine (KDS), STP is able to synthetize alternative sphingoid bases [57] from compatible acyl-CoA [58] and amino acids [59]. SPT is a member of pyridoxal 5V-phosphate (PLP)-dependent α-oxoamine synthases (POAS) family. In mammals, SPT is represented as a heterodimer of 53-kDa LCB1 and 63-kDa LCB2 subunits or SPT1 (SPTLC1) and SPT2 (SPTLC2), respectively, and those subunits are localized in the endoplasmic reticulum (ER) with type I topology. LCB2, when dissociated from LCB1, may become unstable. Activity of SPT, a housekeeping enzyme, is regulated both transcriptionally and post-transcriptionally, and its activation may play a role in apoptosis induced by certain types of stresses [56]. Since both subunits appear crucial for embryonic development, either SPTLC1 and SPTLC2 knockout mice are non-viable [60].

SPT is expressed in normal epithelial and endothelial lung cells, but its subunits vary in specific cell compartments. For example, in adrenomedullary chromaffin cells the LCB1 subunit was found in both nucleus and cytoplasm, whereas LCB2 was primarily found in cytoplasm [61]. The LCB1 subunit's transmembrane domain plays an essential role in upholding the LCB2

component and the SPT integrity in mammalian cells [62]. A recently identified novel SPT subunit, SPTLC3, shows about 68% identity to SPTLC2 and also includes a pyridoxal phosphate consensus motif. SPTLC3 subunit has a high affinity for myristoyl (C14: 0)-CoA and less affinity for palmitoyl (C16: 0)-CoA [63], thus generating C16-sphingoid bases.

Regulation of SPT activity

Members of ORMDL family ER transmembrane proteins are responsible for regulation of SPT activity. These proteins were first discovered during analysis of genes responsible for retinitis pigmentosa [64]. First described in yeast as Orm1 and Orm2, in mammals they are represented by ORMDL1, ORMDL2 [65] and ORMDL3, a gene recently associated with asthma susceptibility in humans [66]. ORMDL proteins interact and inhibit SPT activity. The inhibitory activity of Orm depends on the phosphorylation level of the protein (the higher the phosphorylation – the higher the SPT inhibition), and myriocin (Myr), a potent inhibitor of SPT works by phosphorylation of ORMDL proteins [67].

In yeast, a protein kinase Ypk1 seems to be an essential upstream regulatory factor for Orm protein family. It acts by phosphorylation specific three residues which are also phosphorylated by Myr. The activity level of Ypk1 kinase is also phosphorylation dependent and recent data indicate rapamycin complex kinase 2 (TORC2) as an upstream activator of Ypk1 [68].

2.2.1.2. Ceramide synthases

Ceramide synthases are enzymes that use either dihydroshingosine or sphingosine and specific acyl-coA as substrates [69], [70], [71] (Schematic 1). Discovery of the gene products Lag1p and Lac1p in yeasts and the fact that they were responsible for the production of C26-ceramide [72], [73], resulted in the report of the six paralogs of Lag1 and Lac1 in mammals, including human and mouse, which were named *LASS* (longevity assurance) genes and later *CERS* (Ceramide synthases); in all species studied to date, at least two *LASS* genes have been found in every organism. The *CERS* genes encode for multi-transmembrane (TM) spanning proteins. Although neither the topology nor the exact number of TM domains have not been precisely yet evaluated [70], [74], [75], some conclusions about LASS mammalian proteins structure and function have been made based on studies with yeasts proteins Lag1 and Lac1. Those have eight TM domains, with the N and C termini of the proteins facing the cytoplasm [76], and one TLC domain (after Tram, Lag, CLN8) [77]. There is little information provided about the catalytic synthetic mechanism for LASS enzymes, although some data generated in yeast indicate the importance of two conserved histidine residues within the Lag1 motif [74], [78], [76]. Each mammalian CerS enzyme, with the exception of CerS1 has a Hox domain as well, which appears to be important for CerS5 and CerS6 activity [79]. CerS, like other enzymes of the *de novo* pathway are localized in ER [80], [81], [82], [83], [76]. All CerS enzymes have comparable Km to the sphinganine substrate [84], but they have different affinity for a particular second substrate, acyl-S-CoA. CerS1 is

predominantly responsible for the synthesis of C18 ceramides [82], CerS2 synthesizes C20-C24 ceramides, CerS4 and CerS5 synthetize C18/20 and C16 ceramides, respectively [83]. CerS6 produces C14 and C16 [81], and CerS3 generates C18 and C24 ceramides [85]. CerS have various tissue distribution and expression levels. CerS1 is found in skeletal muscles and testis and is highly expressed in brain tissue, specifically in neurons [86], which correlates with elevated level of C18 ceramides. CerS2 is found in many different human tissues, including brain, kidney, liver and lungs [87], [88], [86]. CerS3 is mostly expressed in testes [89], in the skin [85], especially in keratinocytes [90], where it is responsible for the maintenance of water permeability barrier [91]. CerS4 is found in skin, leukocytes, heart and liver [88]. Moreover, CerS4 may play a role in development of Alzheimer's disease, because it was found increased in the brain of mice with experimentally induced Alzheimer's disease [92]. CerS5 is found to be in high level in the lungs [93] and brain tissue [86]. CerS6 is localized mostly in rapidly developing tissues including embryonic [94] and cancer tissues [95], [96]. Others and our lab demonstrated that in the lungs, CerS2 and CerS5 exhibit the highest activity [88], [93], [77].

Regulation of ceramide synthases

Laviad *et al*. proposed recently that different CerS modulate their activities by dimer formation within ER. This process allows not only for modulation of activities of different CerS isoforms, but also permits increased synthesis of ceramides in the *de novo* pathway [97].

2.2.1.3. Dihydroceramide desaturases

A product of SPT, 3-dehydrosphinganine, undergoes spontaneous reduction by the NADPH-dependent 3-dehydrosphinganine reductase to D-erythrosphinganine [98], [99], [100]. For several years it was not clear whether 3-dehydrosphinganine was first desaturated to form sphingosine and then acylated to yield ceramide or first acylated and then desaturated [71], [56]. The discovery of fumonisin B1, an inhibitor of N-acylation of sphingoid base catalyzed by a group of CerS brought the evidence that dihydroceramide (DHC) was an intermediate in sphingolipid biosynthesis and not sphingosine [56]. D-erythro-sphinganine is first acylated and the subsequent introduction of the 4,5-double bond by the dihydroceramide desaturase leads to the formation of ceramide [98]. There are 2 isoforms of DHC desaturase. The DHC desaturase 1 (DEGS1) presents various affinity to its substrates which seems to rely on many factors such as: alkyl chain length of the sphingoid base (C18 > C12 > C8) and fatty acid (C8 > C18); the stereochemistry of the sphingoid base (D-erythro- > L-threo-dihydroceramides); the nature of the headgroup, with the highest activity for dihydroceramide, but some (about 20%) also for dihydroglucosylceramide [98]. Dihydroceramide desaturase (DEGS) enzymatic action appears similar with the mechanism of delta 9-desaturase (stearoyl-CoA desaturase) [99], [98]. Oxygen is necessary for dihydroceramide desaturase activity and cyanide, divalent copper, as well as antibodies against cytochrome b5, and dithiothreitol act as inhibitors [98]. Oxydative stress inhibits activity of DEGS, leading to the accumulation of DHC. Interestingly, DEGS protein level during exposure to CS is

13

not changed [101]. Data from our lab indicate that DEGS is an oxygen sensor in minor hypoxic conditions, regulating the flow of ceramide production in the *de novo* pathway [102]. The role of DEGS2 is more enigmatic. DEGS2 is able to provide a desaturation of DHC; in addition it serves as hydroxylase [103].

2.2.3. Sphingomyelinase pathway of ceramide synthesis

2.2.3.1. Sphingomyelinases

Shingomyelinases are enzymes (EC 3.1.4.12) responsible for the hydrolysis of sphingomyelin to phosphocholine and ceramide [104]. Sphingomyelinases are classified into 3 main groups based on their optimum pH (acid, neutral and alkaline) and they can be additionally subcategorized based on their cellular compartmentalization and specific cations requirement [105].

Alkaline sphingomyelinase was found almost exclusively in intestinal mucosa of mammals, and in the human liver [106].

Lysosomal acid sphingomyelinase (L-ASMase) was found primarily in lysosomes, but it can be displaced to the outer leaflet of plasma membrane [105], [107]. L-ASMase was first described in 1963 as being active at acidic pH [108] and a deficiency of L-ASMase causes Niemann-Pick disease [109], [110]. A gene encoding for L-ASMase was described as *Smpd1* [111]. A secreted ASMase isoform, first found in fetal bovine serum and localized to the outer leaflet of the plasma membrane, shares also the same gene [112]. Zn^{2+} cations are necessary for activity of both ASMase isoforms: lysosomal ASMase has Zn^{2+} firmly attached, whereas for secreted ASMase, Zn^{2+} needs to be supplemented for its

activity [113], [114]. The secreted form of ASMase may be responsible for paracrine effects leading to upregulation of ceramides at sites other than the source of ASMase.

Neutral sphingomyelinase (nSMase) has been localized to the ER and Golgi apparatus [105], [115] and it was found to be translocated to the inner leaflet of the plasma membrane [116], [115], [117]. There are three different types of nSMases, designated as nSM1, nSM2 and nSM3 with theirs ascribed genes: *Smpd2, Smpd 3* and *Smpd 4*, respectively [118], [119], [115]. The role of nSM1 in cell biology still remains uncertain [120] and nSM1KO mice show no changes in phenotype when compared to WT animals [121]. The nSM2 is universally expressed and is crucial for many processes, including skeletal growth [122]. NSM2 has been shown to be activated in human airway epithelial cells *in vitro* by H_2O_2 or CS exposure [123], [124]. NSMase was found to be responsible for the accumulation of ceramides and apoptosis in the lungs of experimental animals following CS with concomitant over-expression nSM2 in both rodent and emphysematous human lungs [125]. Whereas hydrogen peroxide activates nSM2 similarly to CS, this effect is inhibited by antioxidants, like GSH [124]. NSM3 is a C-tail anchored membrane protein, being associated with both the TNF-α receptor type 1(TNFR1) and the adaptor protein FAN (factor associated with nSMase activation). Interestingly, its mRNA is highly expressed in the heart [115].

Regulation of sphingomyelinases activity

Recent data indicate that nSM2 is a phosphoprotein and its phosphorylation level is regulated by oxidative stress [126]. Calcineurin (CaN) phosphatase, known as PP2B, normally deactivates nSM2 *via* dephosphorylation. Oxidative stress causes degradation of CaN, leading to activation of nSM2, which when fully phosphorylated, activates downstream PKC and p38 MAPK [126]. There are five conserved serine phosphorylation sites on nSM2 and all need to be phosphorylated for full enzyme activity [125, 127]. In addition, aSMase in human airway epithelial cells (HAE) was found upregulated exclusively by peroxynitrite (ONOO−), whereas nSM was not [128].

2.2.3.2. Spingomyelin synthases

Sphingomyelin is a major component of plasma membranes of eukaryotes, especially abundant in mammalian neural tissue [129] and in some prokaryotes [130]. Sphingomyelin synthases (SMS) are enzymes responsible for the synthesis of sphingomyelin from ceramide and phosphocholine, although it has been postulated that SMS can also provide a reverse reaction [131]. SMS have two histidines and one aspartic acid in catalytic domain, which are evolutionary stable [132]. There are 2 SMS isoforms: SMS1and SMS2. SMS1 is localized in the Golgi apparatus, whereas SMS2 is present both in Golgi and plasma membrane [133], [134]. A study suggests SMS2 is also confined to the nuclear membrane and chromatin [135]. In yeast, Sms1 counteracts detrimental

effects associated with the accumulation of ceramide, being functionally opposed to pro-apoptotic BAX [136] and suppression of either SMS isoforms by specific siRNA in mice leads to apoptosis [137]. In addition, SMS1 plays regulatory role in ROS generation, associated with mitochondrial function and controls insulin secretion [138].

SMS2 participates in atherosclerosis development [139], [140] *via* NF kappa B-mediated signaling process [141] and in mice with macrophages deficient in SMS2, the atherosclerosis progress was attenuated [142]. SMS2 may also be involved in controlling certain drug transporters in the brain [143].

Spingomyelin synthases regulation

TNF-α, ceramide, and sphingosine are negative regulators of sphingomyelin synthase activity *via* direct mechanism [144]. IL-2 and PI-3 kinase are known as major positive regulatory factors of sphingomyelin synthase [145].

2.2.3. Recycling pathway of ceramide synthesis

Ceramide is considered a central compound in sphingolipid biochemistry. It can serve as a substrate for the synthesis of varied sphingolipids, like sphingomyelins, as discussed above [139]. Ceramide phosphorylation by ceramide kinase (CK) leads to the synthesis of ceramide 1-phosphate (C1P) [146]. Ceramide can also serve as a substrate for the synthesis of more complex sphingolipids. In this processes glucose or galactose is added to the ceramide through the action of glucose or galactose ceramide synthases, respectively [147].

In turn, the catabolism of ceramide by ceramidases [148], [149], and that of sphingosine-1-phosphate by sphingosine-1-phosphate phosphatases [150] produces sphingosine, which serves as a substrate for the synthesis of ceramides in a salvage pathway or is converted to S1P *via* the action of two sphingosine kinases: SK1 and SK2 [151]. In addition, S1P can be irreversibly metabolized to ethanolamine phosphate and hexadecenal *via* enzyme S1P lyase [152].

3. Apoptosis

Apoptosis is a highly controlled cell death phenomenon, which is important for both a embryonic development and normal tissue integrity in higher organisms [153], [154], [155], [156], [157], [158]. There are characteristic histological changes during late apoptosis, like cell shrinkage, condensation of chromatin, and plasma membrane blebbing, which are visible by light microscopy [159], [160]. However, there is no inflammatory process, no leakage of cellular components is observed and cell content is quickly engulfed by macrophages with no involvement of inflammatory molecules [161], [162].

There are two main pathways leading to apoptosis: the extrinsic or death receptor pathway and the intrinsic or mitochondrial pathway, which can be interrelated *via* molecular crosstalk [163]. A third apoptotic pathway is induced *via* either granzyme B or granzyme A, and is involved in T-cell mediated cytotoxicity [164].

The extrinsic apoptotic pathway starts with binding of specific ligands to their corresponding receptors on cell membrane, and the best described models for this type of interaction are: FasL/FasR and TNF-α /TNFR1. Following receptor clustering, cytoplasmic adapter proteins with death domains are recruited and interact with death receptors. For example, both the interaction of Fas ligand with Fas receptor or TNF-α with TNF-α receptor recruits adapter protein FADD or TRADD, along with binding of FADD and RIP, respectively [165], [166, 167]. Following FADD recruitment of procaspase-8, a death-inducing signaling complex (DISC) is created, leading to activation of caspase-8 and initiation of apoptosis [168].

The intrinsic pathway is a non-receptor mediated pathway, and is triggered by either negative or positive signals, leading to increased inner mitochondrial membrane permeability. Negative signals are described as deficiency of specific factors necessary for maintenance of cellular integrity, like growth factors, hormones and cytokines. Examples of positive signals are radiation, toxins, hypoxia, hyperthermia, viral infections, and free radicals [169]. An important step in the intrinsic apoptotic pathway is opening of the mitochondrial permeability transition (MPT) pore *via* a process called mitochondrial outer-membrane permeabilization (MOMP) [170]. That event causes liberation of two groups of pro-apoptotic proteins from the mitochondrial intermembrane space into the cytosol [171]. Cytochrome c*,* Smac/DIABLO, and HtrA2/Omi [172], [173], [174] are members of the first group of pro-apoptotic proteins, responsible for triggering the caspase-dependent mitochondrial

19

pathway. As soon as cytochrome c is released from mitochondria, it activates both Apaf-1 and procaspase-9. That causes the formation of more complex structure, called "apoptosome" and activation of caspase-9. Activated caspase-9 is an initial signal for executioner caspases pathway, including activation of caspase-3 [175]. In addition, proteins Smac/DIABLO and HtrA2/Omi enhance apoptotic processes by blocking IAP (inhibitors of apoptosis proteins) activity [173], [176]. A second group of pro-apoptotic proteins discharged from mitochondria, include apoptosis inducing factor (AIF), endonuclease G and caspase-activated DNAse (CAD), which are translocated into the nucleus leading to DNA fragmentation [177], formation of oligonucleosomal DNA fragments [178], and nuclear condensation [179], [180]. CAD activation is caspase-3 dependent [181].

The intrinsic apoptotic pathway is largely controlled by proteins from Bcl-2 family. The Bcl-2 family consists of three groups, which are not only functionally different, but also composed of various numbers of Bcl-2 homology domains (BH1-4 domains) [170]. The role of anti-apoptotic Bcl-2 proteins is to bind and hamper pro-apoptotic Bcl-2 proteins. The pro-apoptotic molecules comprise two groups. The effector group, including proteins BAK and BAX is responsible for formation of pores in the outer mitochondrial membrane and subsequent cytochrome c release [182], [183], [184]. The second group consists of the BH3-only proteins and is responsible either for direct enhancement of BAK/BAX-dependent MOMP (BID) [185], or hampering the activity of the anti-apoptotic proteins (BAD) [186], [187], [188]. The final endpoint for both extrinsic and

intrinsic pathways is execution phase. Caspase-3, caspase-6 and caspase-7 are effectors of the execution phase and responsible for many late nuclear and cytoplasm changes, including cleavage of proteins such as PARP and cytokeratins [189].

3.1. Ceramides involvement in apoptosis

Sphingolipids act as signaling molecules, leading to multiple different cellular responses. In general, ceramides are pro-apoptotic, whereas S1P is a pro-survival molecule. Ceramides participate in development of apoptosis *via* several mechanisms. Enhancement of sASMase activity caused immediate ceramide production from sphingomyelin in the plasma membrane, enrichment of specific rafts in ceramides, which leads to the formation of death receptor complexes on plasma membrane, herein augmenting the extrinsic apoptotic pathway [190].

In addition, ceramides activate protein phosphatase 1 (PP1), which regulates the alternative splicing processes in Bcl-2 family with overproduction of pro-apoptotic molecules. Ceramides also activate PPA2, which, in turn, inactivates Bcl-2, an important anti-apoptotic protein, by dephosphorylation at serine 70 [191]. Thus, activation of both PP1 and PP2A turns on the intrinsic apoptotic pathway. Apoptosis is also triggered by ceramide *via* direct activation of cathepsin D [192].

Autophagy or autophagocytosis is a process leading the degradation of a cell's own components by lysosomes [193], [194]. This process plays a normal

part in cell growth and homeostasis, helping to maintain a balance between the syntheses, degradation, and recycling of cellular products. Autophagy can have a protective role, for example against oxidized low density lipoprotein (ox-LDL)-induced injury of human umbilical vein endothelial cells [105], [115]. Autophagic cell death can be initiated by damaged plasma membrane, sphingolipids, and ceramide. For instance, exposure of human umbilical vein endothelial cells to glycated collagen I (GCI) causes lysosomal permeabilization followed by clustering of membrane rafts and it was linked to sphingomyelinase activity, accumulation of ceramide, clustering, and later internalization of lipid rafts [105].

3.2. Cell specific apoptosis in the lung

Not all cells undergo apoptosis in response to ceramides. We noted an intracellular increase in ceramides in human lung endothelial, epithelial cells, and alveolar macrophages (AM) after exposure to CS (Petrusca *et al.*, manuscript in preparation) [195]. Intracellular ceramides trigger apoptosis in lung endothelial cells [77]. However, Petrusca *et al.* and others noted that AM are resistant to ceramide-induced apoptosis [195]. This could be explained by robust activation of signaling pathways that promote survival of AM. Indeed, when ceramide production was amplified by LPS in human macrophages, the activation of PI 3-kinase by those ceramides was observed, which led to activation of pro-survival pathway [196]. Some indicate also a beneficial role of ABCA1, ABCG1 transporters, and HDL in protection and preserving viability of macrophages

22

against oxidative burst following exposure to oxidized phospholipids and/or apoptotic cells [197].

AM are responsible for the elimination of apoptotic cells in a process called efferocytosis [104]. Our laboratory observed that CS-dependent up-regulation in ceramides led to an increase in number of apoptotic alveolar epithelial and endothelial cells in the lung with accumulation of AM. Interestingly, experiments from our lab showed a decrease in efferocytosis of AM in response to either endogenous or exogenous ceramides stimulation [195]. An inhibitory effect of ceramide on efferocytosis was linked to decreased membrane ruffle formation and impairment of Rac1 plasma membrane recruitment. This may imply that the upregulation of ceramides in the lungs causes both apoptosis of parenchymal cells and impairment of efferocytosis by AM, which collectively may augment lung injury [195].

3.3. Ceramide upregulation in lung endothelial cells

Upregulation of ceramides can mediate both extrinsic and intrinsic pathways of apoptosis in various cell types, including endothelial cells, *via* multiple mechanisms, such as death cell receptor clustering [176] and activation of caspase-8 [175], direct activation of protein phosphatases 1 and 2a [15, 20, 177], and direct effect on mitochondrial membrane permeability [198]. In addition to apoptosis, ceramides have been involved in endothelial oxidative stress [199-201], growth arrest [202, 203], cytoskeletal changes [204], and senescence

[205]. Through these effects, ceramides regulate major aspects of lung endothelial cell function and, not surprisingly have been implicated in the pathogenesis of several conditions associated with pulmonary vascular dysfunction.

Ceramides generated by the acid SMase pathway have been implicated in pulmonary edema induced by excessive platelet activating factor in models of acute lung injury or in response to surges in TNF-α that may occur following acute exposure to LPS in sepsis [26, 206]. The mechanism by which ceramide signaling leads to lung injury involves modulation of NO signaling in endothelial cell caveoli in a fashion that appears unique to the pulmonary circulation [207]. Interestingly, the pro-edemagenic effect of ceramides on the lung endothelium appears to be apoptosis-independent [208], the typical cellular response induced by excess ceramides. This dichotomy in the signaling effects of ceramides on the cultured lung endothelium recapitulates that of TNF-α [209] is a key inflammatory cytokine and a potent inducer of ceramides in endothelial cells.

The consequences of sustained or chronic ceramide upregulation in the lung endothelium, induced either by direct instillation of ceramides to the lung or by a decrease in VEGF signaling, or by targeted endothelial mitochondrial damage, have been associated with increased endothelial cell apoptosis, and *in vivo*, with airspace enlargement and a phenotype consistent with lung emphysema [210], [211], [212]. Cigarette smoke, which is the most common cause of emphysema, increases ceramides in endothelial cells and in the whole lung animal models and in individuals who smoke or who have a diagnosis of

emphysema [32, 201, 213-215]. Petrache *et al.* demonstrated, that increased of lung ceramides are sufficient to cause alveolar endothelial and epithelial cell apoptosis, activation of macrophages and matrix proteolysis, which altogether recapitulate the phenotype of emphysema and that upregulation of ceramides *via* the *de novo* pathway of synthesis was necessary for apoptosis and airspace enlargement in the VEGF receptor blockade model of emphysema [32]. More recently, a requirement of neutral SMase-generated ceramides has been reported in relation to cigarette smoke-induced epithelial cell apoptosis [214]. The relative contribution of endothelial and epithelial cell-generated ceramides to apoptosis and airspace enlargement in response to cigarette smoke remains to be elucidated and will be addressed in my thesis. Cigarette smoke exposure may elevate ceramides either by oxidative stress, by VEGF receptor deprivation, or as recently reported, *via* alterations in the function of cystic fibrosis transmembrane regulator (CFTR), which in turn regulates ceramides at the plasma membrane through a process that may involve the *de novo* pathway [216]. Noe *et al.* demonstrated that in lung endothelial cells, CFTR was required for proper ceramide homeostasis through a process that involved intracellular pH regulation that in turn affected both the sphingomyelinase and the *de novo* pathway enzymatic function [217]. These findings complement the elegant work by Gulbins *et al.* which demonstrated the importance to ceramide-mediated effects on epithelial cells with mutant CFTR in models of cystic fibrosis, where acid SMase plays a key role in the pathogenesis of this disease, controlling rates of epithelial cell apoptosis and the susceptibility to chronic lung infection [218, 219].

The mechanisms by which ceramides contribute to emphysema development involve increased oxidative stress and apoptosis, which are linked *via* mutual interaction and self-amplification [201]. In addition, *de novo* synthesized ceramides, and especially downstream production of sphingosine *via* acid ceramidase profoundly inhibit the clearance of apoptotic cells by specialized alveolar macrophages [220]. This is yet another self-perpetuating cycle triggered by ceramides, which both increases apoptosis of structural endothelial and epithelial cells in the lung and inhibits their clearance by macrophages, a process which may contribute to increased inflammation in the lungs of smokers and patients with COPD [221].

The involvement of endothelial cell ceramides in the pathogenesis of pulmonary vascular diseases that include pulmonary hypertension or ischemia reperfusion injury has not been reported, indicating a need for future investigations in these areas.

Harnessing ceramide's pro-apoptotic signaling in the endothelium could be achieved by inhibiting ceramide synthesis in the context of injury, or by counteracting its biological effect through concomitant upregulation of pro-survival pathways, such as those initiated by S1P. Both acid and neutral SMase inhibitors, as well as inhibitors of the *de novo* pathway of ceramide synthesis effectively inhibited ceramide-induced apoptosis in the lung in various acute or chronic injury models *in vivo*, in which these pathways were found activated, as mentioned above, and recently reviewed by Uhlig and Gulbins [222]. Petrache *et al.* demonstrated that inhibition of ceramide synthesis in the context of normal

lung homeostasis may be detrimental, as shown in previous work with fumonisin B1, a ceramide synthases inhibitor, which dose-dependently increased endothelial cell apoptosis, lung apoptosis, and airspace enlargement in naïve mice [32]. Such approach may deplete cells from normally required ceramide for proper sphingolipid metabolism, including that of generating pro-survival metabolites. The role of S1P in cell survival and proliferation has long been recognized [171], an effect that in endothelial cells could be mediated *via* its receptors, also known as endothelial differentiation, G-protein-coupled receptors [223]. Diab KJ *et al.* proposed that, similar to other organs, a balance between proapoptotic ceramide and prosurvival S1P is required for maintenance of alveolar structures in the lung [210]. Treatment of mice with agonists of S1P1 receptor inhibited endothelial cell apoptosis and airspace enlargement typically induced by VEGF receptor blockade [32], suggesting the pro-apoptotic function of ceramide can be antagonized by engaging S1P signaling in the lung [210].

In addition to cell survival, S1P modulates pulmonary endothelial cell motility and barrier function either intracellularly [224], or outside-in *via* specific S1P receptors, such as S1P1, which typically exerts barrier protective actions [225], or S1P2, which is barrier disruptive [226]. There is evidence of a complex interplay between signaling initiated by specific S1P receptors of the presence of intracellular targets of S1P or its synthetic analogs, along with a cell-specificity for responses to S1P [227-229].

3.4. RTP801 and lung cell apoptosis

There is ample evidence that mechanisms of amplification of lung injury lead to destruction of alveolar walls and persistence of inflammatory systemic and lung responses in COPD [8], [230]. Ceramide and RTP801 have been identified as potential signaling relays that are engaged early by CS exposure, which may interact and therefore amplify alveolar wall injury in emphysema [32, 201, 231]. Both ceramide and RTP801 are involved in apoptosis, but it is not known if they are mechanistically linked.

RTP801, also known as REDD1, is a stress response protein and signaling mediator stimulated by oxidative stress generated by CS and triggers NF-κB-mediated inflammation in the lung as well as apoptosis of alveolar structural cells [231]. The upregulation of RTP801 was detrimental to the lung, since mice lacking RTP801 were protected against CS-induced emphysema, concomitant with an increase in trophic factors including VEGF. The finding that lungs of patients with emphysema exhibit increased RTP801 expression [231] spurred on interest in RTP801 as a therapeutic molecular target. Mechanistic studies of RTP801 have been performed in the CS mouse model that recapitulates many aspects of the complex pathogenesis of COPD. A further simplified model which replicates the paucity of VEGF signaling in the lung parenchyma of patients with emphysema and highlights the apoptotic destruction of lung alveoli is obtained by inhibition of the VEGF receptors (VEGFR) [30]. In this murine model, apoptosis-dependent emphysema develops 4 weeks following a single subcutaneous injection of the VEGFR inhibitor SU5416 [30, 32].

Petrache *et al.* measured robust upregulation of ceramide production in the lungs of VEGFR-inhibited rats and mice *via* the *de novo* pathway during the first week following SU5416 injection [32]. The time of ceramide upregulation coincided with increased oxidative stress and apoptosis, all preceding the onset of airspace enlargement [32]. However, it is not known if RTP801 is stimulated in this model, a question I approached in my work.

Based on recent evidence, RTP801 may be one of the earliest stress responses to CS exposure that integrates oxidative stress with lung inflammation and apoptosis [231]. Since both ceramide and RTP801 may be central amplifiers of alveolar wall destruction in emphysema, we investigated if they are mechanistically linked and if RTP801 is one of the mechanisms by which ceramide induces alveolar cell apoptosis.

B. HYPOTHESES

1. Cigarette smoke increases lung ceramides *via* activation of its synthetic pathways.

2. Ceramides are necessary for cigarette smoke-induced alveolar cell death.

3. Ceramide induces alveolar epithelial and/or endothelial cell apoptosis *via* RTP801 upregulation.

C. MATERIALS AND METHODS

1. Chemicals and reagents

All chemical reagents were purchased from Sigma-Aldrich (St. Louis, MO), unless otherwise stated.

2. Mouse strains

C57BL/6 mice 6-10 weeks old females were purchased from Harlan (Indianapolis, IN) and housed in the Laboratory Animal Resource Center at Indiana University School of Medicine (Indianapolis, IN). C57Bl/6 mice were utilized for studies of RTP801 or ceramide C12:0 augmentation and for VEGFR inhibition and CS studies.

DBA2/J2 mice 6-10 weeks old females were purchased from Jackson's laboratory (Bar Harbor, ME) and were used in CS exposure experiments.

Rtp801-null mice (C57bl/6x129SvEv) (females; at least 3 months old) were from Quark Pharmaceutical Inc. Wild type controls of similar genetic background (C57Bl/6 x 129SvEv females; at least 3 months old) were from Taconic, (Fremont, CA). Rtp801-null mice or wild type controls were utilized for studies of ceramide C16:0 augmentation.

All animal studies were approved by the Institutional Animal Care and Use Committee at Indiana University (Indianapolis, IN).

3. Animal experiments

3.1. Cigarette smoke exposure

In vivo CS exposure was performed as previously described [40]. Briefly, C57Bl/6 (female, age 12 weeks; n=5-10 per group), DBA/2J (male or female; age 12-14 weeks; n=5-10 per group) or CerS2KO mice were exposed to CS 5 hours a day 5 days a week or to ambient air for up to 24 weeks. More specifically, mice were exposed to 11% mainstream and 89% side-stream smoke from reference cigarettes (3R4F; Tobacco Research Institute, KY) using a Teague 10E whole body exposure apparatus (Teague Enterprise, CA). The exposure chamber air was monitored for total suspended particulates (average 90 mg/m^3) and carbon monoxide (average 350 ppm). Unless otherwise specified, mice were euthanized and lungs were processed as previously described (3) the day following the last day of CS exposure.

3.2. Intra-tracheal instillation of pro-apoptotic molecules

Indirect method

Mice were anesthetized by brief inhalational halothane exposure, the tongue was gently pulled forward by forceps and the trachea instilled with ceramide-containing or vehicle (ethanol) containing perfluorocarbon solution applied at the base of the tongue *via* a blunt angiocatheter [232], *via* an indirect method of instillation, as previously described [32].

Direct method

After anesthesia, the trachea was exposed in aseptic conditions and either the compound or its vehicle was introduced directly into the trachea using a sterile needle. Following suture of the neck soft tissues, mice were allowed to recover.

Ceramide C12:0, Avanti (Alabaster, AL), was first solublilized in 100%, ethanol and then suspended in sterile perfluorocarbon (15 μl). The oxygen-carrying properties of perfluorocarbon ensured adequate tolerance by the animal at these volumes, while its physical-chemical properties allowed for efficient distal lung delivery following intra-tracheal instillation [32, 201].

Ceramide C16:0 (Avanti) was administered intra-tracheally either as solution in ethanol or conjugated with PEG.

Rtp801 cDNA (50 μg) was delivered intra-tracheally in 80 μl saline.

3.3. Vascular endothelial growth factor receptor (VEGFR) inhibition

The VEGFR inhibition model is an apoptosis-dependent model of emphysema development, and was conducted, as previously described [30]. In this murine model, emphysema develops 4 weeks following a single subcutaneous injection of the VEGFR inhibitor SU5416 Calbiochem (Gibbstown, NJ) [30, 32]. Mice were injected subcutaneously with SU5416 (20 mg/kg) or vehicle (carboxymethylcellulose).

3.4. Pulmonary function tests

Mice were anesthetized with inhaled isoflurane and suspended vertically from their incisors. The neck was transilluminated with a fiber optic light source and the glottic opening was visualized with a custom-made laryngoscope blade. A 0.025" diameter guide wire was probed through the glottic opening, and a 20-gauge Teflon catheter was advanced over the guide wire into the trachea. Following removal of the wire, the animal was mechanically ventilated with a rodent ventilator using room air, at a rate of 140 breaths per minute, a tidal volume of 0.3 ml, and 5 cm H_2O of positive end-expiratory pressure. The animals were placed on a heated (37 ºC) pad and pulmonary function tests were then performed with the Flexi Vent system (Scireq, Montreal, PQ, Canada). Starting at FRC, the system was programmed to deliver 7 inspiratory volume steps, for a total volume of 1 ml, followed by 7 expiratory steps, pausing at each step for at least 1 second. Compliance was calculated by dividing the cumulative volume delivered at each step by the plateau pressure, averaging 3 pressure volumes loops for each mouse. At the conclusion of testing, isoflurane was discontinued, and the animal was allowed to emerge from anesthesia. Once spontaneous respiration had been resumed and reflexes had been returned, the tracheal cannula was removed.

3.5. Animal tissue preparation and analysis

3.5.1. Broncho-alveolar lavage

The broncho-alveolar lavage (BAL) fluid was collected by lavaging the lungs with 3 aliquots of 1 ml each, totaling 3 ml of Ca^{2+} - and Mg^{2+} - free PBS supplemented with 0.1 mM EDTA. Samples were centrifuged (5 min; 500 g; 4 °C). Pellets were collected in 1 ml of red blood cells (RBCs) lysis buffer, left for 5 min on ice, and then resuspended in PBS and counted, using a hemocytomether. Cytospin slides containing 10,000 cells each were made with total volume 350 ml of PBS centrifuged at 1350 rpm for 5 min and stained using a 3 step stain set (Richard-Allan Scientific). The slides were rinsed in water twice and allowed to dry, and then cover glasses were applied with mounting medium (Fisher) and cells were scored by a technician blinded to the identity of the experimental group. The acellular BAL fluid was snap-frozen in liquid N_2 and stored at -80 °C for future analysis.

3.5.2. Lung tissue harvesting

The trachea was exposed and a blunt probe was inserted under the trachea to free it from the surrounding tissue. While trachea was raised, a 4 cm suture was pulled underneath it. Fine tipped scissors were used to cut a small "V" shaped incision of the anterior aspect of the trachea, just below the thyroid cartilage. A cannula was inserted into the trachea and was secured with a suture. Meanwhile, the thoracic cavity was open and the right atrium was punctured with a needle. In some experiments blood was collected to obtain plasma for future

analysis. The lungs were flushed by perfusing 20 ml of PBS through the pulmonary circulation via the RV. The right bronchus was exposed and ligated with a suture. A pre-warmed (up to 57 ^{o}C) 0.25% solution of low melting point agarose (10% formalin with PBS) was slowly introduced into the left lung with constant pressure of 20 cm H_2O. The trachea was then clamped with a haemostatic clamp, the lungs and the heart were dissected *en block*, transferred into 50 ml conical tube, and left on ice (4 ^{o}C) for 10 min. The right lungs were aliquoted and snap frozen in liquid N_2. Left lungs were cut with a sharp blade in a coronal plane into 5 pieces, transferred into a plastic fixation cassette and stored in 10% formalin solution with PBS, and sent to the Histology Core facility for paraffin embedding and sectioning (4-5 μm sections).

3.5.3. Histological assessment

3.5.3.1. Hematoxylin and eosin staining

Tissues on slides were deparaffinized 3 times for 3 minutes each in Clear-Rite 3 (Richard-Allan Scientific) or xylene, followed by immersing (3 times for 1 min) in 100% Flex (Richard-Allan Scientific) and in 95% Flex (1 minute). Slides were then rinsed in running tap water briefly and put for 4 minutes in hot water (60-70 ºC) for 1 min to remove agarose residues, and then rinsed in deionized water. Samples were immersed in hematoxylin solution for 2 min and rinsed in tap water, to remove excess stain. Then slides were put into clarifier (Richard-Allan Scientific) for 30 seconds, rinsed in tap water, immersed in Bluing Reagent for 1 min and rinsed in tap water for 1 min. Slides were then stained in Eosin-Y

for 30 sec and were immersed (3 times for 1 min) in 100% Flex, then in xylene (3 times for 1 min each), followed by mounting of cover glasses, using mounting media.

3.5.3.2. Detection of Rtp801 by immunohistochemistry

Rtp801 IHC was performed after deparaffinization of slides and antigen retrieval with citrate solution (pH 6.0; 30 min). After inhibition of endogenous peroxidase activity by incubation in H_2O_2 (3% methanol; 30 min) slides were rinsed in TBS and blocked in goat serum (10% in TBS; 30 min). Primary antibody against RTP801 was applied (Proteintech; 1:200; 1 h), followed by secondary biotinylated goat anti-rabbit antibody (1:200; 1 h), streptavidin peroxidase (30 min), and chromogen (DAB; 5 min). A set of sections was then counterstained with Mayer's hematoxylin.

3.5.3.3. Detection of active caspase-3 by immunohistochemistry

Active caspase-3 IHC was performed on lung sections, as previously described [233]. Briefly, following deparaffinization and hydration, sections were blocked with goat serum (10%) and incubated with anti-caspase-3 antibody (Cell Signaling; 1 h at room temperature or overnight at 4 ºC). Slides were then stained with biotin-conjugated goat anti-rat IgG secondary antibody (1:100; Vector Laboratories, Burlingame, CA) and streptavidin-coupled phycoerythrin or fluorescein isothiocyanate (1:1,000; Vector). Sections were counterstained with DAPI and mounted with Mowiol 488 (Calbiochem). Microscopy was performed on either Nikon Eclipse (TE200S) inverted fluorescence or a combined confocal/multiphoton inverted system (Spectraphysics laser, BioRad

MRC1024MP). Images were captured in a masked fashion and quantitative data were obtained by Metamorph Imaging software (Molecular Devices, Sunnyvale, CA) as previously described [233].

3.5.4. Morphometric analysis

Morphometric analysis was performed on coded slides as described previously, using a macro developed by Dr. Tuder for MetaMorph [234].

3.5.5. Apoptosis assessment by flow cytometry

Besides apoptosis evaluation with IHC, apoptosis of specific lung cell populations was measured in cell suspensions isolated after lung disintegration, followed by the detection of cleaved caspase-3 using flow cytometry. For channel setup, we used Jurkat cells (Lymphoma T cells from ATCC; 10^6 in 100 μl) stained with FITC labeled anti CD3 (eBioscience) for FL1 and with Phycoerythrin (PE) labeled anti CD3 (eBioscience) for FL2. Cell suspensions were incubated with anti CD32/16 antibody (Santa Cruz Biotechnology; 1 μg/10^6 cells; 10 min), followed by washing and transfer into flow cytometry tubes. Labeling of selected cell populations was achieved with rat anti-mouse CD31 FITC conjugated antibodies (BD Pharmingen; 30 min) for the detection of endothelial cells, using as isotype control a rat IgG 2 FITC conjugated (eBiosciences). For the detection of type I pneumocytes, Alexa Fluor 488 Golden Syrian Hamster IgG anti Podoplanin antibody (eBiosciences) was used, with an isotype control Golden

Syrian Hamster IgG FITC conjugated (eBiosciences) antibody as control. Cell suspensions stained for alveolar type II cell markers were first prepared for intracellular staining. All samples underwent fixation and permeabilization with paraformaldehyde (1% in PBS) and Triton-X 100 (0.1% in PBS), respectively. Pro-surfactant C rabbit anti-mouse FITC labeled Abs were used, which were obtained by labeling rabbit polyclonal anti-pro-surfactant C IgG antibodies (Millipore/Abcam) with FITC using a kit (Pierce), following the manufacturer's instructions. For isotype control, cells were stained with rabbit anti-mouse polyclonal IgG antibody (SouthernBiotech) which was labeled with FITC using a similar kit. Staining for active caspase-3 in lung cell suspensions was achieved by using PE conjugated affinity purified polyclonal rabbit antibody raised against active caspase-3 (BD Pharmingen), and an isotype PE conjugated IgG antibody (Southern Biotech). Following staining (30 min), samples were washed, centrifuged (500g; 5 min; RT) and cell pellets were suspended in BSA (1% in PBS) for flow cytometry analysis.

3.6. Enzymatic caspase-3 activity assay

3.6.1. Preparation of samples

3.6.1.1. Preparation of cells: Media was discarded and cells were washed 2x in PBS and harvested in caspase-3 lysis buffer with fresh protease inhibitors cocktail (1/100), using approximately 230 μl for each well from 6-well plates. Cells were collected on ice (4 ºC) by scraping, transferred into Eppendorf tubes, and sonicated for 20 sec. Then samples were centrifuged for 10 min, 4 ºC, at

39

10,000 rpm. The supernatants were collected into clean tubes and stored at minus 80 °C.

3.6.1.2. Preparation of tissue: Lung tissue (4 - 5 mm^3) was homogenized with electric homogenizer in caspase-3 lysis buffer with fresh protease inhibitors cocktail 1/100, using approximately 600 μl of buffer for each sample. Then, samples were sonicated for 20 sec and centrifuged for 10 min, 4 ^{o}C, at 10,000rpm. The supernatants were collected into clean tubes and stored at -80 °C.

For preparation of homogenates we used the following caspase-3 lysis buffer: 50 mM HEPES (pH 7.4); 100 mM NaCl; 0.1% CHAPS; 1 mM DTT; 0.1 mM EDTA.

3.6.2. Caspase-3 activity assay

While working on ice (4 ^{o}C), 50 μl of each sample was added into each of a 96 well plate in duplicates. Next, 50 μl of substrate for caspase-3, 2-DEVD-R110 (x100) (Promega) (1/100 dilution in caspase-3 assay buffer) was added into each well. A 1.5 hour kinetics assay was performed using λ= 485 nm for excitation and λ= 538 nm for emission in a fluorometer plate reader (Promega, Fitchburg, WI).

Human caspase-3 (active) recombinant protein (Chemicon International, 25 units) was used as positive control. The negative control was caspase-3 assay buffer: 50 mM HEPES (pH 7.4), 100 mM NaCl; 0.1% CHAPS; 1 mM DTT;

0.1 mM EDTA; 10% glycerol. The results of caspase-3 activity were normalized by the protein concentration of the sample.

4. Cells culture experiments

4.1. Cell lines used in experiments

HLMVEC-human lung microvascular endothelial cells; Lonza, (Walkersville, MD); media: EBM-2 Basal Medium 500ml with EGM-2 SingleQuot Kit Suppl. & Growth Factors, all from Lonza.

L2-primary rat lung epithelial cells; ATCC, (Manassas, VA), cultured in Hams F12 media with 10% FBS, (American Type Culture Collection**,** ATCC).

RLMLEC-rat lung microvascular endothelial cells were from the University of South Alabama, (Mobile, AL), cultured in DMEM; Cellgro (Herndone, VA) and supplemented with 10% FBS and penicillin/streptomycin.

SAEC-small airway epithelial cells (human) were from Lonza; cultured in SABM Basal Medium 500 ml with SAGM with SingleQuot Kit Suppl. & Growth Factors (Lonza).

All cells were cultured in a humidified 37 $^{\circ}$C, 5% CO_2 incubator.

4.2. Preparation of CS extract

An aqueous CS extract was prepared from filtered research grade cigarettes (1R3F) from the Kentucky Tobacco Research and Development

41

Center at the University of Kentucky. A stock (100%) CS extract was prepared by bubbling smoke from 2 cigarettes into 20 ml of PBS at a rate of 1 cigarette per minute to 0.5 cm above the filter, modifying a method developed by Carp and Janoff (30). The extract's pH was adjusted to 7.4, followed by filtration (0.2 μm, 25 mm Acrodisc; Pall, Ann Arbor, MI) and used in cell culture experiments within 20 min. A similar procedure was used to prepare the control extract, replacing the CS with ambient air.

4.3. Preparation of treatment media for all culture studies.

Prior to addition to cell culture media, sphingosine-1 phosphate (S1-P) (Sigma) was dissolved in DMSO. D-sphingosine *(*Sigma) was dissolved in methanol. FTY-720 was dissolved in DMSO. Ceramide C16: 0 was dissolved in ethanol. CS extract (100%) was diluted volume: volume at the indicated concentrations.

4.4. Whole lung disintegration

Mice were sacrificed using isoflurane and immediately cannulated with an intra-tracheal catheter. Vessels on both sides of the neck were open and lungs were perfused via the right ventricle with PBS without calcium and magnesium ions, at 37 °C. Large vessels and bronchi were discarded. The remaining lung tissue was placed in 60 mm tissue culture dishes, each containing disintegration solution and then dissected and minced into 1-2 mm diameter fragments, followed by immediate transfer into 50 ml conical tube. The lung tissue

disintegration solution contained fetal bovine serum in Dulbecco's modified Eagle medium (10%), DNase I, (6.5 μg/ml, Stemcell Tech, Vancouver, Canada). and collagenase A (12 μg/ml) (Roche). Lung fragments were disintegrated in this solution (30 min; 37 °C) until a clear cell suspension was obtained. Cell suspension was filtered through a cell strainer (70 μm; Fisher Scientific, Fair Lawn, NJ), followed by centrifugation (10 min, 300 g, 4 °C). Cell pellets were resuspended in PBS followed by the addition of Geye's solution (erythrocyte cell lysis buffer) and repeated centrifugation. Cell pellets were then resuspended in 1ml of PBS with 1% FBS. All procedures in above protocol for isolation of cells for culture purposes were performed in sterile conditions.

4.5. Isolation of lung endothelial cells

For isolation of lung endothelial cells, we used positive selection of CD146$^+$ cells from mouse using CD146 for liver sinusoidal endothelial cells (LSEC) MicroBeads (Miltenyi Biotec, Cambridge, MA). All procedures followed Miltenyi Biotec guidelines.

4.5.1. Magnetic labeling of cells

Following whole lung disintegration using the above protocol, the cell number in each sample was determined. Cells were centrifuged for 10 min, 300 g, at 4 °C and supernatants were discarded. Cell pellets were resuspended in 90 μl of MACS buffer per 10^7 total cells and 10 μl of CD146 (LSEC) MicroBeads per 10^7 cells were added. Samples were mixed well and incubated for 15 minutes at 4 °C. Cells were washed by adding 1-2 ml of MACS buffer per 10^7 cells and

centrifuged at 300 g for 10 minutes. The supernatant was aspirated and cells were resuspended in 500 μl of MACS buffer up to 10^7 cells, followed by magnetic separation.

4.5.2. Magnetic separation with MS columns

The column was placed in the magnetic field of suitable MACS separator. The columns were prepared by rinsing with the 500 μl of MACS buffer. Previously prepared cell suspensions were applied onto the columns and flow - through containing unlabeled cells was collected. The columns were washed 3 times with 500 μl of MACS buffer. Unlabeled cells were collected for efficiency analysis. Washing steps were performed by adding buffer aliquots only when the column reservoir was empty.

The column was then removed, placed at a distance from the separator in a suitable collection tube. 1 ml of MACS buffer was added onto the column and the magnetically labeled cells were immediately flushed out by firmly pushing the plunger into the column. The cell suspension was saved for culture or experimental evaluation.

4.6. Flow cytometry analysis of apoptosis using Annexin-V/PI detection kit

4.6.1. Cells harvest

At the end of the experiment, either SAEC or HLMVEC were washed in PBS (w/out Ca and Mg), trypsinized and collected in media, followed by centrifugation at 500 g for 5 min at RT. Next, they were washed in 500 μl of cold 2% BSA in PBS (with Ca and Mg) and centrifuged again at 500 g for 5 min RT.

4.6.2. Evaluation of apoptosis

Apoptotic and necrotic events were quantified by Annexin V/PI staining using an apoptosis detection kit (R&D Systems, Minneapolis, MN) the flow cytometry evaluation was performed with a Beckman Coulter Cytomics FC500 cytofluorimeter (Beckman Coulter, Fullerton, CA) with CXP software. As a positive control UV-treated Jurkat or rat thymocytes were used.

4.7. Proliferation assay

RLMVECs were cultured overnight in 96-well plate in full DMEM medium. Then cells were pretreated with 2% FBS DMEM media for 1 h and treated with CS along with BrdU labeling solution. After appropriate time of incubation (from 6 to 72 h) cell proliferation was measured *via* BrdU incorporation using Cell Proliferation ELISA BrdU Kit, Roche (Indianapolis, IN).

5. Evaluation of lipids

5.1. Lipids extraction

Lung tissue was added into 2 ml methanol, homogenized, and 1 ml of chloroform was then added. For samples prepared for mass spectrometry analysis, 20 μl of 1 ng/μl Cer 17:0 standard was added. Samples were vortexed briefly and sonicated for about 20 sec to break down tissue/cells clumps. Then samples were left 2-3 h at RT or at 4 ºC overnight. Chloroform (1 ml) and 0.1 N HCl (1.3 ml) were added, samples were vortexed vigorously (1 min) and centrifuged (16 min at 2,600 g). The lower chloroform phase was transferred with

a Pasteur pipette into 4 ml clear glass. The solvent was evaporated under nitrogen stream in the heating block and the lipid film was re-dissolved in 1 ml of solvent (methanol: chloroform 3:1) and stored for further analysis.

Cell lysates were prepared in 1 ml of methanol (body fluids or supernatants were prepared in 2 ml of methanol), and then assayed as above, using ratios of methanol to chloroform to water (or 0.1 N HCl) at 1:1:0.9.

5.2. Lipid phosphorus (Pi) determination by optical density

The key assumption of this experiment is that one mole of phospholipids contains one mole of phosphate (Pi) that is released with heat treatment in the presence of perchloric acid. Therefore, by measuring released (Pi) one can estimate the phospholipids content of the cell lysate/tissue that is proportionate to the total amount of the cell/tissue used. The amount of ceramides normalized by (Pi) is then compared among samples within the same experiment. 200 μl of the lipid solution (for physiological fluids) or 100 μl (for tissue) was transferred to 8 ml glass tube and dried out under the nitrogen stream in. Then 50 μl of 70% $HClO_4$ with 1% $Na_2MoO_4*2H_2O$ was added into each tube, which was covered with Teflon tape and baked in a heating block at 200 ºC for 40 min. While the samples were exposed to heat, working reagents were prepared from 2.6 ml of 1 N H_2SO_4 and 6.85 ml of ddH_2O.

Eight standard solutions of Pi via serial dilution using the stock standard (100 mM $K_2HPO_4*3H_2O$ with 0.01% NaN_3) were prepared. The sample and standard tubes were cooled down to RT, followed by the addition of 0.45 ml of working reagents to each tube. 50 μl of ddH_2O was added to the samples and 50 μl of the standard Pi concentration to the standard tubes. The tubes were capped tightly, sealed with Teflon tape and boiled in a water bath for 15 min. Then they were cooled down to RT and 200 μl of each was transferred in duplicates in 96-well plate for colorimetric measurement (absorbance 815 nm).

A standard curve was prepared, subtracting the background of the 0 nmol/50 μl standard. The Pi values in the samples were interpolated.

5.3. Ceramide quantification

The sphingolipids were ionized via electrospray ionization (ESI) with detection via multiple reactions monitoring (MRM) by our collaborator, Dr. Walter Hubbard. Analyses of the sphingolipids were performed by combined liquid chromatography/ tandem mass spectrometry (LC/MS/MS). The instrumentation employed was an API4000 Q-trap hybrid triple quadrupole linear ion-trap mass spectrometer (Applied Biosystems, Foster City, CA) equipped with a turboionspray ionization source interfaced with an automated Agilent 1100 series liquid chromatograph and autosampler (Agilent Technologies, Wilmington, DE) [235], [236]. S1P and DHS1P were quantified as bis-acetylated derivatives with C17-S1P as the internal standard employing reverse-phase HPLC separation,

negative ion ESI, and MRM analysis. Details of this approach are described in [236, 237].

6. Enzymatic activity assays

6.1. Serine-palmitoyl transferase assay

Lungs were homogenized in SPT lysis buffer, containing 10 mM HEPES (pH 7.5 in NaOH); 250 mM Sucrose; 1 mM EDTA; proteinase inhibitor cocktail in ddH$_2$O. An equal volume (100 μl) of each sample was used in 100 μl of SPT assay buffer, containing 0.1 M HEPES (pH 8.3); 2.5 mM EDTA; 50 μM pyridoxal phosphate; 5 mM DTT; 1 mM L-serine, prepared in ddH$_2$O. SPT activity was determined by measuring the incorporation of (^{3}H) L-serine (American Radiolabeled Chemicals, Inc., St. Louis, MO) into palmitoyl-CoA and expressed as a number of counts per minute, measured using a scintillation plate reader. The results were normalized by protein concentration. A boiled tissue sample was used as a negative control.

6.2. Ceramide synthase-2 and -5 (CerS2 and CerS5) assays

Cells or lung tissue were homogenized in ceramide synthase lysis buffer: 5 mM EGTA; 25 mM Hepes pH 7.4; 50 mM NaF; 1 μg/ml Leupeptin; 10 μg/ml Soybean trypsin inhibitor in ddH$_2$O. First, D-erythro-sphinganine (C16 dihydrosphingosine, Avanti) was added to each glass tube and dried under N$_2$. Next, it was resuspended in assay buffer, containing 2 mM MgCl$_2$; 20 mM Hepes; 0.5 mM DTT; 20 mM defatted BSA. For CerS 2 activity assay, "cold' behenyl-

CoA with radioactive ^{14}C behenyl-CoA was utilized. For CerS 5 activity assay, "cold" palmitoyl-CoA, and ^{14}C palmitoyl-CoA (American Radiolabeled Chemicals) were used. After 1 hour incubation at 37 ^{o}C, samples were dried out under $N_{2,}$ resuspended in 20 μl chloroform and methanol (1:1) containing 1 mg/ml bovine brain ceramide and 1 mg/ml diacylglycerol, and 15 ml of this mixture was loaded onto silica TLC plates. Liquid chromatography was performed in TLC solvent, containing chloroform, methanol and 3.5 N aqueous ammonium hydroxide in a ratio 85:15:1, respectively. Particular bands on silica plate were captured by Phosphoimager. Activities of ceramide synthases were calculated by densitometric analysis and normalized by the protein concentration of the homogenate.

6.3. Sphingomyelinase activity assays

The activities of specific sphingomyelinase isoforms were evaluated with Amplex Red Sphingomyelinase Assay Kit (Molecular Probes, Eugene, OR), following manufacturers protocol. Tissues were homogenized in lysis buffers specific for each isoform [238]. For lysosomal ASM, we used cell lysis buffer, composed of: 0.2% TritonX-100; 100 mM sodium acetate (pH 5.0); 2 mM EDTA; 0.1 mM Na_3VO_4 (fresh); 1 mM PMSF (fresh); 10 μl/ml aprotinin (fresh); 10 μl/ml leupeptin (fresh), adjusted to 10 ml of ddH_2O; for secreted acid sphingomyelinase: 0.2% TritonX-100; 100 mM sodium acetate (pH 5.0); 0.1 mM Na_3VO_4 (fresh); 1 mM PMSF (fresh); 10 μl/ml aprotinin (fresh); 10 μl/ml leupeptin (fresh), adjusted to 10 ml of ddH_2O; and for neutral sphingomyelinase cell lysis

buffer: 0.2% TritonX-100; 20 mM Hepes, pH 7.4; 2 mM EDTA; 10 mM MgCl$_2$; 5 mM DTT (added fresh); 10 mM Beta-glycerophosphate; 0.75 mM ATP (fresh); 0.1 mM Na$_3$VO$_4$;10 μl/ml Aprotinin (fresh); 10 μl/ml Leupeptin (fresh), adjusted to 10 ml of ddH$_2$O. The kinetics for both acid and neutral sphingomyelinases was measured using a fluorescence microplate reader. Hydrogen peroxide and purified neutral sphingomyelinase were used as positive controls. The enzyme activity results were expressed normalized to protein concentration.

7. Evaluation of protein concentration

Protein concentration was evaluated using BCA Protein Assay Kit (Pierce).

8. Western blotting

Detection of Rtp801. Lung tissue or cells were homogenized in a lysis buffer containing 20 mM HEPES, (pH 7.5), 1.5 mM MgCl$_2$, 150 mM NaCl, 10% glycerol, 1% Triton X-100, 2 mM EDTA, 2 mM Na$_3$VO$_4$, 50 mM NaF, 1 mM PMSF, and protease inhibitor cocktail Set I (Calbiochem). Protein lysates were run on SDS- PAGE and transferred to nitrocellulose membrane, using the Criterion system (Biorad). The membranes were blocked with Superblock blocking buffer (Pierce Biotech) and incubated with indicated primary antibodies overnight (rabbit anti-mouse Rtp801, Quark Pharmaceuticals Inc.), and with secondary antibodies conjugated with horseradish peroxidase (Vector). The blots were developed using enhanced chemiluminescence kit (GE Healthcare).

9. Additional buffers and media

PBS w/Ca,Mg: 0.1 g of $CaCl_2$ (anhydrous), 0.1 g of $MgCl_2$-6H20, 0.2 g of KCl, 0.2 g of KH_2PO_4, 8 g of NaCl, 2.1 g of Na_2HPO_4-7H_2O in 1000 mL of ddH_2O (pH 7.4).

PBS w no Ca,Mg: 8 g NaCl, 0.2 g KCl. 1.44 g of Na2HPO4 and 0.24 g of KH2PO4 in 1000 ml of ddH2O water (pH 7.4).

Geye's Lysis Solution (Red cell lysis buffer); Solution A: In a 1 L beaker, 17.5 g of NH_4Cl, 0.925 g of KCl, 0.225 g of Na_2HPO_4 (anhydrous), 0.055 g of KH_2PO_4, 0.25 g of glucose were added to nearly 500 ml of dd$H_2$0, adjusted to a final volume of 0.5 L and then the buffer was filter-sterilized; **Solution B:** In a 0.5 L beaker, 1.05 g of $MgCl_2$*6H_2O, 0.36 g of $MgSO_4$*7H_2O, 0.85 g of $CaCl_2$ were added to nearly 250 ml of dd$H_2$0, adjusted to a final volume of 250 ml and then the buffer was autoclaved; **Solution C:** In a 0.5 L beaker, 5.625 g of $NaHCO_3$ was added and adjusted to 250 ml with ddH_2O and then was autoclaved.

Geye's Solution was then constituted by adding: 10 ml Solution A, 2.5 ml Solution B, 2.5 ml Solution C and 35 ml dH2O. To lyse RBC, 12 to 13 ml Geye's solution was added and incubated for 5 min at +4 ^{o}C.

10. Statistical analysis was performed with Sigma Stat (Systat Software Inc, Chicago, IL), using unpaired Student t-test, ANOVA, or Kruskal-Wallis One Way Analysis of Variance on ranks, as appropriate. Statistical significance was accepted at $p < 0.05$.

D.RESULTS

1. Cigarette smoke (CS) exposure effect on lung cells ceramides and apoptosis *in vitro* and *in vivo*

1.1. Lung epithelial and endothelial cells upregulate ceramides and undergo apoptosis in response to CS

1.1.1. CS exposure inhibits cell proliferation *in vitro*

Chronic CS exposure of decades leads to lung emphysema in susceptible individuals. In mice, emphysematous changes are observed as early as after 4-6 months after CS, depending on the strain. Both lung epithelial and endothelial cells have been shown to undergo apoptosis in emphysema models. To investigate the role of ceramide in CS-induced apoptosis, I first studied the ability of a soluble cigarette smoke extract (CSE) to affect primary lung alveolar cell function. Prior to the onset of programmed cell death due to CS, there are many changes in cellular physiology, including inhibition of cell proliferation. I asked if CSE affects proliferation of endothelial cells, using rat lung microvascular endothelial cells (RLMVECs) as an experimental model. First, I wanted to determine the CSE concentration that inhibits cell proliferation of RLMVECs. I exposed RLMVECs for 48 h to 1, 1.5, and 2.5% CSE concentrations and measured proliferation by BrdU incorporation using Cell Proliferation ELISA BrdU Kit. I found a significant inhibition of RLMVECs proliferation at 2.5 % CSE (Figure 1A), which is considered typically a low CSE concentration, as cell death is usually noted only with 5-10% CSE in these cells. Then, I used 2.5% CSE in

order to determine how cell proliferation is affected in RLMVECs during different time points of CSE. I exposed RLMVECs to CSE (2.5%) for 6, 24, and 72 hrs. There was a statistically significant inhibition of proliferation in all CSE treated cells when compared to air control (AC) extract (Figure 1B). These data indicated that even low CSE concentrations inhibit cell proliferation in RLMVECs, and even helped select CSE concentration and timepoints for our next experiment.

1.1.2. CS exposure causes lung cell apoptosis *in vitro*

To test whether CS causes apoptosis in a relevant *in vitro* model, I exposed human lung endothelial or human lung epithelial cells to increasing CSE concentrations (from 0.1 to 10%) for 6 h. I used commercially available human lung microvascular endothelial cells (HLMVEC) and small airway epithelial cells (SAEC), which are primary cells harvested from human lungs. After CSE exposure, cells were harvested and analyzed for apoptosis. Apoptotic events were quantified by Annexin-V/PI staining, using the Apoptosis detection kit (R&D Systems) and flow cytometry. In HLMVEC, there was increase in apoptosis when exposed to 5% and 10% CSE, which was dose-dependent (Figure 2A). In SAEC, I observed a similar response, albeit more robust and with less variability (Figure 2B). These data may suggest that SAECs are more sensitive to CSE than HLMVEC and both cell types undergo apoptosis in response to increasing CSE concentration.

1.1.3. CS exposure increases lung cell ceramides content *in vitro*

Since ceramide upregulation causes cell apoptosis, I investigated if human alveolar cells in culture upregulate ceramide in response to CS. Both SAEC and HLMVEC were exposed to increasing CSE concentrations, specifically from 0.1 to 10% of CSE for 24 hours. Cells were harvested and analysed for total ceramide content. I found increased ceramides in a dose-dependent manner in both SAECs and HLMVECs following CSE treatment (Figure 3). Interestingly, the ceramide content in HLMVEC was higher than that in epithelial cells both at baseline and following CSE treatment. That might be attributed to a known large pool of acid sphingomyelinase in the endothelium [239]. These data show that CSE leads to the accumulation of ceramides in both lung epithelial and endothelial cells, and the rate and pathway of ceramide accumulation may determine apoptosis outcomes.

1.1.4. CS upregulates enzymes responsible for ceramide synthesis *in vitro*

If CS-induced apoptosis is due to the overproduction of ceramide, I should observe an increase in enzymatic activities responsible for ceramide synthesis after CSE treatment. Since endothelial cells are highly abundant in ASMase, I next determined if their activities are triggered by CS in human primary lung endothelial cells (HLMVEC) exposed to 5% or 10% CSE for 1, 4 and 24 h. There was a trend for lysosomal ASMase activation, by both moderate and high CSE concentrations (Figure 4A), while the secretory ASMase was significantly and robustly activated at 24 h (Figure 4B). In contrast, HLMVEC did not activate nSMase in these conditions (Figure 4C).

CSE of rat lung epithelial cells (L2) triggered activation of both the *de novo* and the sphingomyelinase pathways. In lung epithelial cells, exposure to moderate CSE concentration (5%) elicited significant activation of SPT (Figure 5A) at 4 h, with brief but not significant elevations of CerS5 and CerS2 activities (Figure 4b). By 24 h of exposure, both CerS (Figure 5B and 5C) and lysosomal ASMase (Figure 6A) were actually inhibited by CS. Higher concentration of CSE (10%) also activated SPT even earlier (at 1 h) (Figure 5A), having a positive early (4 h) increase in CerS5 and CerS2 activities (Figure 5B, 5C), without reaching significance. ASMase was also activated by high CSE concentrations in a sustained manner (Figure 6A and B). No change in activity was observed for nSM during these conditions (Figure 6C). These data show that CS activates ceramide enzymatic pathways in both epithelial and endothelial lung cells with different kinetics and amplitudes, having in epithelial cells robust activation of SPT and exhibiting increase of ASMase activity in endothelial cells.

1.2. CS exposure *in vivo* increases lung ceramides
1.2.1. CS exposure increases total lung ceramides and DHC

Chronic CS is associated with alveolar cell apoptosis and causes emphysema in susceptible individuals after decades of exposure. In mouse models, airspace enlargement develops after 4-6 months of CS exposure and apoptosis is detected as early as 1-4 weeks of exposure. To address my hypothesis that ceramide is involved in CS- induced apoptosis, I first measured ceramide following 1 or 4 weeks of CS exposure, in C57Bl/6 mice. Lung tissue

was harvested, ceramide and DHC levels were evaluated by LC-MS/MS and normalized to lipid phosphorus content. I observed increased levels of ceramide in the whole murine lungs at 4 weeks of CS, compared to mice of similar age exposed to ambient air or to those exposed to CS for only 1 week (Figure 7A). Interestingly, DHC, the ceramide precursor in the *de novo* pathway , was also upregulated after 4 weeks of CS (Figure 7B). these data are in concordance to previous studies in our lab, showing increase ceramide levels in DBA2/J mice exposed to CS at 4 weeks [210], and an increase ceramide levels in smokers lungs in humans [32], [102].

1.2.2. CS exposure activates the nSMase *in vivo* in both endothelial and epithelial type I cells

Since cells in culture may behave differently than in situ, I investigated if ceramide synthetic pathways are activated in lung endothelial and epithelial cells type I *in vivo*, I exposed DBA2/J mice to CS for 1 week. Following CS exposure, lungs were immediately harvested, enzymatically disintegrated and sorted for the collection of both endothelial cells and epithelial type I cells using a Miltenyi Biotec system (Figure 8A). I used specific antibodies with iron microbeads and positive selection process. Podoplanin-specific Abs and CD146-specific antibodies were used for isolation of epithelial type I and endothelial cells, respectively. I then determined the activities of lysosomal ASMase, nSMase, and caspase-3 activities in both endothelial cells (Figure 8B, C and D) and epithelial

cells type I (Figure 8E and F). Of all enzymes investigated, I found a significant increase in nSMase in both cell types (Figure 8C and 8E). Only in epithelial type I cells I found a significant increase in caspase-3 activity, which indicates increased apoptosis in these types of cells following in vivo CSE for this short time (Figure 8F).

1.2.3. CS exposure rapidly activates the SMase pathway of Cer synthesis in the whole lung

SMases are known to be highly activated by stress, but their activities may be short-lived. I investigated if; unlike in the chronic model of CS exposure when mice are allowed to recover from CSE before harvest, immediately following CSE, lungs may show activation of sphingomyelinases. DBA2/J mice were exposed to CS for 0.5, 1, 2, and 5 hours (Figure 9A). Lung tissue was harvested immediately following CS and activities of sphingomyelinases were determined. I found a significant increase in the activities of both acid sphingomyelinase isoforms: lysosomal and secreted after 1 hour following CS, with return to baseline after 5 hours (Figure 9B). In a separate experiment, I noted that both ASMase and nSMase are activated as early as 30 min following CSE (Figure 9C). This indicates acute activation of lung sphingomyelinases during CSE. In contrast, the activity of CerS5, which is responsible for the synthesis of ceramide C16: 0, one of the most abundant lung ceramide, showed a trend for decreased activity after 1 hour of CS (Figure 9D).

1.2.4. Chronic CS activates the *de novo* pathway of ceramide synthesis in the whole lung

Given that the upregulation of DHC suggested the activation of *de novo* ceramide synthesis, I measured the activities of enzymes in this pathway. SPT is the first enzyme responsible for the committed step in the *de novo* ceramide synthesis. I determined SPT activities in the whole lung tissue following 1, 2, and 4 months of CS (Figure10). After an initial decrease after 1 month, SPT activity significantly increased later, at 4 months of CS exposure (Figure 10). These data provide evidence of upregulation of the *de novo* pathway following chronic CS exposure in DBA2/J mice.

I next evaluated CerSs in response to CS. There are six CerS, responsible for synthesis of different Cer species. It is not known about the abundance of specific CerS in the lung. Previous work indicated that CerS5 is abundant in lung epithelial cells [32].

In collaboration with Dr. Futerman, our lab studied the relative expression levels of all CerS in the C57Bl/6 lung during CS exposure. They measured CerS expression using real time PCR of mouse lung homogenates. CerS2 and CerS5 were the most abundant CerS in the lung (Figure11). In response to CS, CerS2 mRNA expression was elevated late, after 6 months of CS (Figure11). Interestingly, the mRNA levels of one of the most abundant isoform, CerS5 decreased starting at 1 week of CS, with return towards baseline after 6 months of CS (Figure11). The mRNA levels of both CerS1 and CerS4 showed a steady

decrease with time of CS. The only CerS, that exhibited an early upregulation in the expression of mRNA level, was CerS3, which increased after 1week of CS (Figure 10), but the low abundance of transcripts makes the significance of this increase unclear. In the C57Bl/6 mice, the mRNA levels for CerS2 was preceded by increased activity of CerS2 after 2 months of exposure (Figure12A), while CerS5 activity was upregulated at 2 months of CS (Figure11B), followed by return to (Figure 12A and B) or even below baseline activity in the C57Bl/6 (Figure12C) late in the course of CS.

Interestingly, there were no changes in the enzymatic activity of sphingomyelinases after prolonged CS, compared to control lungs (Figure 13A, B, C). Of note, lungs were harvested 16-24 hours following removal from active CS exposure. This data suggest that the *de novo* pathway is activated by chronic CS (2-4months), in particular SPT and CerS2.

2. Effect of inhibition of enzymes responsible for ceramide synthesis on lung apoptosis following CS

My hypothesis is that ceramide are necessary for CS-induced alveolar cell apoptosis. It has been shown previously that accumulation of ceramides was associated with VEGF blockage model of emphysema development and that direct instillation of ceramides led to extensive apoptosis of lung parenchyma [32]. If my hypothesis is true, downregulation of ceramide production will

decrease apoptosis. That could be achieved by using various inhibitors of enzymes responsible for ceramide synthesis.

2.1. Effect of inhibition of ASMases on CS-induced lung apoptosis

I first tested the effectiveness of amytryptiline (Amy), a known inhibitor of ASMases to prevent the activation of ASMase after acute CS exposure. I compared the effectiveness intra-peritoneal (i. p.) or intra-tracheal (i. t.) administration of Amy on the inhibition of lung ASMase (Figure14A). The i.p. administration of Amy significantly inhibited the activities of both lysosomal and secreted isoforms of ASMase in the lung following 1h CS exposure (Figure 14B and C). I therefore administered Amy i.p. in a chronic model of CS exposure in DBA2/J mice to test if the acute activation of ASMase is important for lung apoptosis after chronic CS exposure. Mice were exposed to CS smoke for four months and one group was injected with Amy for the first 2 consecutive months, as an early intervention (Figure 15A). Another group was injected with Amy for only the last two months of CS exposure, concomitant with CS exposure, as a late intervention (Figure 15A). After 4 months lungs from animals were harvested and alveolar tissue apoptosis was determined by IHC.

There was a significant increase in caspase-3-expressing cells in the lung parenchyma of mice from CS group vs. AC group. There was a significant decrease in active caspase-3-expressing cells in the lungs of mice from early Amy treatment group exposed to CS (Figure 15B), compared to untreated CS-

exposed mice (Figure 15B). These early inhibition of ASMase was not as effective at inhibition apoptosis at 4 months of CS. These data suggest that inhibition of ASMase late in the course of CS inhibits CS-induced apoptosis.

2.2. Effect of inhibition of SPT on lung apoptosis due to CS

SPT is the first enzyme in the *de novo* pathway of ceramide synthesis, and because I observed previously an increase in SPT activity in DBA2/J mice after 2 months of CS I asked if administration of myriocin (Myr), a potent inhibitor of SPT, would decrease CS-induced apoptosis. I exposed DBA2/J mice to either CS or ambient air for 2 months and appropriate groups were concomitantly administered with Myr (Figure 16A). After two months, lung tissue was harvested and analyzed. As expected, Myr downregulated the SPT activity in response to both CS and at baseline (Figure 16B). Treatment with myriocin did not significantly affect ASMase activity at 2 months of CS exposure (data not shown).

However, nSMase was found significantly activated in the myriocin-treated group (Figure 16C), suggesting a compensatory feedback. Myriocin-treated mice had a significant decrease in caspase-3 activity of the whole lung, when compared to untreated CS exposed mice (Figure 16D). However, I could not detect any difference in caspase-3 activity in the whole lung after 2 months between CS and air control groups. (Figure 16D). I therefore evaluated lung parenchyma-only apoptosis, using IHC for active caspase-3. Indeed, there was increase in active caspase-3-expressing lung cells in alveolar tissue of CS-exposed mice (Figure

61

16E). Unexpectedly, Myr treatment actually increased the number of cells expressing active caspase-3 in CS exposed animals (Figure 16E). These data suggest that inhibition of ASMase was more effective at reducing lung parenchyma apoptosis following CS exposure than inhibition of SPT.

3. Role of RTP801 on ceramide-induced lung cell-specific death

3.1. RTP801 is upregulated in the lung ceramide-dependent model of emphysema

I asked if RTP801 is involved in the mechanism of ceramide-induced apoptosis. As a first step in elucidating the crosstalk between RTP801, ceramide, and apoptosis, it was documented by the Petrache lab, that the oxidative stress-responsive RTP801 was upregulated in the lungs during the first 7 days following VEGFR inhibition (Figure 17A). In this model, ceramide is upregulated and causes apoptosis. Interestingly, treatment of mice with the ceramide synthesis inhibitor FB1 inhibited the VEGFR-inhibitor-induced RTP801 protein expression, suggesting ceramide synthesis may be upstream of RTP801 upregulation in this model (Figure 17A). These data, together with previous work on RTP801 as a stress response molecule in the CS model of emphysema [32] indicated a possible interrelation between RTP801 and ceramide expression in the lung. To investigate if induction of RTP801 expression can increase ceramide levels, the Petrache lab in collaboration with Dr. Tuder and Dr. Feinstein, overexpressed RTP801 in the lung.

3.2. Rtp801 is sufficient to trigger lung apoptosis, airspace enlargement, and to increase lung ceramides

I measured outcomes of another experiment, that overexpressed RTP801 cDNA ($50\mu g$) or empty plasmid *via* intra-tracheal instillation [240]. At day 3 following administration, when compared to control mice that received empty plasmid, the lungs of mice instilled with RTP801-expressing plasmid exhibited increased RTP801 protein (Figure 17B), and increased active caspase-3 as measured by IHC (Figure 17C). In RTP801-instilled mice, I measured an increased number of enlarged alveoli (Figure 17D). Interestingly, there was a marked increase in lung ceramides in response to RTP801 instillation, which was prevented by pretreatment with the ceramide synthase inhibitor FB1 (Figure 1E). These results suggested that VEGFR inhibition can increase RTP801 in a ceramide-dependent manner while, conversely, upregulated RTP801 suffices to trigger ceramide synthesis.

3.3. Direct augmentation of ceramides in the lung increases endogenous ceramides and causes apoptosis, airspace enlargement, and RTP801 upregulation

It was previously demonstrated that a single intra-tracheal instillation of ceramides with a 12-carbon fatty acid side chain (C12:0; 1 mg/kg) administered with perfluorocarbon vehicle [32], caused overproduction of endogenous ceramides and lung cell apoptosis at 24h and 48h associated with an increase in

alveolar size [32, 201]. To further characterize the lung changes induced by ceramide, I instilled mice intra-tracheally with ceramide (C12:0; 1 mg/kg) or a with control vehicle (sham) and compared them with untreated mice. To distinguish exogenous from endogenous ceramides, I used tandem mass spectrometry to identify and measure only endogenous sphingolipids with longer than 14-carbon fatty acid chain. Since ceramide is the precursor of sphingosine-1 phosphate, an important pro-survival sphingolipid, in collaboration with Dr. Berdyshev, I measured the ratio of ceramide to sphingosine-1 phosphate in the lungs following C12:0 ceramide instillation, as a better reflection of a pro-apoptotic sphingolipid imbalance. The endogenous lung ceramide/S1P ratio increased at 4 h and was highest at 24 h after ceramide instillation, followed by a return to sham levels at 48 h (Figure 18A). Ceramide induced activation of executioner caspases-3/7 after 4 h, which persisted for 48 h following instillation (Figure 18B and C). As expected, ceramide instillation decreased alveolar surface area/lung volume, which became significant at 48 h (Figure 18D). To determine if ceramide increases are sufficient to elevate RTP801 expression in the lung, I next administered *via* a similar protocol of intra-tracheal instillation as C12:0 ceramide a more common endogenous ceramides, C16:0 ceramide, using this time polyethylene glycol conjugation to achieve improved solubilization of this more hydrophobic molecule. Compared to sham-instilled mice, the lungs of mice in which C16:0 was augmented had a 2-fold increase in RTP801 expression in the lung parenchyma (Figure 18E and F). These results suggest a mutual interaction of ceramide and RTP801 induction in the lung.

3.4. Rtp801-null mice are protected from ceramide-induced epithelial cell apoptosis and emphysema-like disease

I next asked if RTP801 induction was necessary for the pathogenic effects of ceramide in the lung. I instilled ceramide C16:0 intra-tracheally in the lungs of Rtp801-null mice, which were previously characterized in detail [231]. Compared to wild type mice, RTP801-deficient mice had significantly less caspase-3/7 activity in whole lung tissue homogenates following ceramide augmentation (Figure 19A). Because of differential susceptibility of distinct lung alveolar cells types to ceramide *in vivo* is not known, I evaluated caspase-3/7 activation in specific alveolar structural cell types isolated from the lung at 48 h following ceramide instillation. I enzymatically disintegrated lungs and investigated the vulnerability to apoptosis of lung endothelial, epithelial type I, and epithelial type II cells in both Rtp801 KO and WT mice. Alveolar cell-type markers (CD31, podoplanin, and prosurfactant-C, respectively) and active caspase-3 were detected using labeling with specific antibodies followed by flow cytometry. Ceramide instillation significantly increased apoptosis in both lung endothelial and epithelial type II cells in wild type mice (Figure 19B). Interestingly, in Rtp801-null mice only type II pneumocytes were protected against ceramide-induced apoptosis (Figure 19B). Given that RTP801 is largely upregulated in type II cells (but not in endothelial cells) after exposure to cigarette smoke *in vivo* [231], these findings concordantly demonstrate that RTP801 is necessary for ceramide to activate caspase-3 in alveolar type II epithelial cells.

To determine if other features of emphysema-like disease induced by ceramide are impacted by RTP801, we measured lung inflammation by counting inflammatory cells in the bronchoalveolar lavage fluid of mice. There was a relative increase in the polymorphonuclear (PMN) cells following ceramide instillation in wild type mice, which was significantly reduced in the *rtp*801-null mice (Figure 19C). As expected, alveolar macrophages exhibited reciprocal changes (Figure 19D).

To measure the effect of ceramide 16:0 and the role of RTP801 on lung parenchyma morphology and function, following lung function testing, the left lung was inflated under constant pressure and airspace size was determined by morphometry. Compared to wild type mice, where ceramide augmentation increased airspace size measured by mean linear intercepts (MLI) from 37.1 to 39.1 μm (p=0.02), in *rtp*801-null mice ceramide had a negligible effect on changes in MLI from 36.5 to 37.8 μm (p=0.3), suggesting that the lack of RTP801 was protective against ceramide-induced apoptosis (Figure 20A and B). Similarly, wild type mice exhibited significant increases in the lung static compliance (p=0.01) in response to ceramide instillation, whereas *rtp*801-null mice did not (Figure 20C). Interestingly, ceramide instillation also elevated the airflow resistance in mice and this, similar to the increase of airspace size was more pronounced in wild type than in *rtp*801-null mice (Figure 20D). These data show that ceramide induces a COPD-like physiological phenotype, which is ameliorated by absence of RTP801.

66

E.DISCUSSION

1. Cigarette smoke (CS) exposure increases ceramides both *in vitro* and *in vivo*, which leads to lung cell apoptosis

1.1. Lung epithelial and endothelial cells increase ceramide levels in response to CSE, which leads to a programmed cell death

1.1.1. CS exposure inhibits cell proliferation *in vitro*

I showed inhibition of proliferation in RLMVEC when exposed to even low CSE concentration. This response allowed me to select CSE concentration parameters for subsequent studies. It is not known, how CSE inhibits cell proliferation. Excess of cellular ceramides has known pro-apoptotic effect, but basal levels of ceramides are necessary for cell viability, because ceramides serve as intermediaries for synthesis of other sphingolipids, including those with pro-survival and pro-proliferative role, like S1P. It is possible that the reduction in cell proliferation in CS exposed cells is due to either increase of DHC, increase ceramide to S1P ratio, or molecular changes unrelated to ceramide.

1.1.2. Lung alveolar cells exhibit an increase in apoptosis in response to CS

Both human lung endothelial and epithelial cells exhibited increased apoptosis in response to CSE, in a dose dependent manner. SAEC had a more consistent apoptotic response than HLMVEC when exposed to similar

concentrations of CS. There was no measurable necrosis in response to CSE as measured by Annexin/Pi. This is, to my knowledge, the first comparison between the apoptotic responses of these two cell types, which suggests, that HLMVECs have more robust survival response to CS than SAEC.

1.1.3. CS generates ceramides *in vitro*

CSE levels that caused apoptosis were associated with increased ceramide levels in both epithelial and endothelial cells, in a dose dependent manner. Interestingly, the highest increase of ceramides was observed in HLMVEC, cells which also had the highest baseline ceramide levels. This may be attributed to acid sphingomyelinase levels, which are the highest in endothelial cells. Interestingly, the decrease in the level of ceramides in HLMVEC at 10% CSE concentration when compared to 5% might be attributed to complete blockage of the *de novo* ceramide synthesis *via* DEGS inhibition or to complete utilization of available stores of membrane sphingomyelin *via* activated sphingomyelinases. The fact that HLMVEC had the highest ceramide content, but were more apt for survival than SAEC suggests that either pro-survival S1P is equally robustly increased, or that it is not the total content, but rather the rate of increase and the manner of increase in specific ceramides that induce apoptosis.

1.1.4. CS activates enzymes involved in the synthesis of ceramides

The upregulation of the *de novo* and sphingomyelinase pathways by CS was cell type-, time-, and concentration-specific. Both ASMase and nSMase were briskly activated, whereas SPT and CerS were early on inhibited or unaffected, followed by late activation. Epithelial cells relied more on nSMase, whereas endothelial cells upregulated ASMase more robustly.

1.2. CS upregulates ceramides *in vivo*

1.2.1. Total lung Cer and DHC are increased following chronic CS exposure

Chronic CS exposure upregulated ceramides along with DHC, indicating upregulation of at least the *de novo* pathway. Fact that the magnitude of DHC increase was higher than ceramide increase indicated a partial inhibition of DEGS, possibly *via* oxidative stress. Alternatively, ceramide might be quickly utilized for the synthesis of other metabolites.

1.2.2. Acute CS exposure activates the sphingomyelinase pathway in the whole lungs

Both isoforms of ASMase were found to be upregulated after 1h following CS exposure. This data are in agreement with previous reports of quick sphingomyelinase activation by stress, including oxidative stress [125]. The decrease in CerS5 activity after 1 h of CS exposure may indicate an early

inhibition of the *de novo* pathway, but whether this acute downregulation is due to inhibition by DHC or other regulatory processes remains to be determined.

1.2.3. Chronic CS exposure activates the *de novo* pathway of ceramide synthesis in the whole lung

The activity of SPT, the first enzyme from the *de novo* pathway was found to be upregulated after 4 months of CS exposure after initial inhibition at 4 weeks of CS exposure. These findings correlate well with the occurrence of lung cell apoptosis as detected in lung IHC after 4 months of chronic CS. CerS are enzymes, which are responsible for the synthesis of various dihydroceramides, depending on utilization of specific acyl chains. CerS (LASS) exist in 6 isoforms, having specific organ distribution and activity. Interestingly, the expression of mRNA level of given CerS does not correspond always with their activity level. Of all CerS isoforms, only the mRNA level for CerS2 correlated with its activity which was the highest at 6 months of CS exposure. The downregulation of CerS mRNA expression early in the CS course may suggest involvement of specific transcriptional regulatory mechanisms to prevent overproduction of ceramides or DHC in the lungs. My data imply that the *de novo* pathway is activated by prolonged CS exposure, in particular with SPT and CerS2 involvement, with no significant coactivation of SMase pathway. However, the timing of harvest of lung tissue (16-24 hours) following removal from CS doesn't exclude a brisk participation of sphingomyelinases (minutes) in the generation of ceramides even this late in the course of CS exposure.

2. Effect of enzyme inhibition on lung apoptosis following CS

2.1. Inhibition of SPT with Myr does not inhibit lung parenchyma apoptosis due to CS

I noted discordant results between total lung caspase enzymatic activity and apoptotic caspase composition by IHC in lungs treated with the SPT inhibitor, Myr. This may be explained by the contribution of other lung cells to caspase-3 activity. In contrast, IHC only focuses on the lung parenchyma. Only on lung parenchyma I detected increases in apoptosis in response to CSE. Myr did not decrease it; in contrast it increases apoptosis in response to CS. This may suggest that compensatory production of ceramides *via* neutral sphingomyelinases in face of blocked *de novo* pathway has contributed to apoptosis of alveolar cells.

2. 2. Inhibition of ASMase with Amy inhibited lung parenchyma apoptosis due to CS

Amytryptiline is an inhibitor of ASMase accelerating its lysosomal degradation. Both ASMase isoforms activated early by CS exposure were effectively inhibited by Amy. The i. p. administration of Amy was more effective at inhibition of lung ASMase than i. t. administration. Using IHC methodology, we demonstrated significant increase in caspase-3 activity following chronic CS. The i. p. administration of ASMase inhibitor decreased active caspase-3, induced by chronic CSE. Collectively, this data indicate that ceramides produced by ASMase

during chronic CS are pro-apoptotic. Although ceramides are produced by both *de novo* and sphingomyelinase pathways, ceramide provided by ASMase, even when only briefly activated have a role in triggering caspase-3 activation in alveolar parenchyma.

3. RTP801 is required for ceramide-induced cell-specific death in the murine lung

I used *in vivo* gain of ceramide function approaches, which are characterized by alveolar cell apoptosis and oxidative-stress dependent airspace enlargement. I have shown that ceramide augmentation induces apoptosis of both lung endothelial cells and type II epithelial cells and is associated with alveolar wall apoptosis and enlargement of airspaces accompanied by an increase in static compliance, suggesting an emphysema phenotype. The airspace enlargement was inhibited in mice lacking RTP801, which showed lack of apoptosis of epithelial type II cells in response to ceramide. These results causally implicate RTP801 as an upstream sensor of lung cellular stresses in lung epithelial cells. Although alveolar destruction also involves capillary endothelial cells, our data positions type II cells as key in the amplification of the alveolar destruction mediated by the interaction of ceramide and RTP801. Interestingly, type I cells not only were not protected from apoptosis in the RTP801 null mouse, but they exhibited heightened caspase-3 activation in response to ceramides. This may suggest a possible crosstalk between stress-

protected alveolar type II cells, which are considered precursors of type I cells, and the type I cells, which are bona-fide structural components of the alveolo-capillary membrane. It is possible that rescued type II cells may replace apoptosing type I cells at a rate sufficient to preserve airspace size, and/or that RTP801 has opposing roles in the two cell types, being pro-apoptotic in type II cells, but anti-apoptotic in type I cells.

A common denominator linking ceramide and RTP801 upregulation could be oxidative stress, a known inducer of both molecules, which is also generated downstream of both ceramide and RTP801 upregulation [32, 201, 231, 240]. Oxidative stress caused directly by CS or endogenous sources, such as inflammatory and parenchymal cells, plays a central unifying roles in all stages of emphysema. Reduction in anti-oxidant defenses in NRF-2 knockout mice leads to increased susceptibility to emphysema, which is characterized by heightened alveolar cell death [241]. Oxidative stress is most likely sensed by a susceptible host as a cellular stress in the setting of exposure to CS. RTP801, a negative regulator of mTOR signaling, is therefore activated as part of a prototypic response to adverse cell stress responses. However, its activation promotes cellular injuries triggered by CS, including further oxidative stress, cell death, and alveolar inflammation. Excessive ROS could also have been responsible for RTP801 increases in response to VEGFR inhibition [234]. In addition, we have shown that ceramide-induced airspace enlargement is dependent on oxidative stress [201], which may have also upregulated RTP801 in response to intra-tracheal ceramide administration.

Ceramide is a prototypic lipid-signaling molecule, which we have shown to amplify lung injury due to CS [32, 77, 201, 220, 242]. Prior studies have also highlighted that ceramide not only amplifies, but its synthesis is triggered by oxidative stress [201]. I present novel evidence that RTP801 is not only sufficient but also necessary to mediate increases in lung ceramide *via* the *de novo* pathway of ceramide synthesis. These data position RTP801 in type II cells as upstream of ceramide synthesis *in vivo*, in settings that reproduce features of CS-induced alveolar injury. Of note, increases of lung expression of either RTP801 or ceramide levels suffice to lead to alveolar enlargement and alveolar cell death. Whether ceramide mediates all or part of RTP801 dependent pathogenesis due to CS will await further experimentation in mice deficient of ceramide synthetic enzymes.

The significance of increased airflow resistance in response to ceramide upregulation and its attenuation in the RTP801 null animals is yet to be clarified. This airway response was associated with increased RTP801 expression in the larger airways as well as airway inflammation, as suggested by elevated levels of inflammatory cells (PMN) in the bronchoalveolar lavage fluid of wild type animals, which was largely RTP801-dependent. The mechanism by which RTP801 triggers this large airway inflammation is not known.

The data that VEGF receptor inhibitor also triggers RTP801 expression further expands the concept of RTP801 as a stress sensor, in that alterations in alveolar maintenance, such as those caused by interruption of VEGF survival signals, may be also interpreted as part of a lung cellular stress response. CS

has been shown to decrease VEGF signaling in the alveolar lung tissue and VEGFR blockade is sufficient to upregulate ceramides, induce oxidative stress, and trigger alveolar cell apoptosis, events that precede the onset of airspace enlargement [30, 32, 234, 243]. Furthermore, as increases in lung ceramide activate RTP801 expression; endogenous lung stress responses may perpetuate this pathogenic loop. It will be important to elucidate whether lung injury is more severe when these responses become repetitive, possibly exhausting repair mechanisms.

In conclusion, my results highlight the concept of self-amplifying injury in response to CS exposure, the role of ASMase activation in lung cell apoptosis, the importance of alveolar type II cell apoptosis in this process, and the cell-specific apoptotic signaling of ceramide *in vivo*. Early interruption of such self-perpetuating stress responses may prevent emphysema development, or may allow proper repair mechanisms to prevail.

F.FUTURE STUDIES

I demonstrated *in vitro* and *in vivo* studies that ceramides play an important role in the development of lung cell apoptosis in response to CS. There are still many unanswered questions. Lungs consist of more than 50 different cell types and there are multiple complex interactions between them, including various type of signaling. Both epithelial and endothelial cells from alveolar units are the first line of cells responsible for apoptotic changes due to harmful insults, including CS exposure. *In vitro* studies, although well conducted, can delineate only some aspects of pathophysiologic changes due to exogenous insults, including CS exposure. *In vivo*, when embedded in a complex microenvironment, particular cells responses to noxious stimuli may differ to those observed *in vitro*. This is specifically important when studying ceramide synthesis due to CS exposure. Particular cells may differ in the way they synthesize ceramides. Even the same cells can activate different biosynthetic pathways depending on stimulus. For example, endothelial cells may produce ceramides acutely *via* acid spingomyelinase activity due to CS exposure or TNF-α, which can eventually activate the *de novo* pathway. Thus, further studies on particular cell lines *in vivo*, using sorted cells following rapid lung disintegration may be needed for precise cell-specific kinetics of ceramide activation and apoptosis.

Other studies should be directed for biochemical compounds for targeted inhibition of pathways for ceramide synthesis. Pharmacological inhibition of the enzymes involved in the synthesis of ceramides could have off target effects.

Furthermore, since ceramides are important intermediaries for more complex

sphingolipids, including those responsible for activating pro-survival pathways,

the inhibition of ceramide synthetic patways may lead to scarcity of ceramides in

certain cells, and paradoxically, to enchanced apoptosis. For this reason

research should be directed to specifically inhibit the synthesis of ceramides only

in these cells which are extremaly sensitive to ceramides.

Schematic 1

Sphingolipids metabolism and interconnection of bioactive sphingolipids
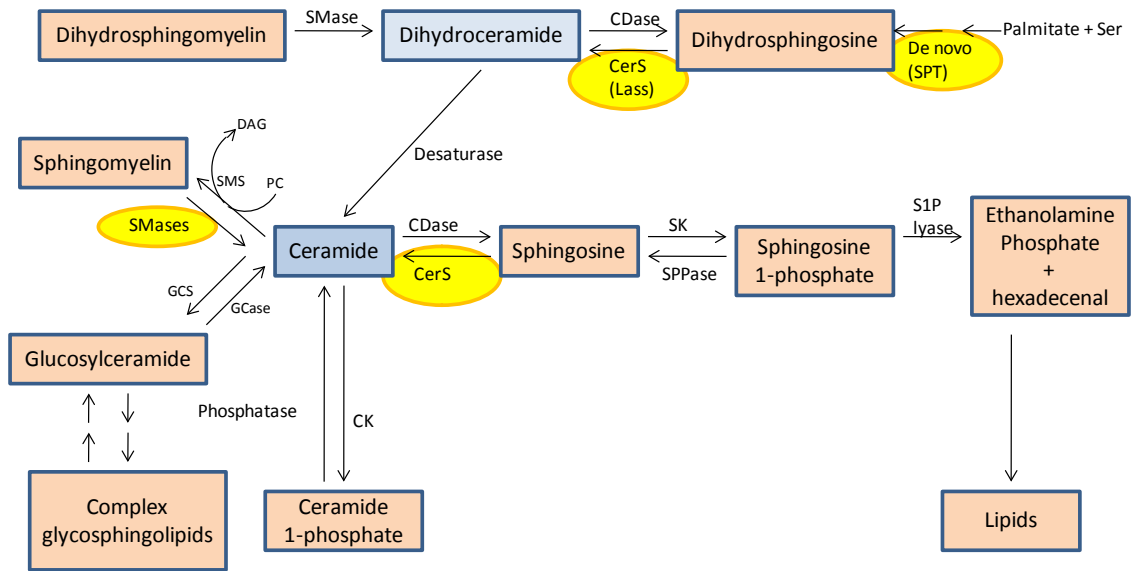
From: Yusuf at al. Principles of bioactive lipid signalling
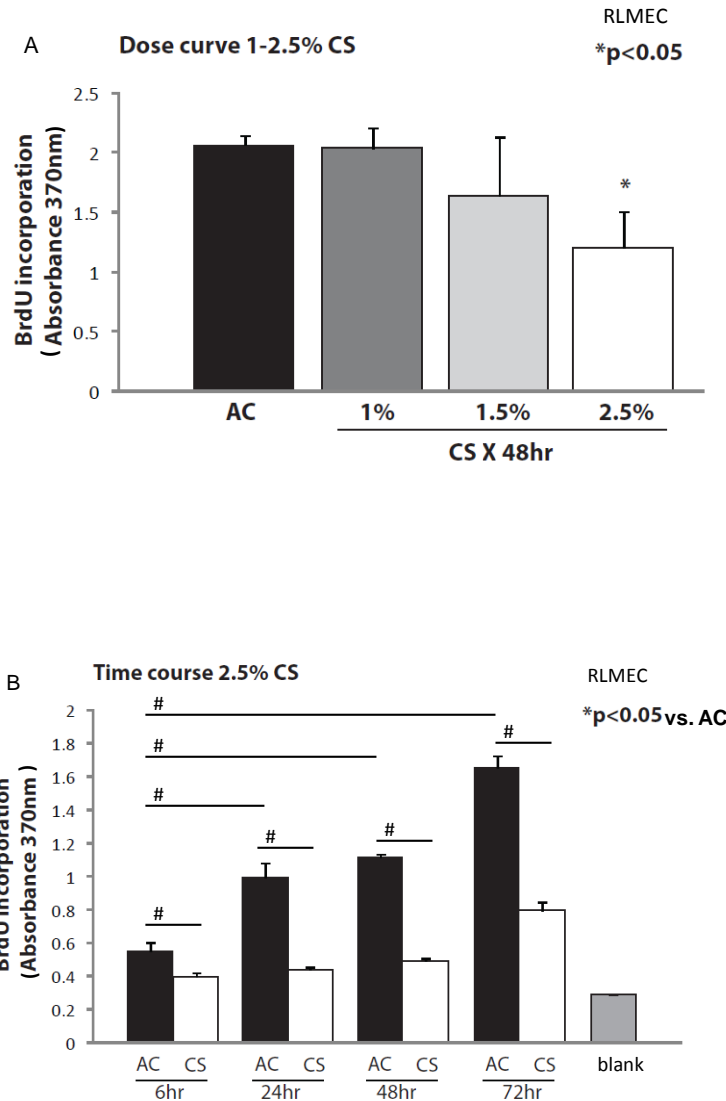
Figure 1. Proliferation assay performed on rat lung endothelial cells following CS exposure. That assay was determined with BrdU incorporation using ELISA. (A) Proliferation of cells exposed for 48h to the indicated concentrations of CSE. Mean +SEM; * p,0.05; n=3. (B) Proliferation of cells exposed to CS (2.5% CSE) for the indicated time. Mean +SEM; #: p<0.01; n=3. AC - air control; CS - cigarette smoke.
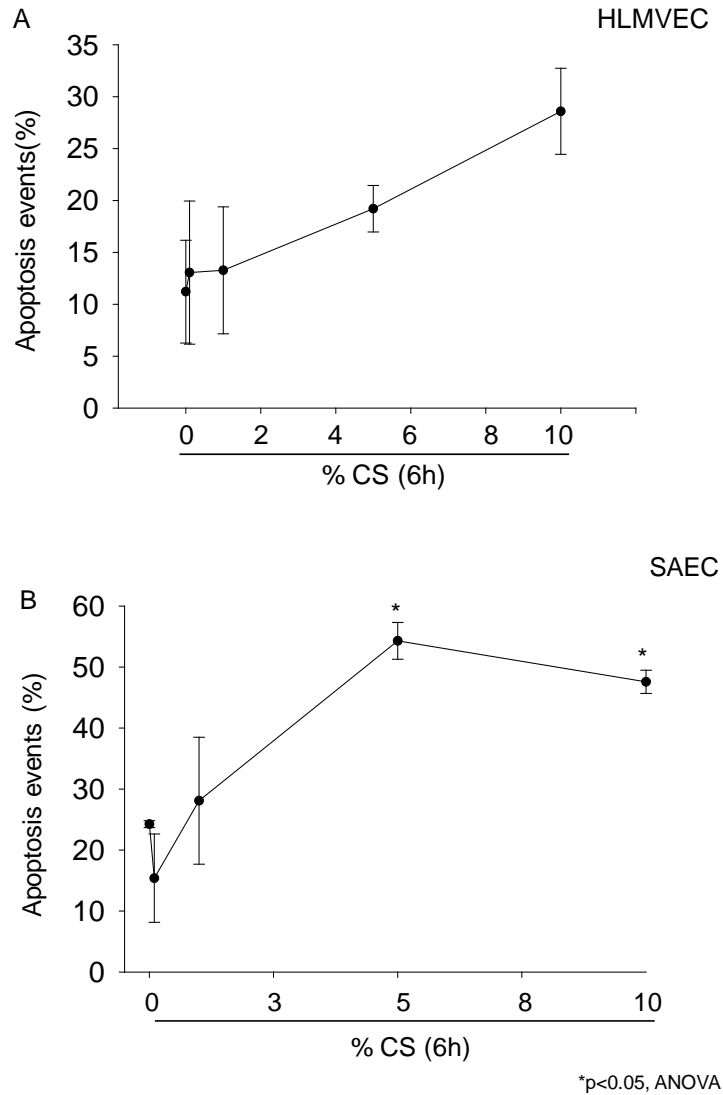
Figure 2. Evaluation of apoptosis events in lung alveolar cells following different

CS exposure. Apoptotic events were quantified by Annexin-V/PI staining and flow

cytometry. (A) Apoptosis measured in small airway epithelial cells (SAEC)

following CS exposure (0.1 to 10% CSE) for 6 h. Mean+ SEM; *: p<0.05,

ANOVA; n=2-3/group. (B) Apoptosis measured in human lung microvascular

epithelial cells (HLMVEC) following CS exposure (0.1 to 10% CSE) for 6 h.

Mean+ SEM; ANOVA; n=2/ each concentration.
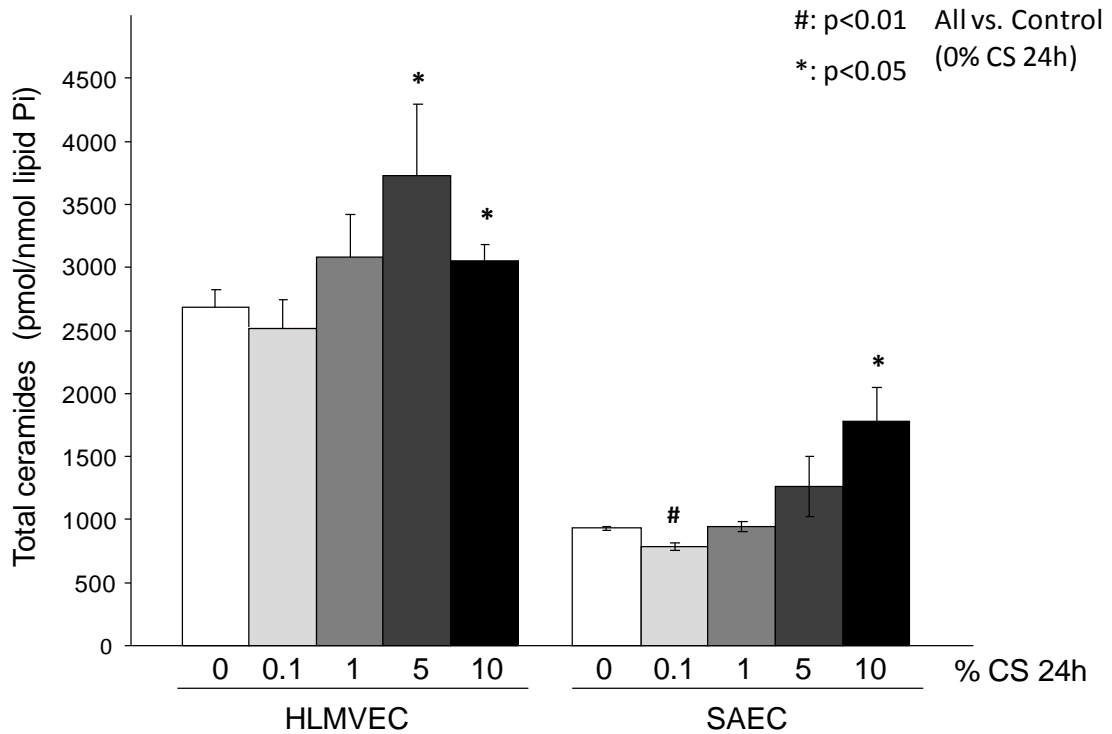
Figure 3. Ceramide content of lung cells following CS exposure. Total ceramides

levels in lung microvascular endothelial cells (HLMVEC) or small airway epithelial

cells (SAEC) exposed to CS (0.1, 1, 5, 10%) for 24 h. Mean+ SEM; *p<0.05;

n=3/HLMVEC and 5/SAEC/group.

A. HLMVEC — Lysosomal ASMase activity (mU/min/ug); CON, 5% CS (1h, 4h, 24h), 10% CS (1h, 4h, 24h)

B. HLMVEC — Secreted ASMase activity (mU/min/ug); CON, 5% CS (1h, 4h, 24h), 10% CS (1h, 4h, 24h)
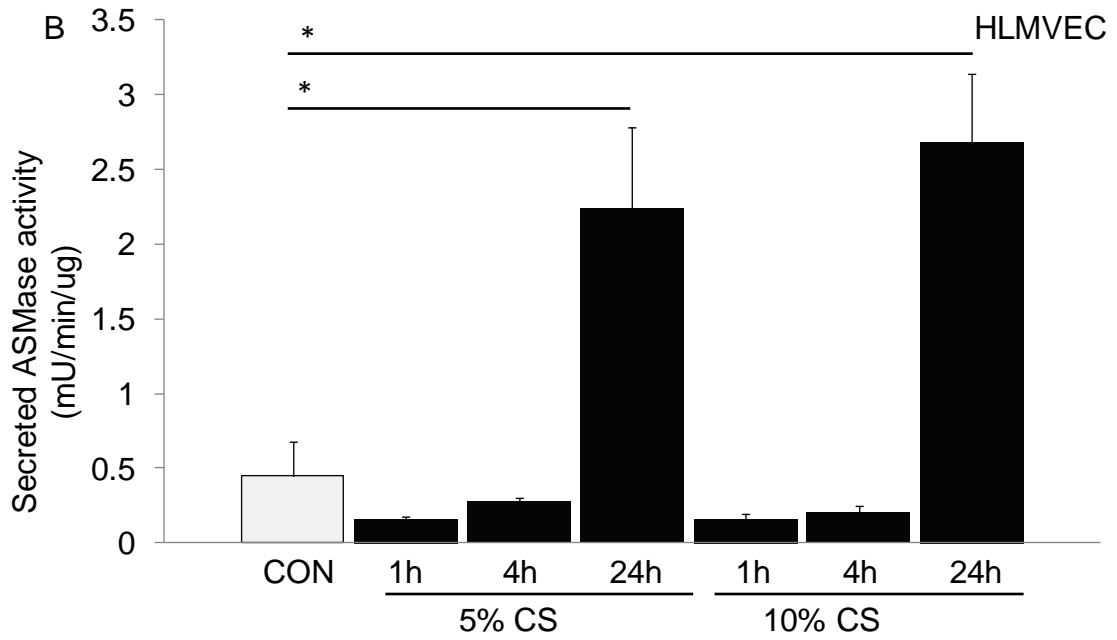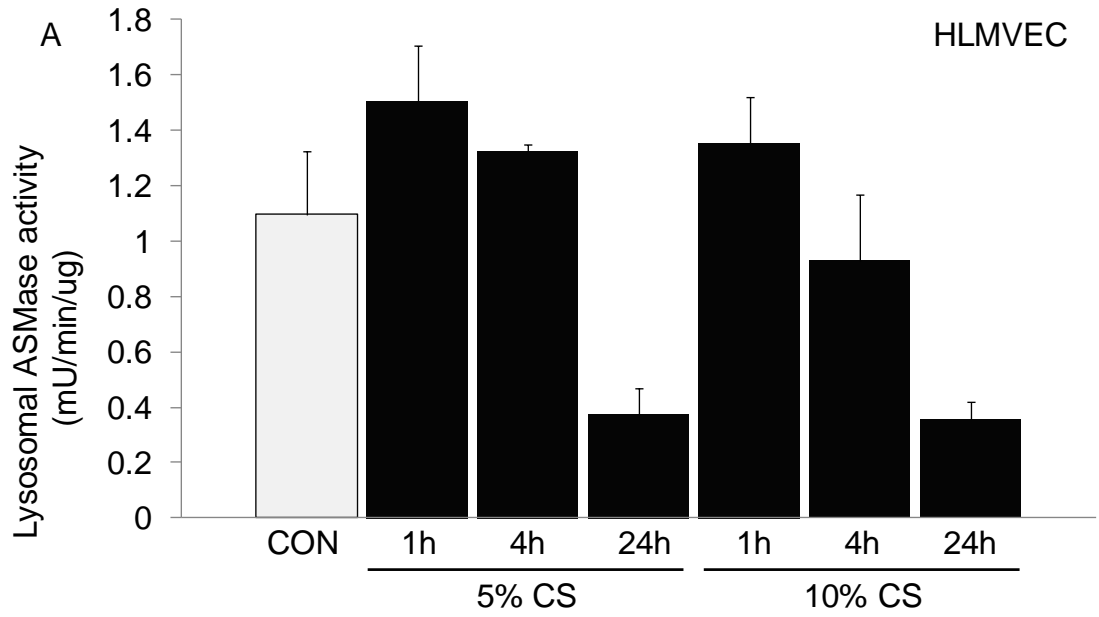
*p<0.05, ANOVA
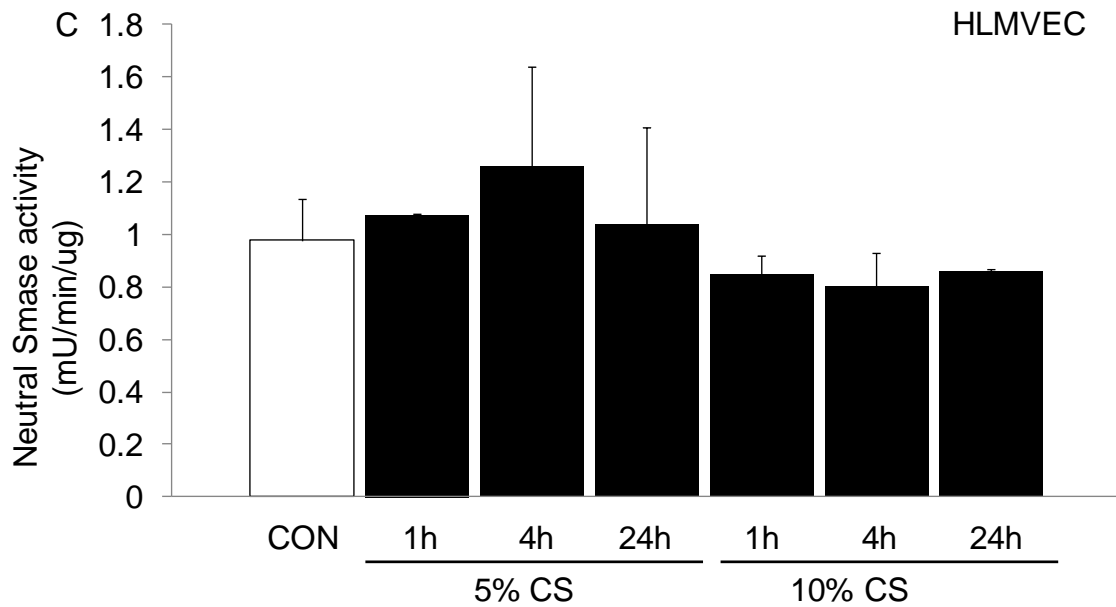
Figure 4. Effect of CS exposure on the activity on the sphingomyelinase pathway in cultured human lung endothelial cells. Cultured cells were exposed to CS (5 or 10%) for the indicated time. (A) The lysosomal ASMase activity, (B) secreted ASMase activity, and (C) neutral SMase activity, were expressed as activity rates normalized by protein concentration. Mean+ SEM; n=2-3/group.

A — Lung epithelial cells. SPT activity (AU/µg) for CON, 5% CS (1h, 4h), and 10% CS (1h, 4h).

B — Lung epithelial cells. Ceramide synthase 5 activity (AU/µg) for CON, 5% CS (1h, 4h, 24h), 10% CS (1h, 4h, 24h), and neg.
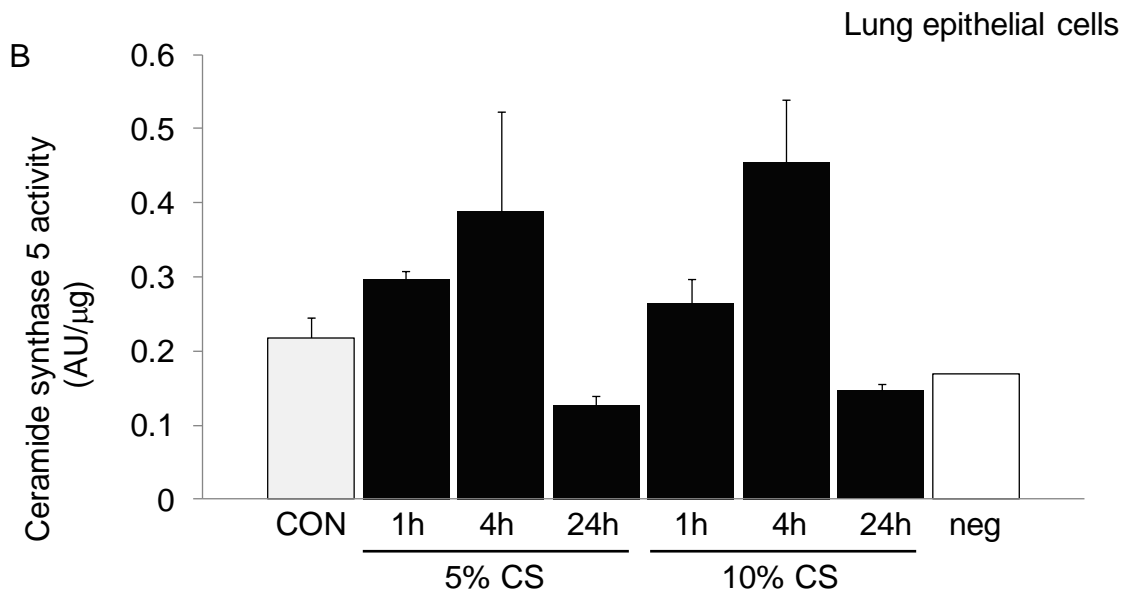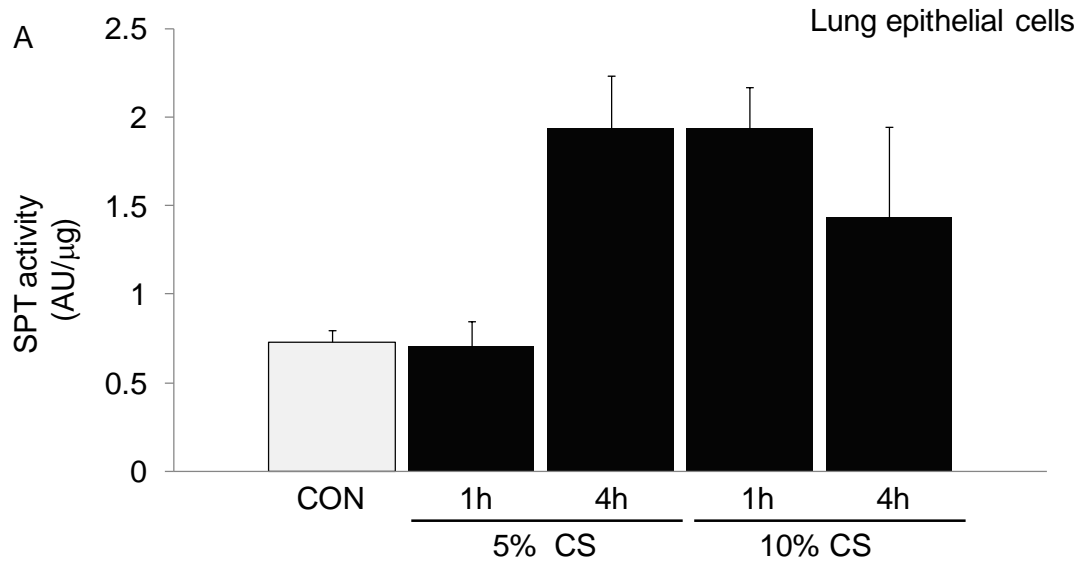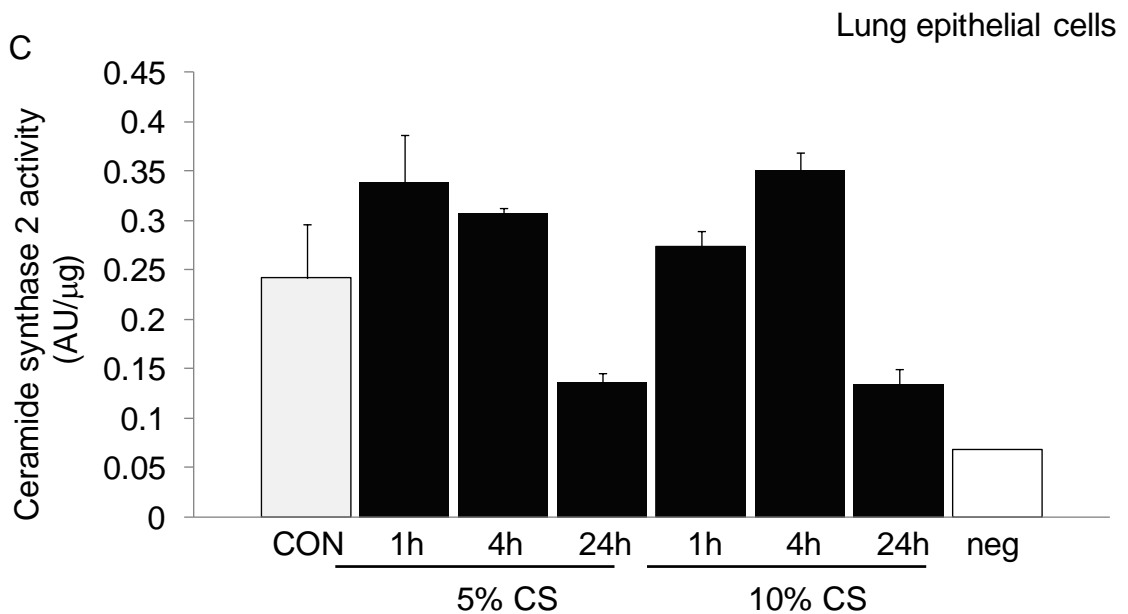
Figure 5. Effect of CS exposure on the enzymatic activities in the *de novo* ceramide synthesis pathway in rat lung epithelial cells. Cultured cells were exposed for the indicated time to CS (5 and 10% CSE). (A) SPT activity was expressed as arbitrary units (AU) derived from the number of scintillation counts per minute, normalized by the protein concentration of the sample. Mean+ SEM; n=2-3/group. (B) Ceramide synthase-5 activity was expressed as AU derived from densitometric density of TLC bands, normalized by the protein concentration. Mean+ SEM; n=2-3/group. (C) Ceramide synthase-2 activity was expressed as AU derived from densitometric density of TLC bands, normalized by the protein concentration. Mean+ SEM; n=2-3/group.
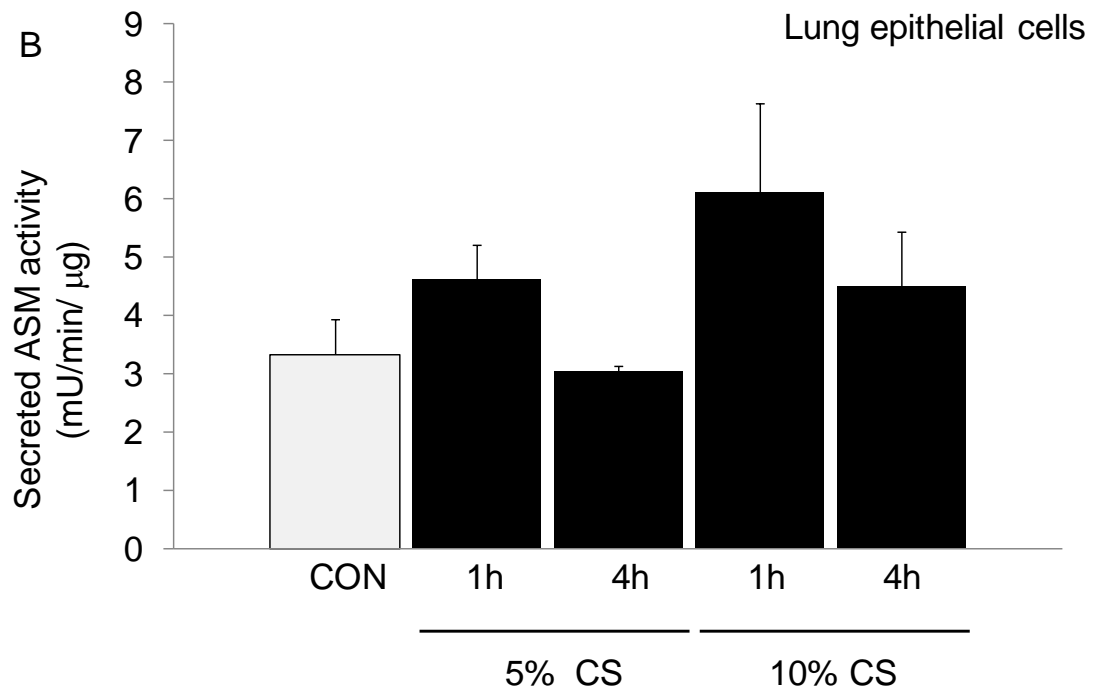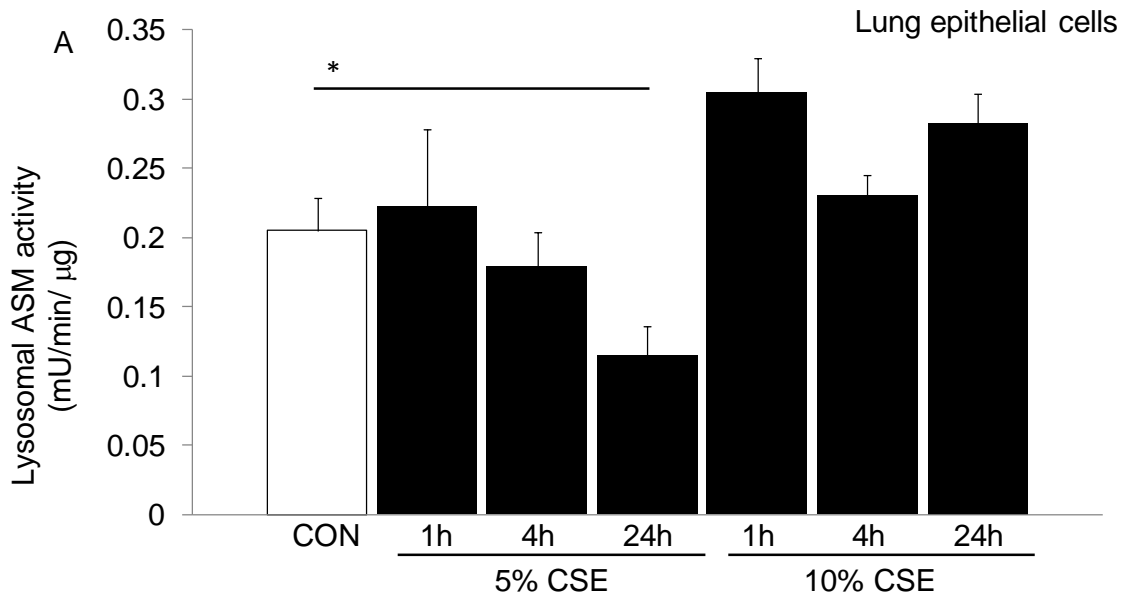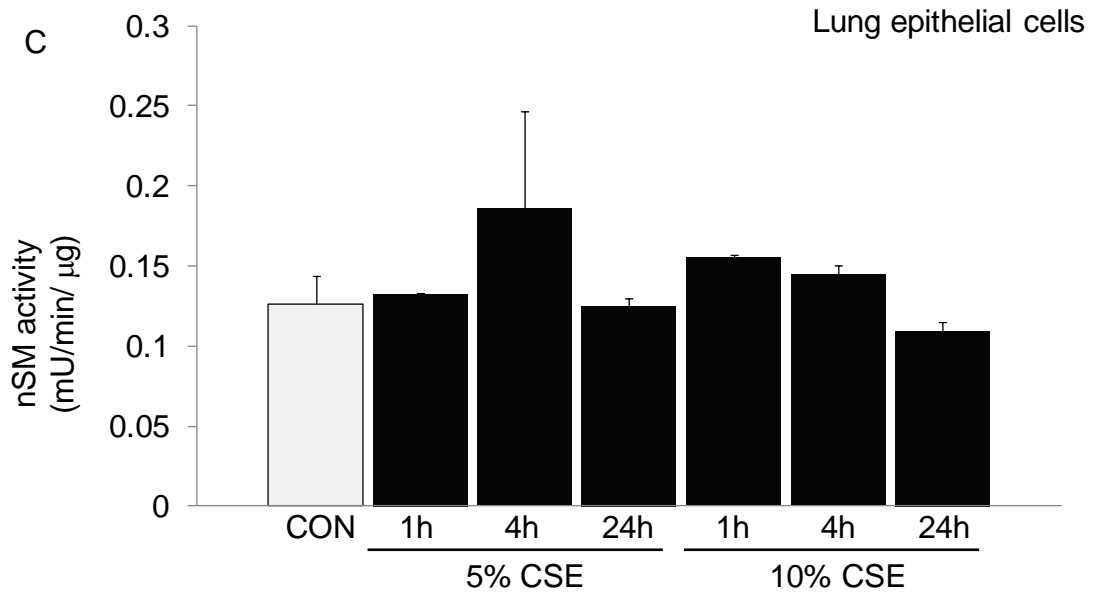
Figure 6. Effect of CS exposure on the activity of enzymes in the sphingomyelinase pathway in rat lung epithelial cells. A-C: Cultured rat lung epithelial cells (L2) were exposed for the indicated time to CS (5 and 10% CSE). (A) Lysosomal ASMase activity; (B) secreted ASMase activity; and (C) neutral SM activity were each normalized to protein concentration. Mean+ SEM; n=2-3/group. *: $p < 0.05$, ANOVA.
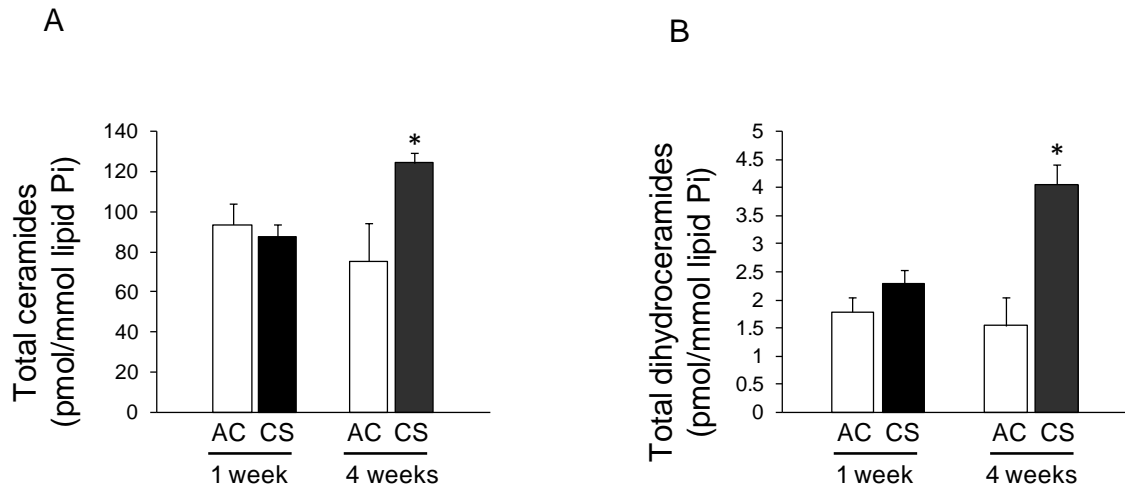
Figure 7. CS exposure increases production of ceramides *in vivo*. Lung

ceramide levels in response to CS exposure for 4 weeks in C57Bl/6 mice. Left

panel: total ceramide level adjusted to lipid phosphorus concentration. Mean+

SEM; p<0.05 vs. control AC; n=5/group. Right panel: total dihydroceramide level

adjusted to lipid phosphorus concentration. Mean+ SEM; p<0.05 vs. control AC;

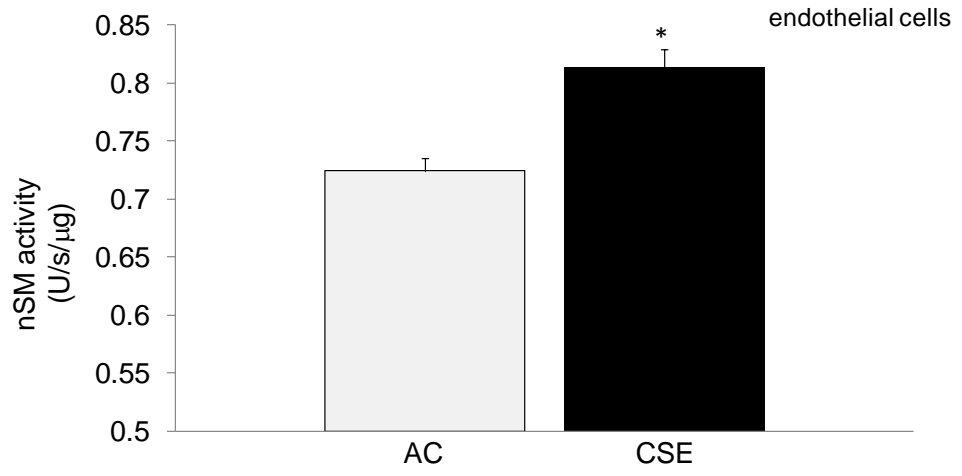n=5/group. Ceramide content was evaluated by Walter Hubbard, JHU.

A

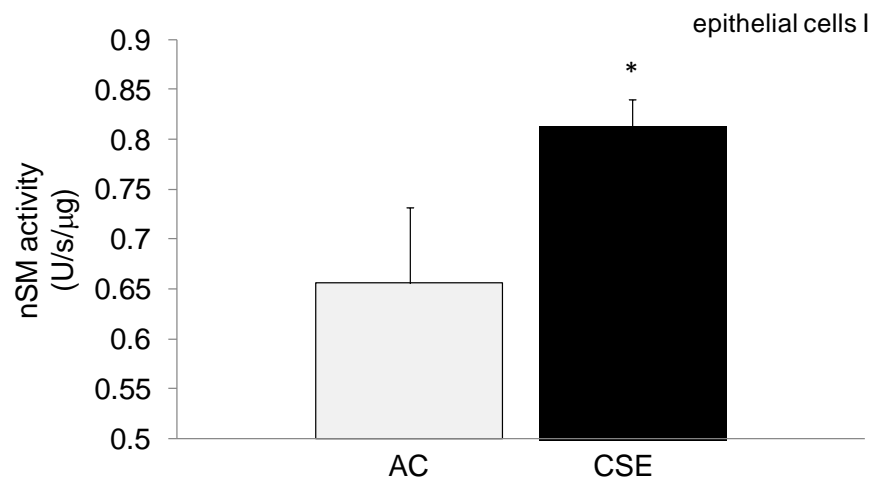Isolation of epithelial type I and endothelial cell from whole lung

B

C

D

E

epithelial cells I
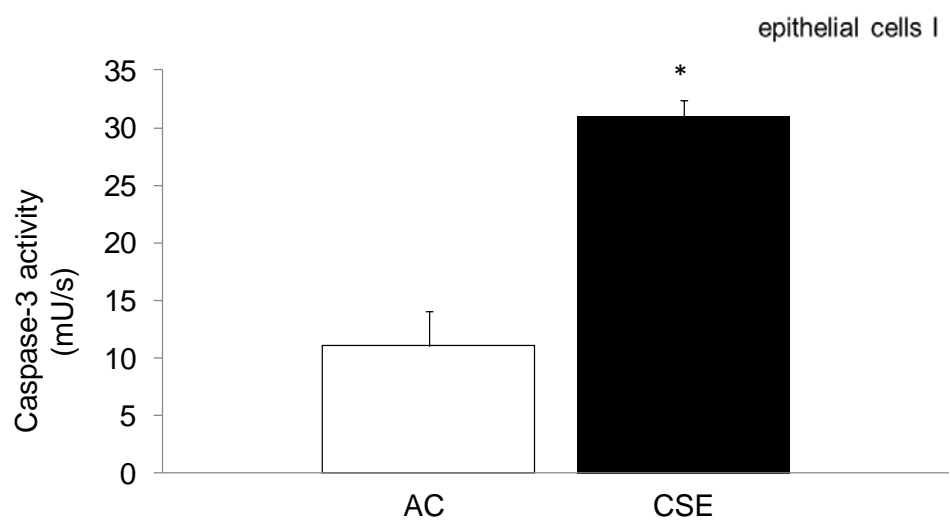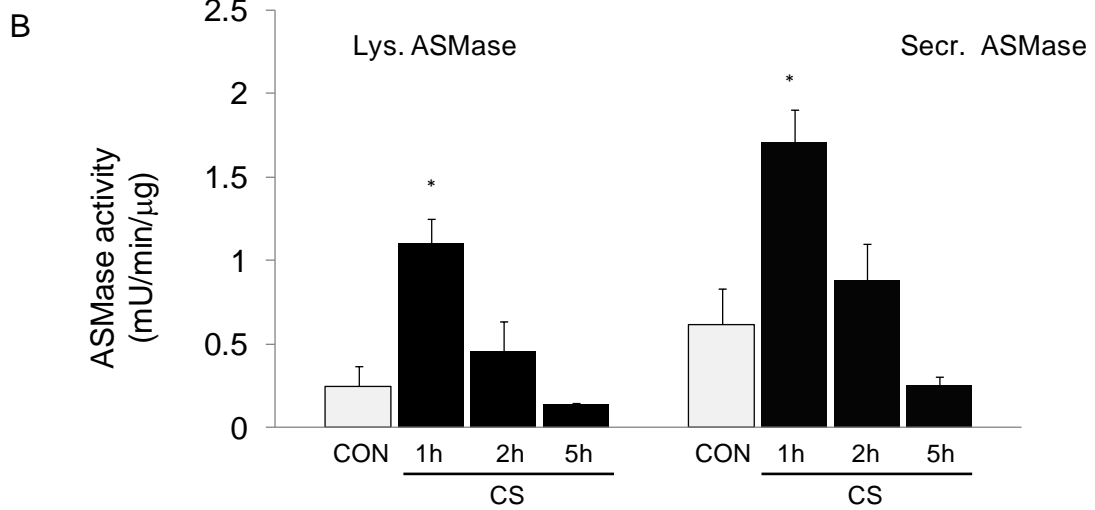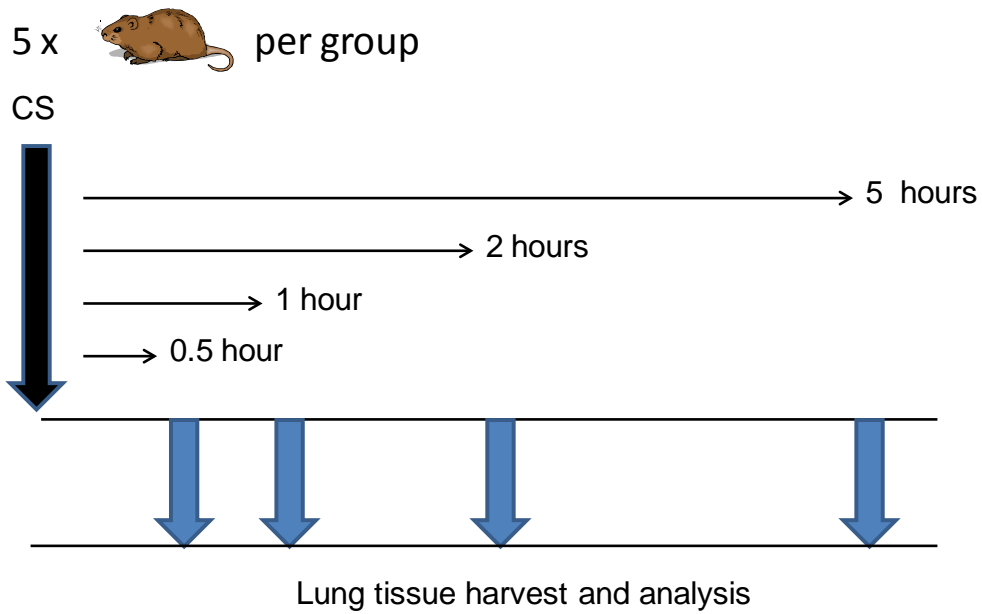
F
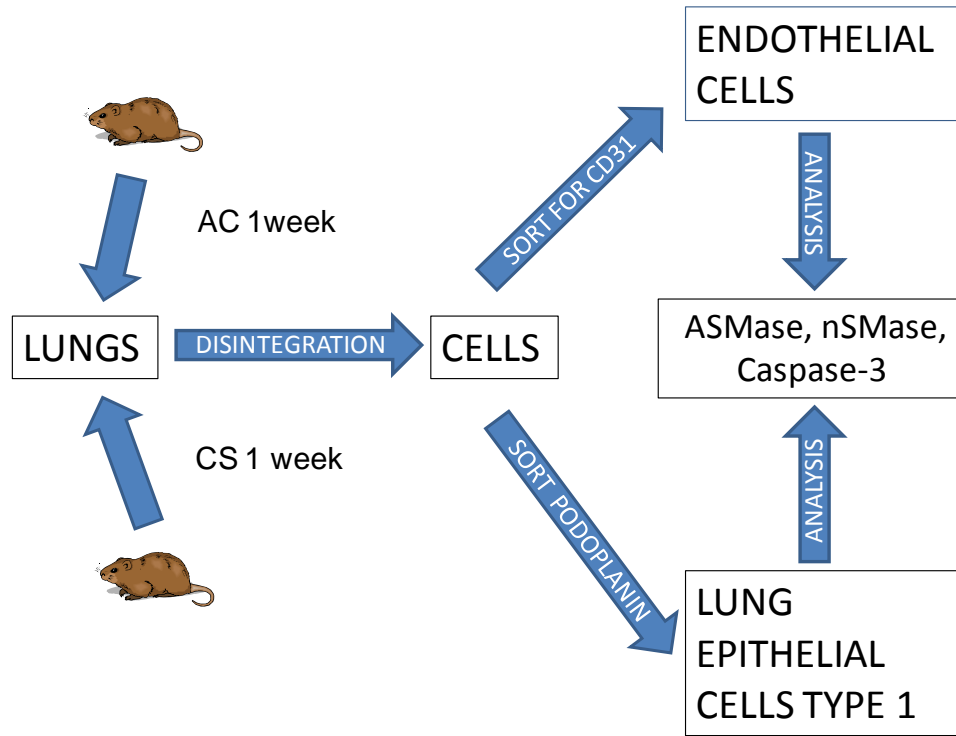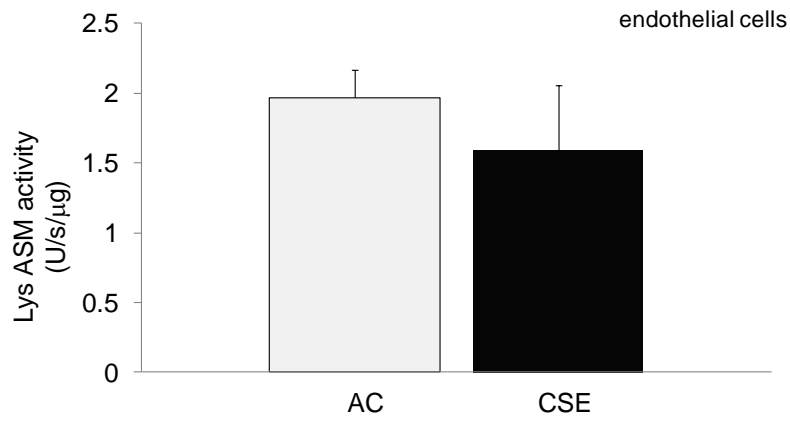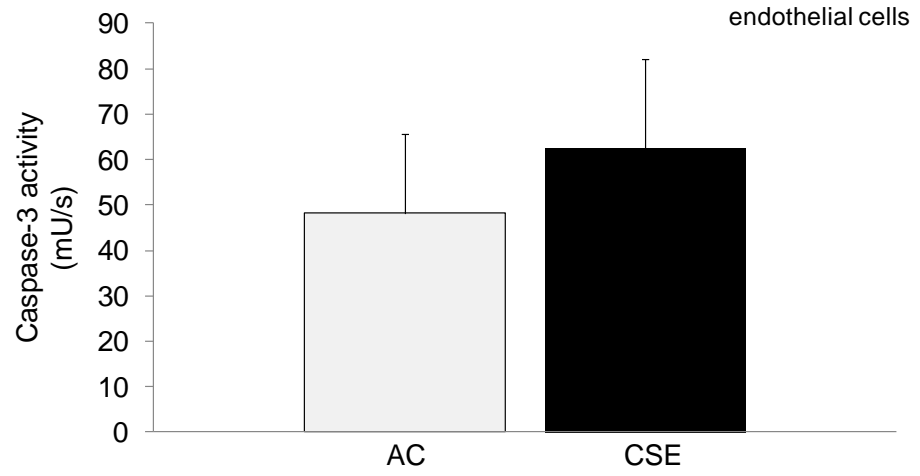
epithelial cells I

Figure 8. Determination of enzymatic activities in sphingomyelinase ceramide synthesis pathway in both endothelial and epithelial cells type I isolated from enzymatically disintegrated lungs, following 1 week of CS exposure. (A) Design for the experiment: DBA2/J mice were exposed to CS for 1 week, lungs were enzymatically disintegrated and sorted for endothelial and epithelial type I cells. In both groups of cells the activities of lysosomal ASMase, neutral SMase and caspase-3 were determined. (B) Lysosomal ASMase activity in endothelial cells normalized to protein concentration. Mean+ SEM; n=4-5/group. (C) Neutral SMase activity in endothelial cells normalized to protein concentration. Mean+ SEM; n=4-5/group (D) Caspase-3 activity in endothelial cells (measured in 16.86 μg of protein per sample). Mean+ SEM; * p< 0.05; n=4-5/group. (E) Neutral SMase activity in epithelial cells type I normalized to protein concentration. Mean+ SEM; * p< 0.05; n=4-5/group. (F) Caspase-3 activity in epithelial cells type I (measured in 16.86 μg of protein per sample). Mean+ SEM; * p< 0.05; n=4-5/group.

A ACUTE cigarette smoke exposure

5 x per group

CS

5 hours

2 hours

1 hour

0.5 hour

Lung tissue harvest and analysis

B

Lys. ASMase

Secr. ASMase

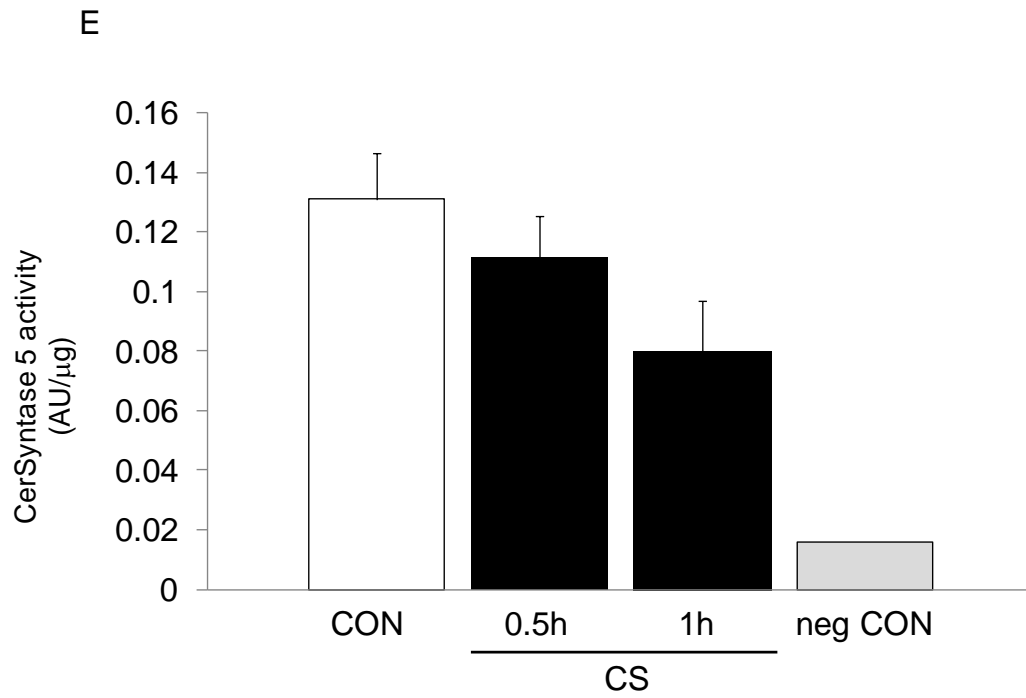ASMase activity (mU/min/μg)
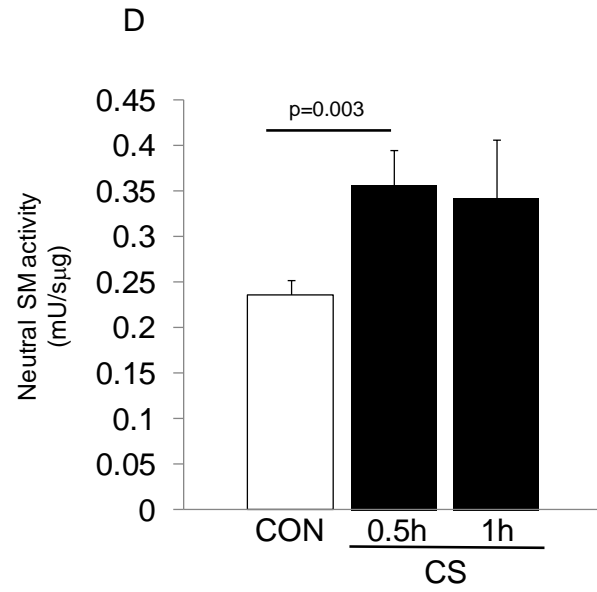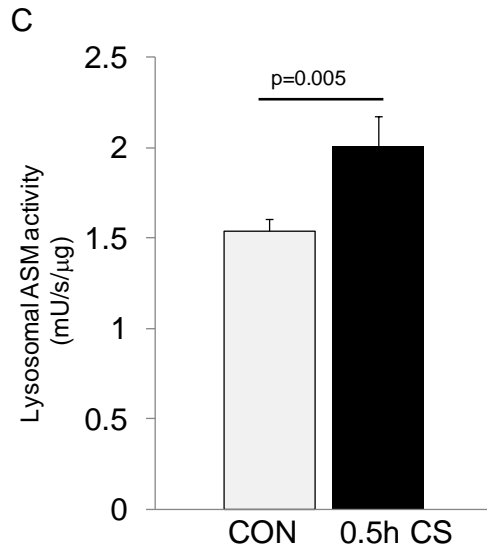
CON 1h 2h 5h
CS

CON 1h 2h 5h
CS

Figure 9. Effect of short term CS exposure on the activity of ceramide synthesis enzymes in the whole lung tissue of DBA2/J mice. (A) Experimental design for acute CS exposure in. (B) Lysosomal and secreted acid sphingomyelinase activities normalized by protein concentration. Mean+ SEM; * p<0.05; n=5/group. (C) Lysosomal and (D) neutral sphingomyelinase activities normalized by protein concentration. Mean+ SEM; * p<0.05; n=4/group. (E) Ceramide syntase 5 activity expressed as arbitrary units calculated from densitometry units normalized to protein concentration. Mean+ SEM; n=5/group.
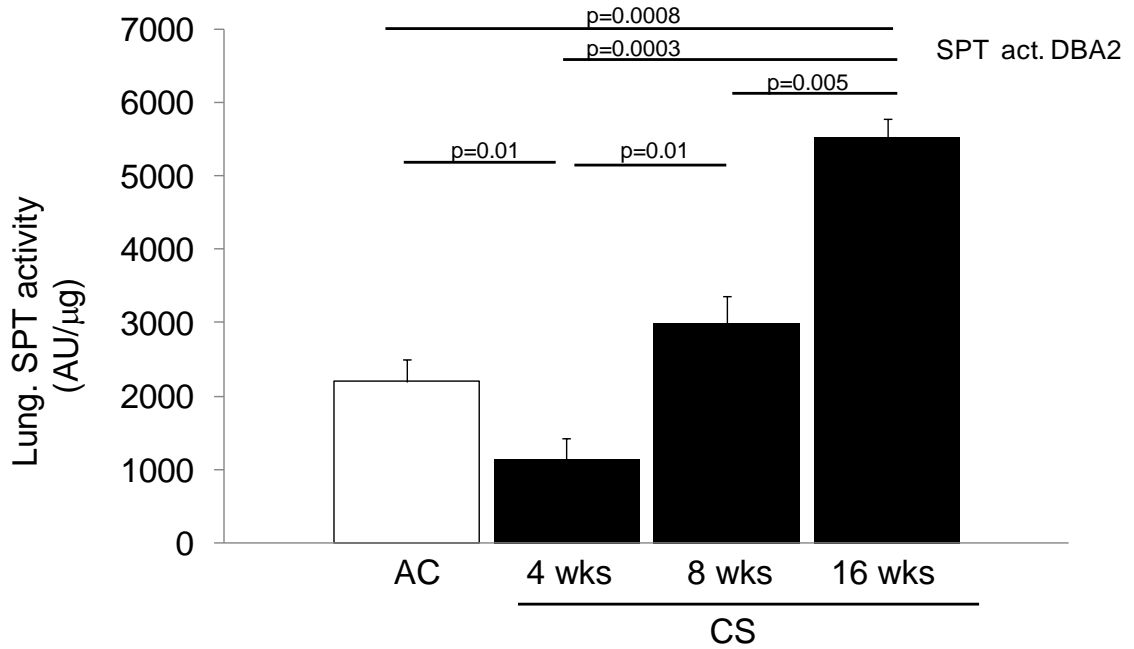
Figure 10. Effect of CS on enzymes of the *de novo* ceramide synthesis pathway

in the whole lungs. Mice (DBA2/J) were exposed to CS for the indicated time and

SPT activity was determined using tritium-labeled L-serine and expressed as

arbitrary units normalized by protein concentration. Mean+ SEM; p< 0.05;

n=3/group.

Effect of CS on the expression of lung CerS mRNA isoforms in C57Bl/6 mice
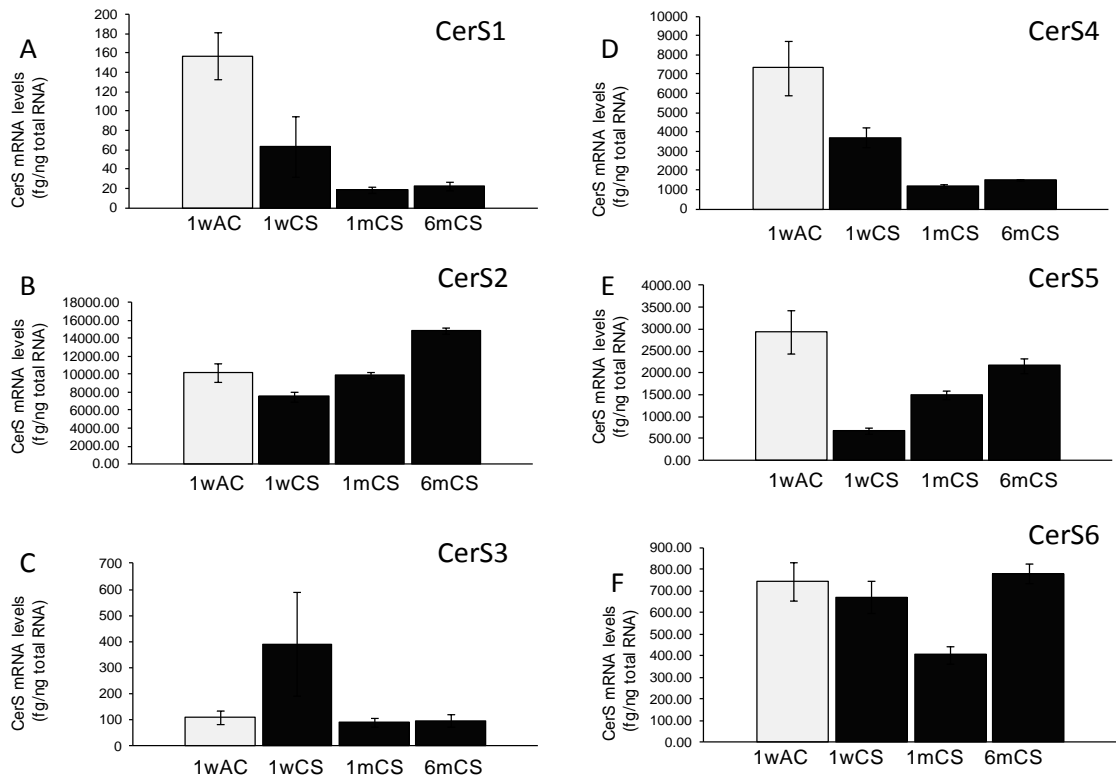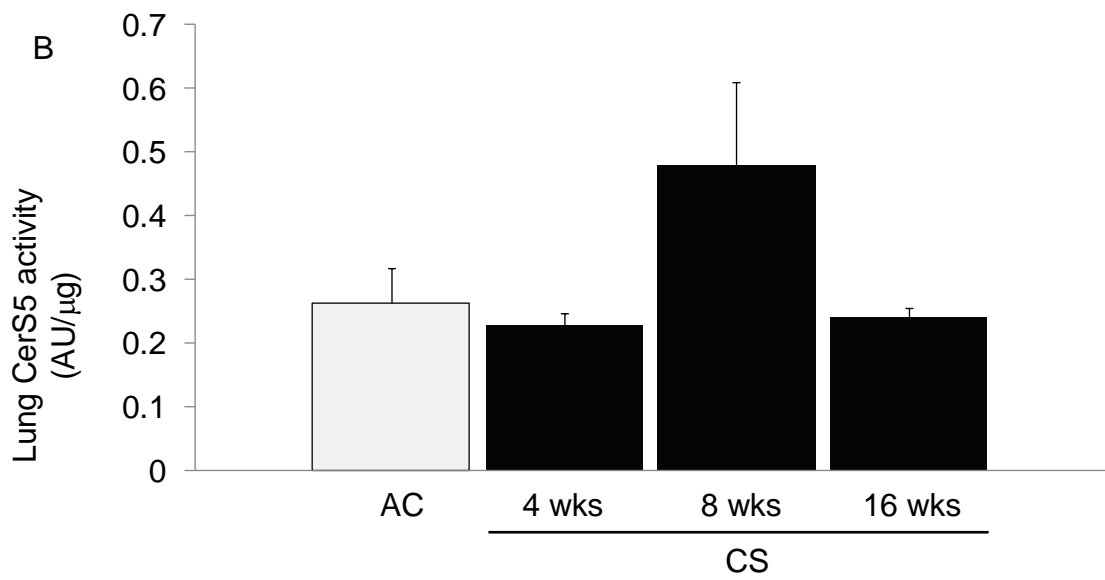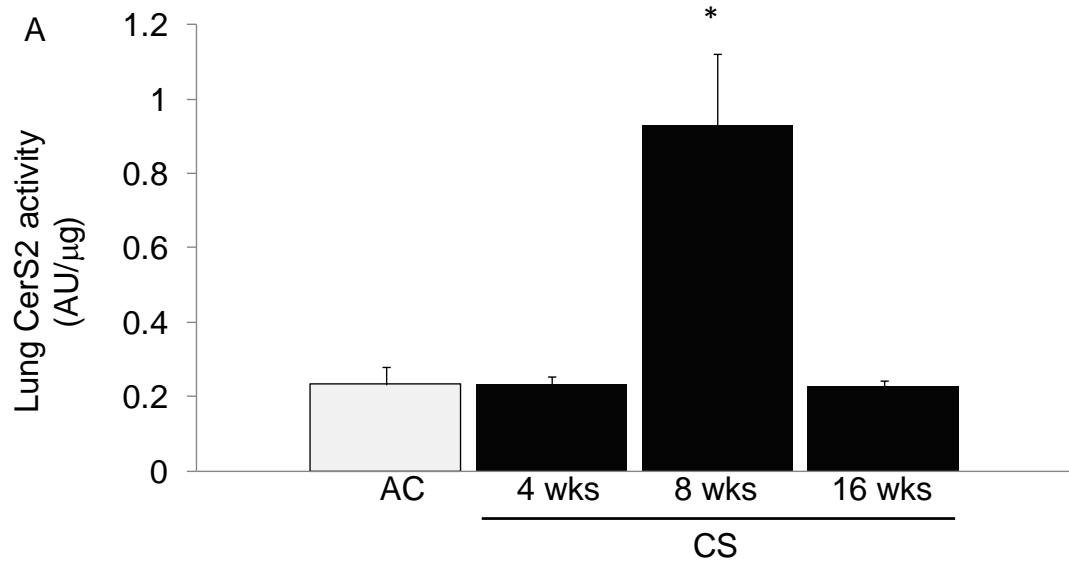
Figure 11. Expression of mRNA levels of distinct lung ceramide synthase isoforms in the whole lung of C57Bl6 mice following CS exposure for the indicated time. (A-F) mRNA levels were measured by real time PCR. For all panels: Mean+ SEM; * $p < 0.05$ vs. air control; n=5. Data provided by Dr. A. Futerman (Weizmann Institute, Israel).
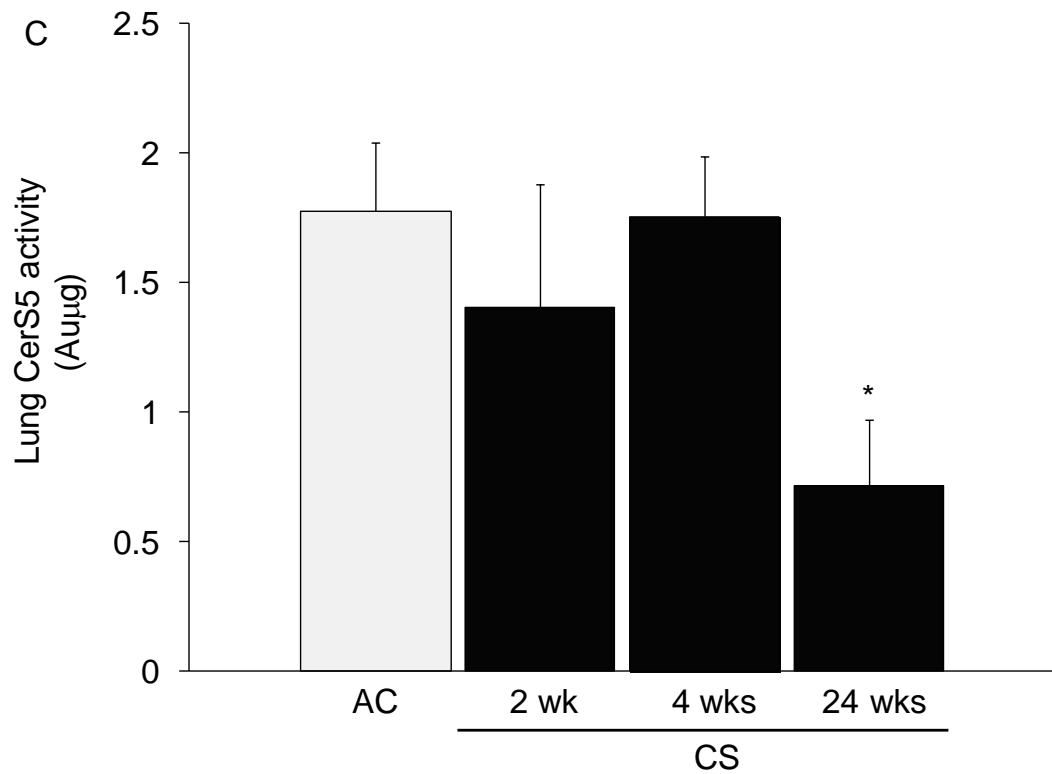
Figure 12. CS exposure activates enzymes of the *de novo* pathway in the lungs of DBA2/J mice. (A) Ceramide synthase 2 activity in lungs of DBA2/J mice, expressed as arbitrary units (AU) of densitometry normalized by protein concentration. Mean+ SEM; $p < 0.05$ vs. AC; n=5/group. (B) Ceramide synthase 5 activity in lung of DBA2/J mice, expressed as arbitrary units (AU) of densitometry normalized by protein concentration. Mean+ SEM; $p < 0.05$ vs. AC; n=5/group. (C) Activity levels of lung ceramide synthase 5 in C57Bl/6 mice during chronic CS exposure, expressed as arbitrary units (AU) of densitometry normalized by protein concentration. Mean+ SEM; $p < 0.05$ vs. AC; n=5/group.
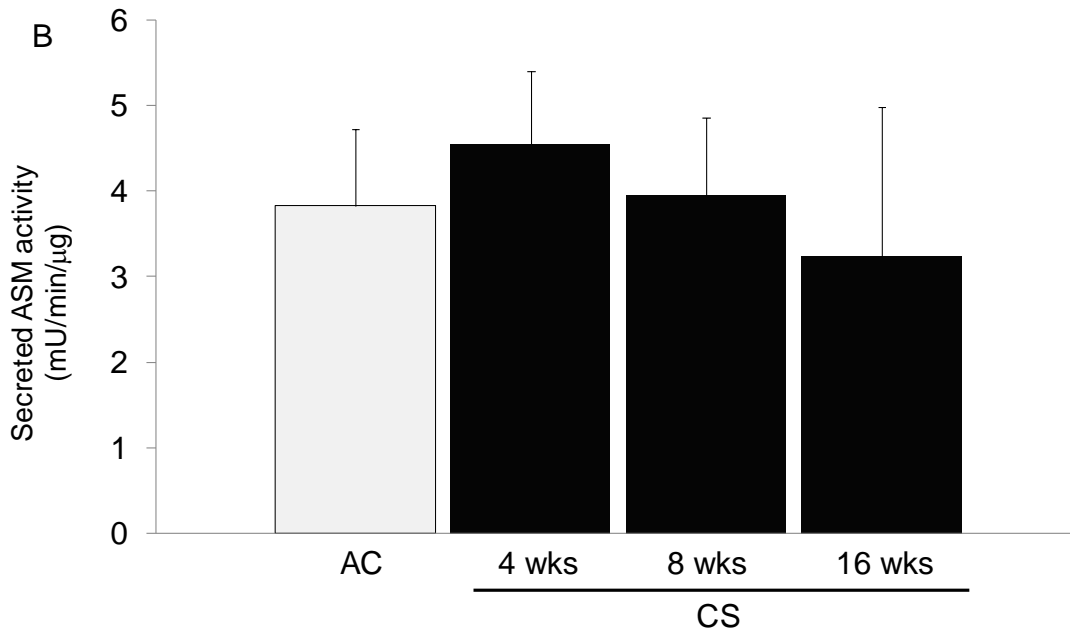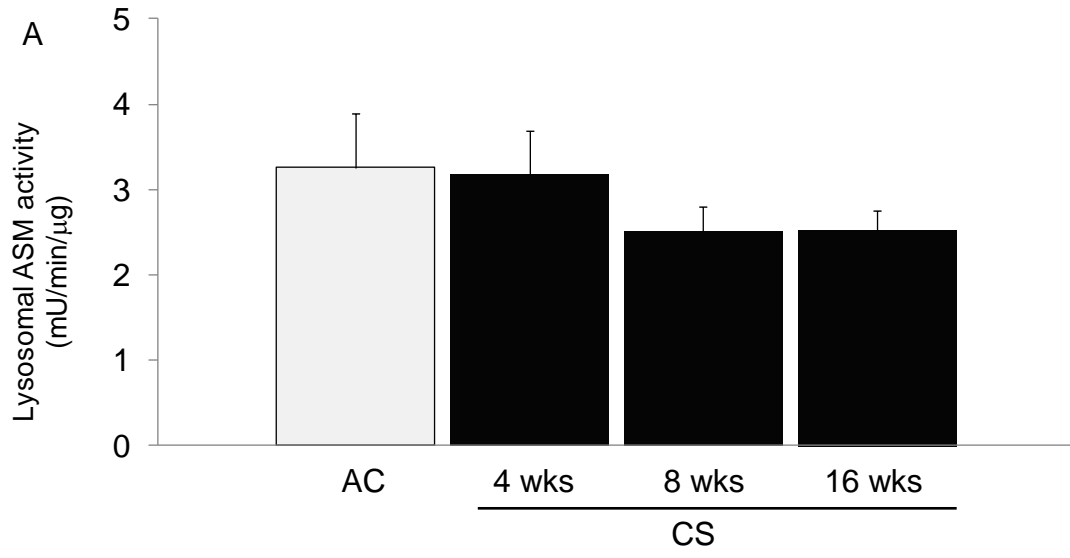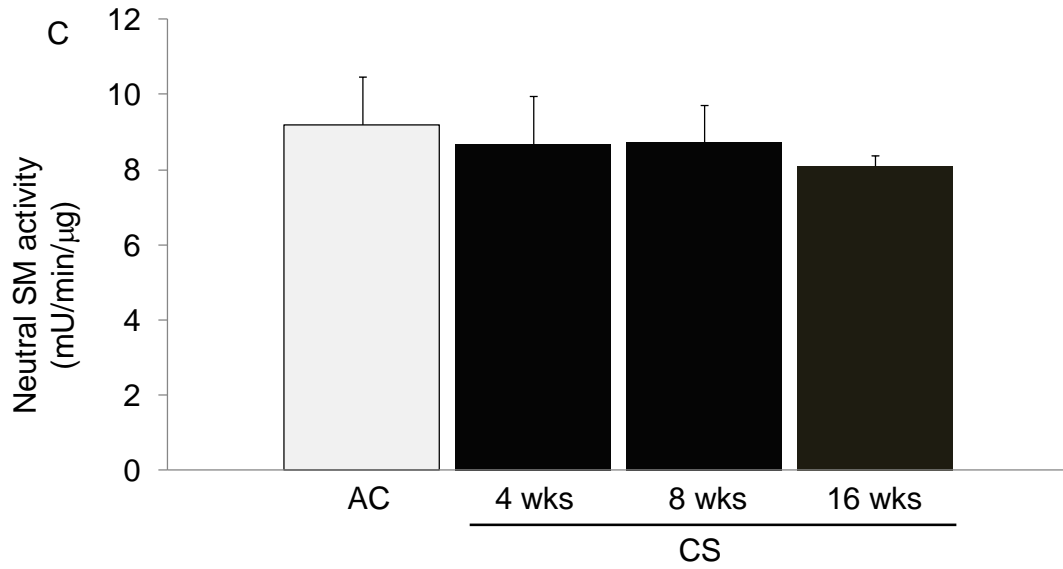
Figure 13. Effect of CS exposure on the activity of enzymes in the sphingomyelinase pathway in the whole lung tissue of DBA2/J mice. (A) Lysosomal acid sphingomyelinase, (B) soluble acid sphingomyelinase, and (C) Neutral sphingomyelinase activities were measured following CS exposure for the indicated time and were normalized by protein concentration. Mean+ SEM; n=4/group.

Short term cigarette smoke exposure of DBA2/J mice with blockade of **ASMase**
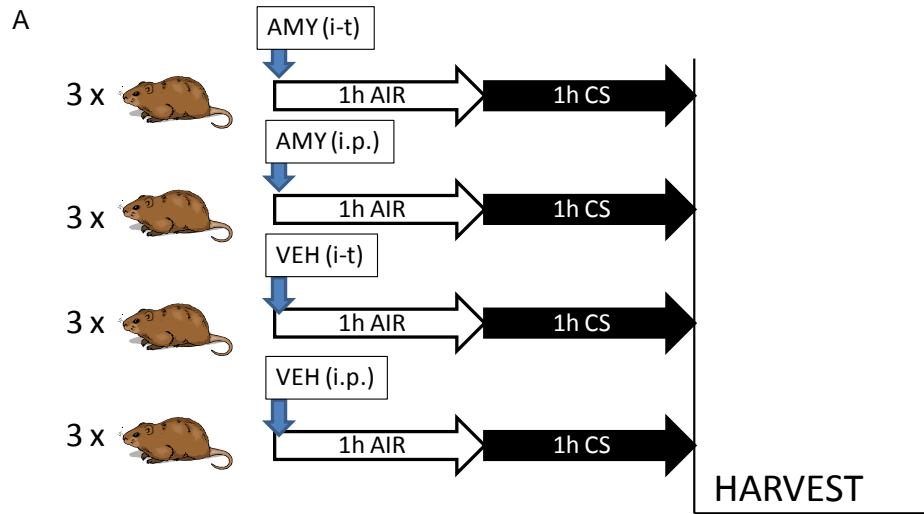
Amytryptylline (AMY) was intratracheally instilled or injected i.p. once, 0.3 mg/kg
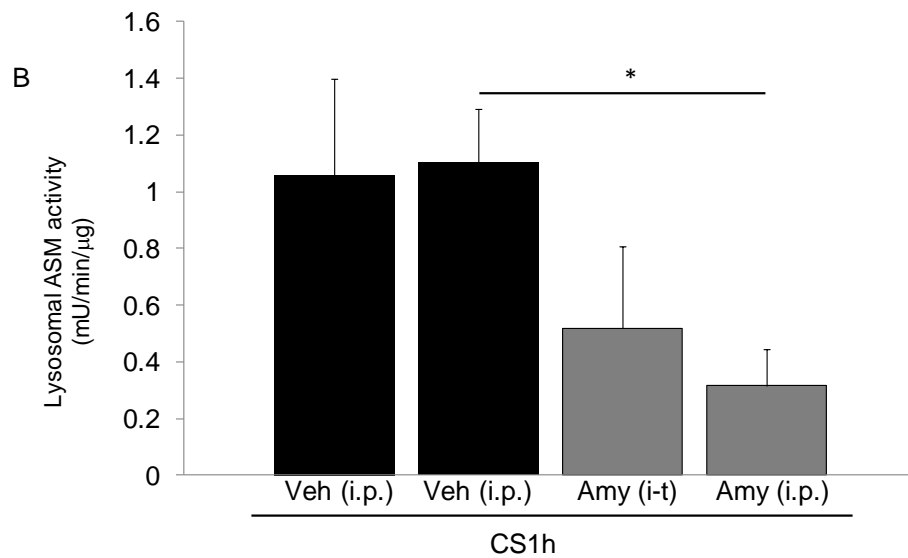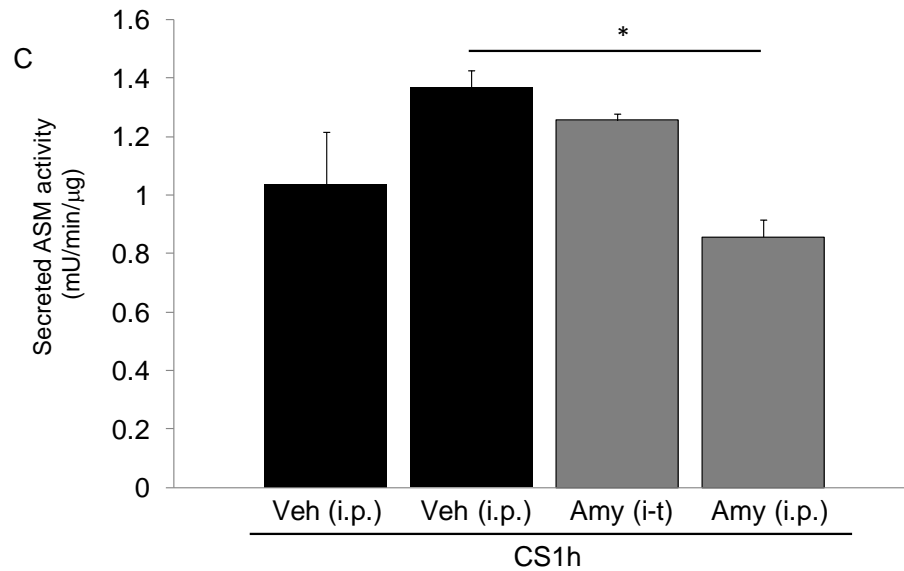
Figure 14. Effect of the ASMase inhibitor amytryptilline (Amy) on the lysosomal and secreted ASMase activities induced by short term CS exposure in lungs of DBA2/J mice. (A) Experimental design: mice were intratracheally instilled or intraperitoneally injected with Amy (0.3 mg/kg, once) or with vehicle (PBS) 1 h prior to exposure to CS (for 1 h). Whole lung (B) lysosomal and (C) secreted sphingomyelinases activities were normalized to protein concentration. Mean + SEM; * $p < 0.05$; n=4/group.

Long term cigarette smoke exposure
Inhibition of ASMase

A

AC

16 wks AMY control

16 wks CS

8 wks AMY
16 wks CS

Amy-P ("Prophylaxis")

8 wks AMY
16 wks CS

HARVEST

Amy-T ("Treatment")
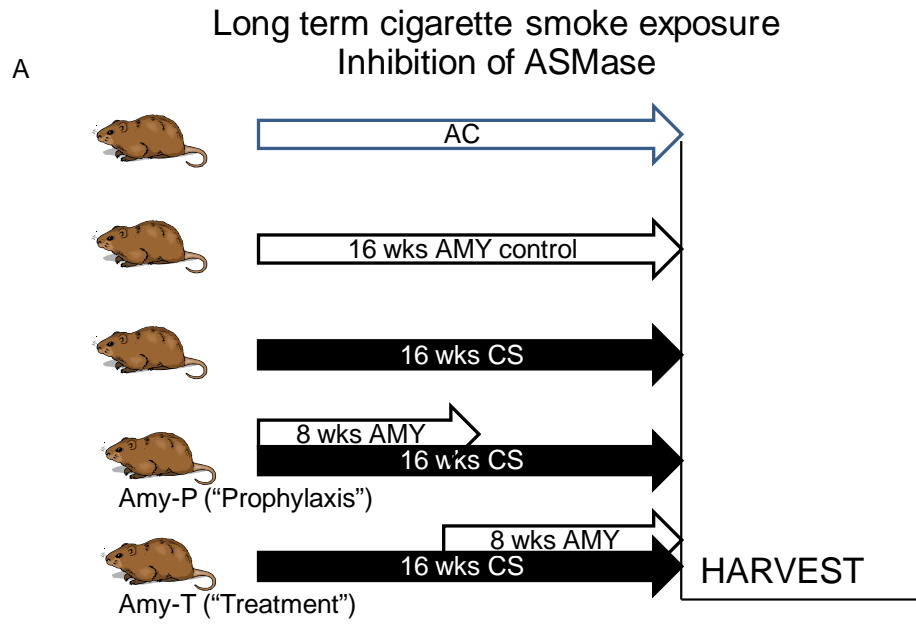
Amytryptylline (AMY) was injected i.p. 3 times/week 0.3 mg/kg

ASM inhibition downregulates CS-induced apoptosis

B

#: p<0.05
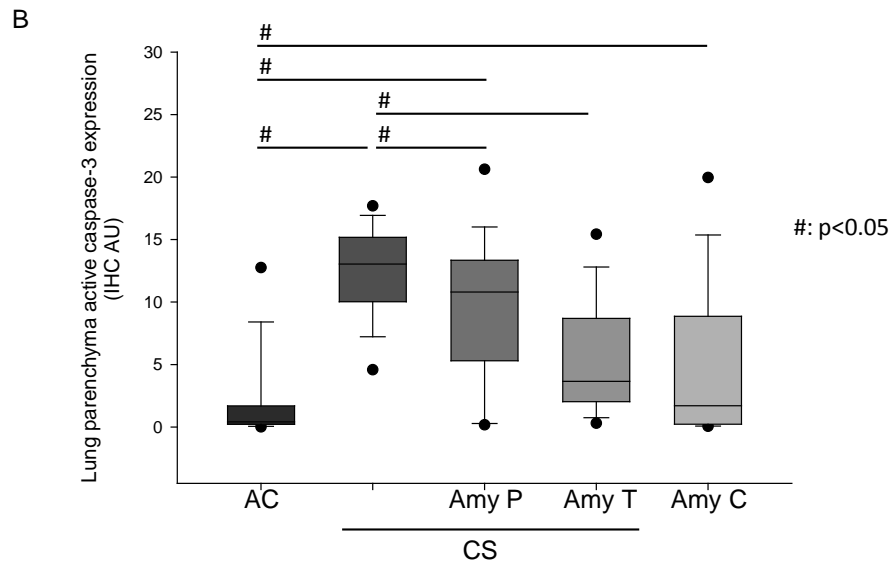
Figure 15. Effect of ASMase inhibition with amytryptilline on lung apoptosis following chronic CS exposure in DBA2/J mice. (A) Experimental design. (B) Caspase-3 activity measured by IHC with active caspase-3 antibody and image analysis of lung parenchyma only. Boxplot (box indicating the 25th and 75th percentile with the middle line showing the median and the 5th and 95th percentiles indicated by whiskers); Abbreviations: AmyP: Amy prophylactic, AmyT: Amy treatment, AmyC: Amy Control: ANOVA; *p<0.05; n=5-10/group.

Long term cigarette smoke exposure
Inhibition of the de novo pathway (SPT) with myriocin

A

2m AC

2m MYR

2m CS

2m MYR
2m CS

HARVEST
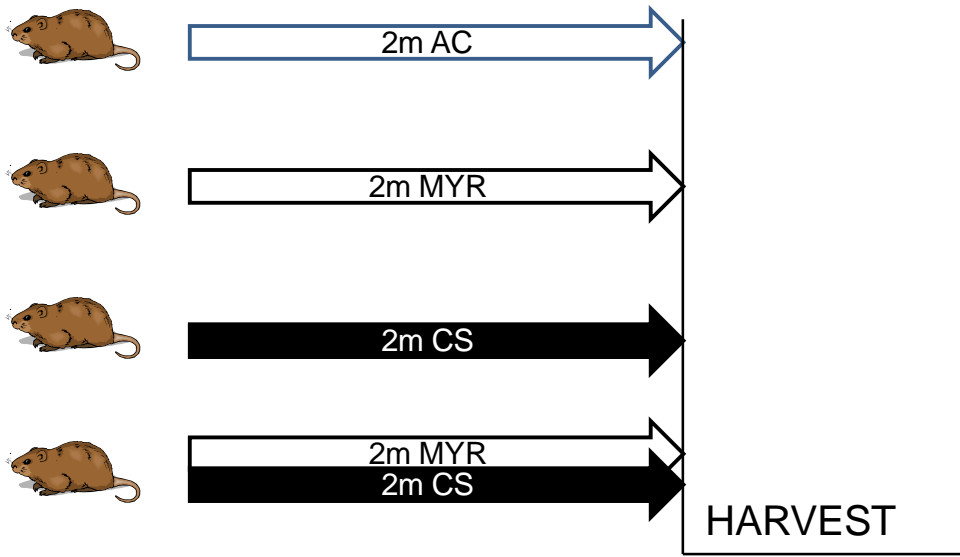
Myriocin (MYR) was injected 1mg/kg i.p. 3 times/week

B

SPT activity (ct/50µg)

AC   Myr   CS   CS+MYR
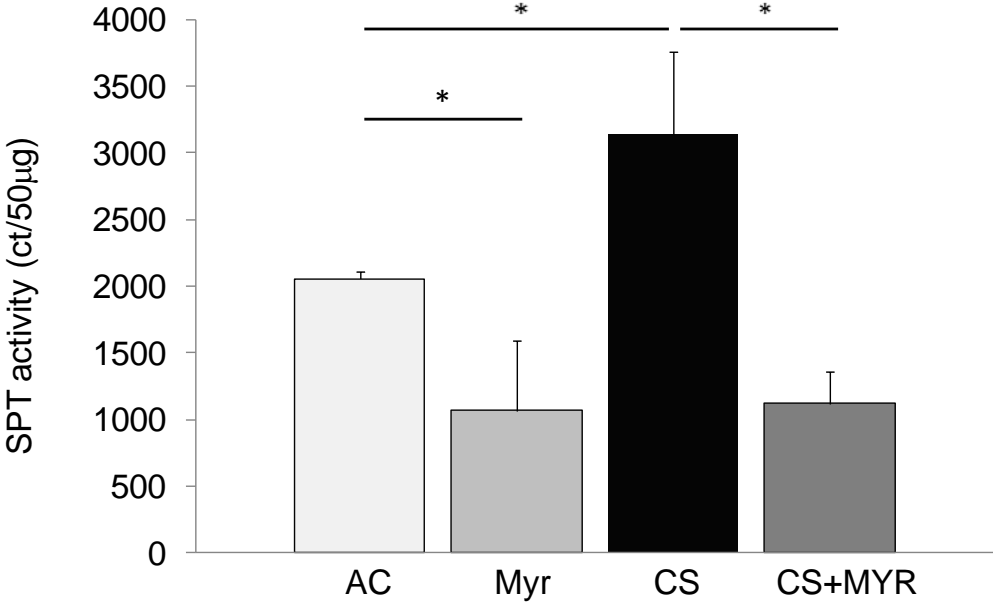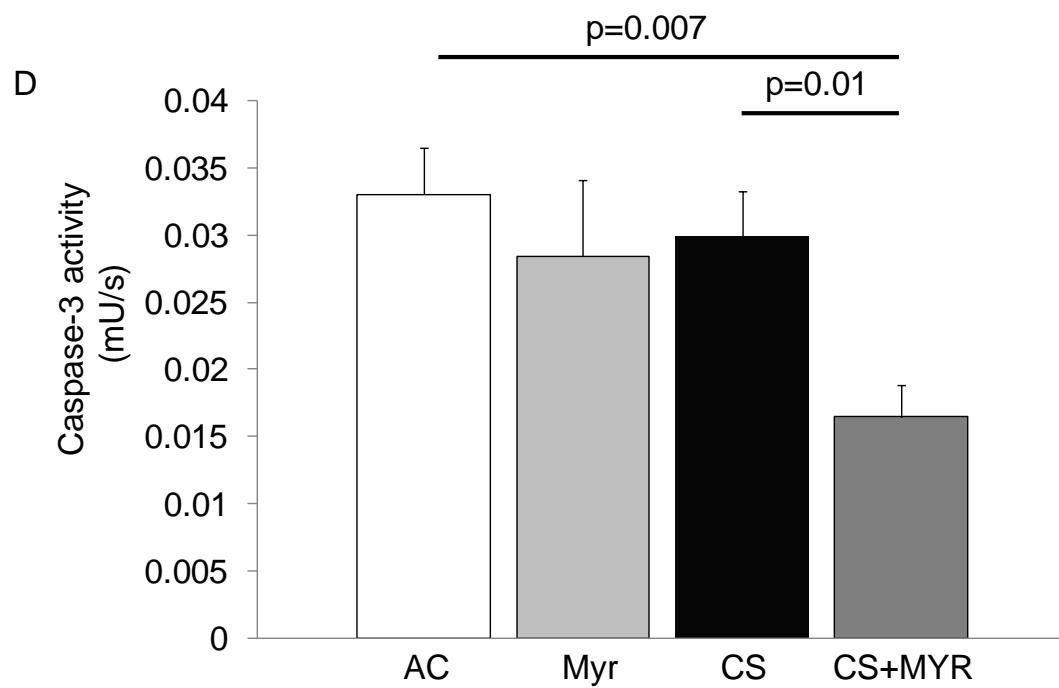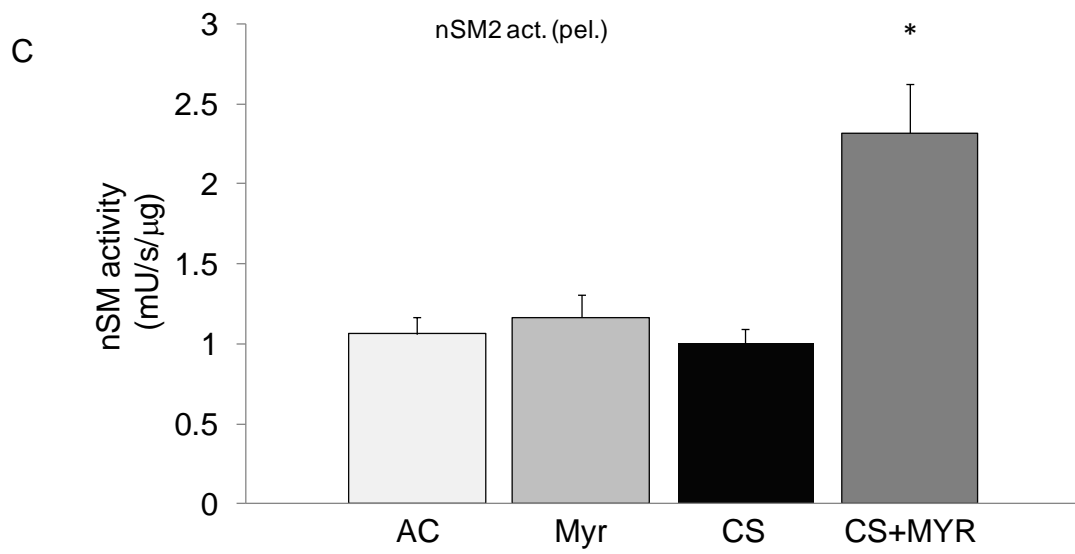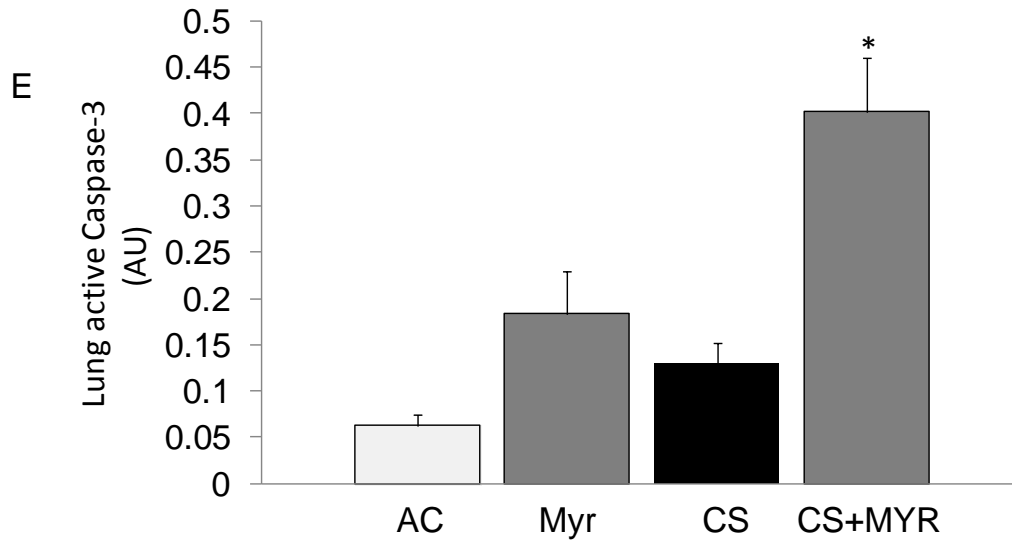
Figure 16. Effect of SPT inhibition with myriocin on lung apoptosis following chronic CS exposure of DBA2/J mice. (A) Experimental design. (B) Whole lung SPT activity expressed as arbitrary units (AU) derived from scintillation counts, normalized to 50 mg tissue protein. Mean + SEM; n=4-5/group. (C) Whole lung neutral SMase activity normalized to protein concentration. Mean+ SEM; $p<0.05$; n=4-5/group. (D-E) Apoptosis measured *via* caspase-3 activity in the whole lung tissue normalized per 11.49 ug protein (D) or specifically in the lung parenchyma by immunohistochemistry (E) using active caspase-3 antibody and image analysis. Mean+ SEM; * $p<0.05$; n=4-5/group.

A

Days following
SU5416 treatment

| Vehicle | 3 | 5 | 7 | 7 | 7 | 7 | FB1/SU5416 | RTP801 |

Vinculin

B

Control   RTP801

RTP801

Vinculin

C

Control   RTP801

Active Caspase-3 IHC

D

Vehicle
RTP801

Frequency (%)

Alveolar diameter (μm)

Control   RTP801

Hematoxyllin-eosin

E

Ceramide (AU/nmol lipid Pi)
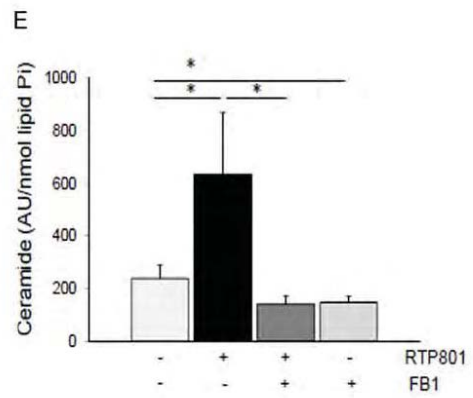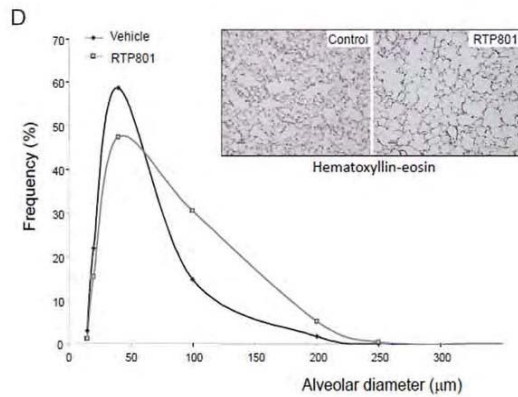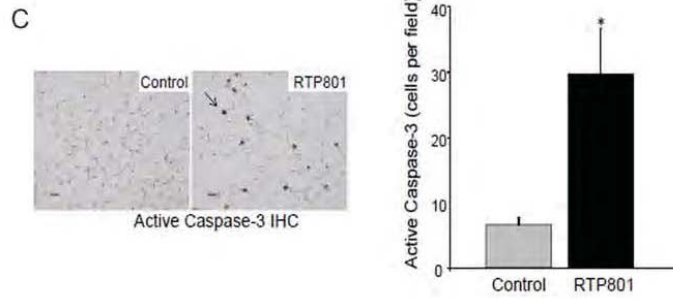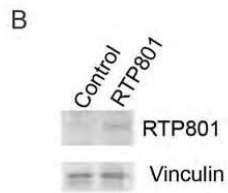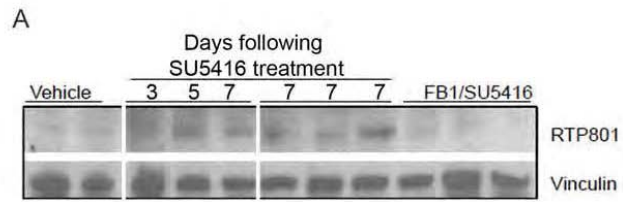
				RTP801
-	+	+	-	RTP801
-	-	+	+	FB1

Figure 17. Elevation of lung RTP801 is associated with increases of airspace

size, apoptosis, and ceramide levels. (A) In a model of apoptosis-dependent

emphysema by vascular growth factor receptor inhibition expression of RTP801

is increased in the lung tissue. RTP801 protein expression was measured by

Western blotting in lung homogenates from individual mice treated with SU5416

(20 mg/kg; s. c. once) and harvested after the indicated number of days, with

vehicle control (Veh; s.c. once, lungs harvested at day 7), or with SU5416 and

ceramide synthase inhibitor Fumonisin B1 (FB1; 1.1 mg/kg, i.p. daily; lungs

harvested at day 7). Each lane represents a different mouse lung. Vinculin

immunoblotting was used as a loading control. (B-E) Effects of intra-tracheal

instillation (i-t) of RTP801-expressing plasmid (50 mg) in the lung: (B) Increased

RTP801 protein measured in the lung homogenates by Western blot following

RTP801 instillation compared to control plasmid. (C): The left panel shows active

caspase-3 positive cells detected by immunohistochemistry (brown; arrow) in

fixed lung tissue from control animals following intra-tracheal instillation of empty

plasmid (50 mg; lungs harvested after 3 days) or of RTP801-plasmid; size bar 10

mm. The right panel represents quantification of data from IHC; Mean + SEM,

*$p < 0.05$ vs. control; Student's t test; n=3 mice/group; 8-10 lung fields/mouse). (D)

Airspace enlargement was measured by morphometry of the hematoxyllin-eosin-

stained fixed lungs (inset) 3 days after RTP801-plasmid instillation and

expressed as the mean frequency of alveoli of a certain diameter. Note a shift the

right (towards a higher frequency of larger diameter alveoli) in mice instilled with

RTP801-plasmid (grey line) compared to control (black line); n=3/group. (E) Total

ceramide content of mouse lungs at 3 days following RTP801-plasmid instillation, with or without ceramide synthase inhibitor fumonisin B1 (FB1; 2.2 mg/kg), measured by DAG kinase assay and expressed as arbitrary units (from densitometric analysis of ceramide on TLC plates) normalized by lipid inorganic phosphorus (lipid Pi). Mean + SEM, *p<0.05; ANOVA; n=3-5/group.

A

B

C

D

E

RTP801 IHC/ Hematoxyllin

Sham   WT   RTP801KO

Ceramide C:16

F

Lung RTP801 expression (AU)

5
4.5
4
3.5
3
2.5
2
1.5
1
0.5
0

Sham   WT   RTP801KO
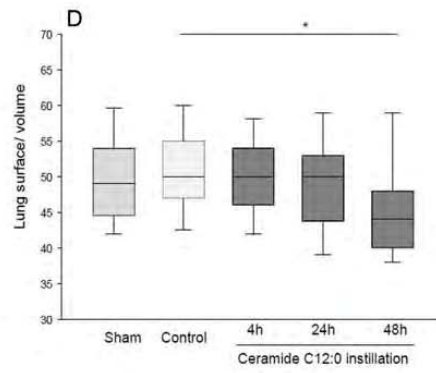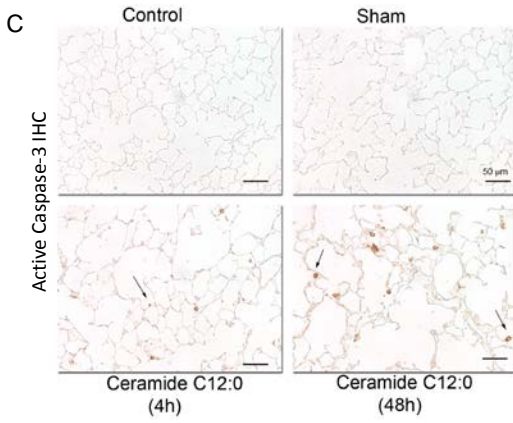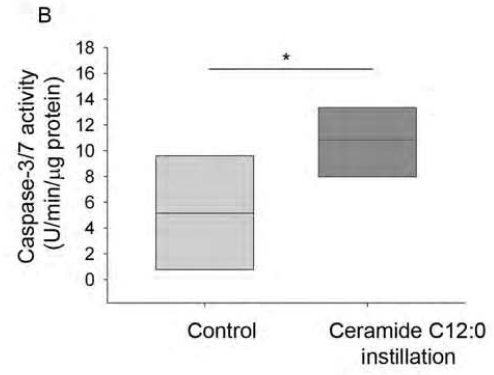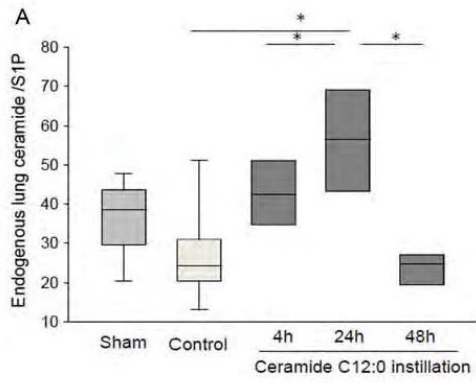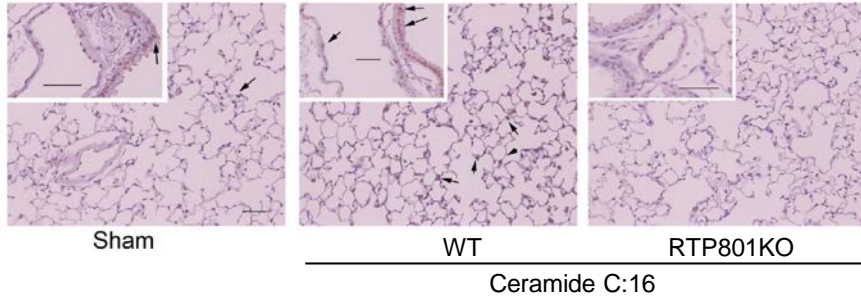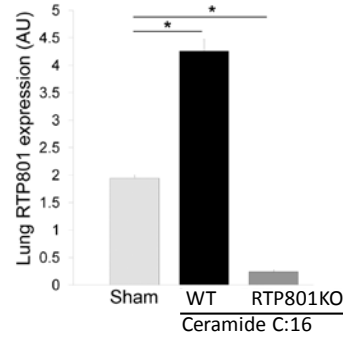
Ceramide C:16

*: p<0.05

Figure 18. Increases in lung ceramide content are associated with airspace enlargement, apoptosis, and RTP801 upregulation. Effect of a single intra-tracheal instillation of ceramide C12:0 (A-D) or C16:0 (E-F) (5 mg/kg) in mice on: (A) Endogenous ceramides/sphingosine-1 phosphate (S1P) ratio in lung tissue homogenates at the indicated time in sham-operated mice (that underwent exposure of the trachea only), negative control mice (that were administered the vehicle only) or mice that received exogenous C12:0. Boxplot (box indicating the 25th and 75th percentile with the middle line showing the median and the 5th and 95th percentiles indicated by whiskers); ANOVA; *p<0.05; n=4-5/group.(B) Lung caspase-3/7 enzymatic activity was measured in whole lung lysates of mice that were instilled with C12:0 (n=7) and expressed relative to the activity measured in control mice (n=5). Mean ± SEM; *: p<0.05 vs. control; Student's t test). (C) Lung active caspase-3 expression detected by IHC (brown, arrows) shown in representative micrographs (size bar 50 mm). (D) Lung surface/volume ratio determined by standardized lung morphometry of alveolar spaces of mice following ceramide instillation timecourse and 48h, respectively. Boxplot, ANOVA; * P<0.05; n=2 (Sham); n=3-4/group; 8-10 lung fields/mouse. (E) RTP801 expression detected by IHC in the lung sections of mice following C16: 0 instillation compared to control animals or *rtp*801-null mice. Note an increase in RTP801 (brown, arrows) in the lung parenchyma and also (see insets) in the vascular (v) endothelium as well as bronchial (b) epithelium in ceramide-instilled mice. (F) RTP801 expression in the lung parenchyma was quantified via blinded image analysis software and expressed as arbitrary units (AU); Mean + SEM, *:

p<0.05, Student's t test; n=4, except for RTP801-null mice, which was n=2; 8-10

lung field/mouse.

A

B

C

D

116
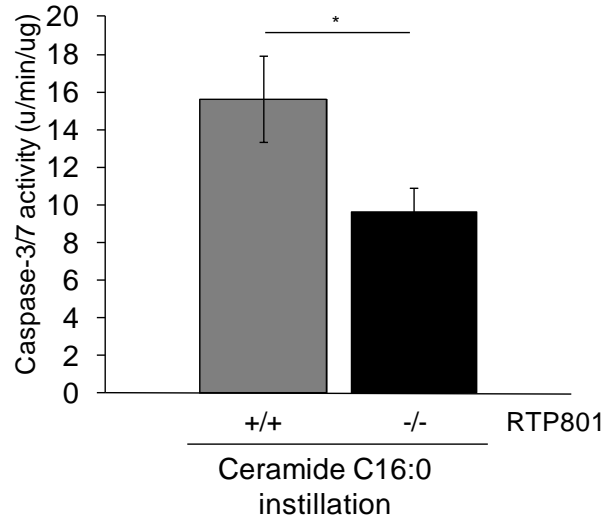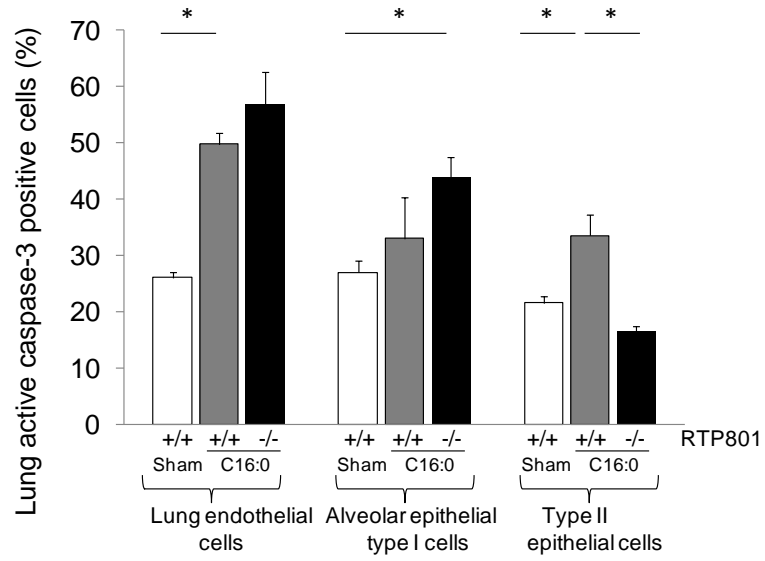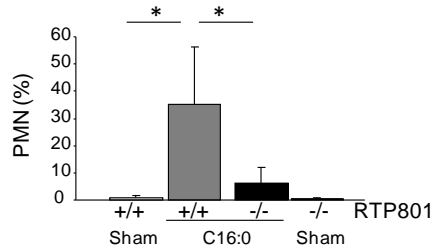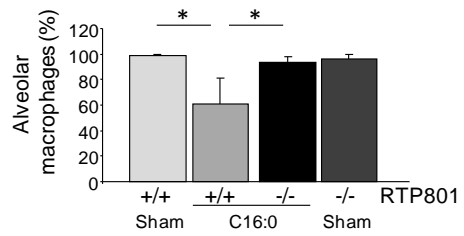
Figure 19. Requirement for RTP801 in ceramide-induced apoptosis of type II epithelial cells and neutrophil infiltration. (A) Caspase-3/7 activity levels in whole lungs homogenates normalized by protein concentration. Mean + SEM; *: $p < 0.05$; Student's t test; n=2-4/group. (B) Cell specific apoptosis expressed as relative abundance (%) apoptotic active caspase-3/7- positive cells among lung endothelial (CD31-positive), alveolar epithelial type I (podoplanin positive) and type II (pro-surfactant-C positive) cells in murine lung cell suspensions, detected by flow cytometry with fluorescence-labeled specific antibodies. Mean + SEM; *: $p < 0.05$; n=4-5/group. Note that only type II epithelial cells were protected against ceramide-induced apoptosis in *rtp*801-null mice. (C-D) Analysis of abundance (% of total cells) of polymorphonuclear cells (PMN), (C) and alveolar macrophages (D) counted in cytospins of the bronchoalveolar lavage fluid in mice. Mean + SEM, *: $p < 0.05$; n=4-5/group.

A
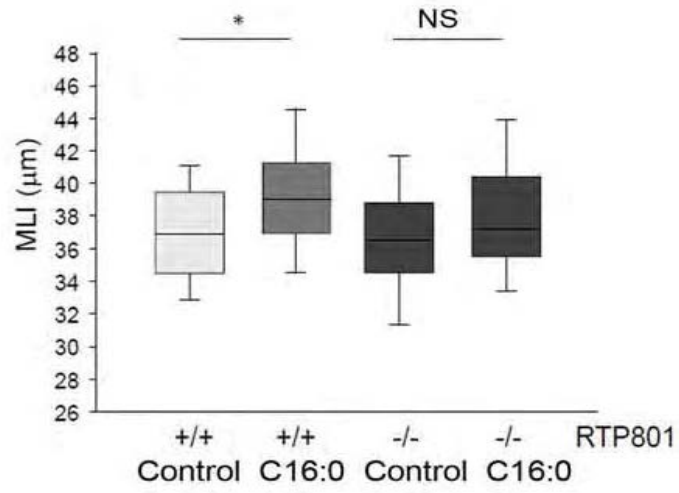
B
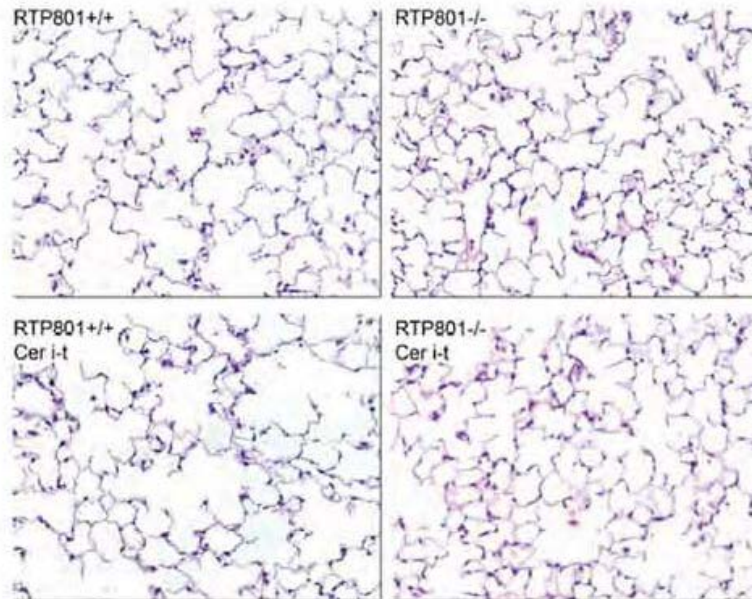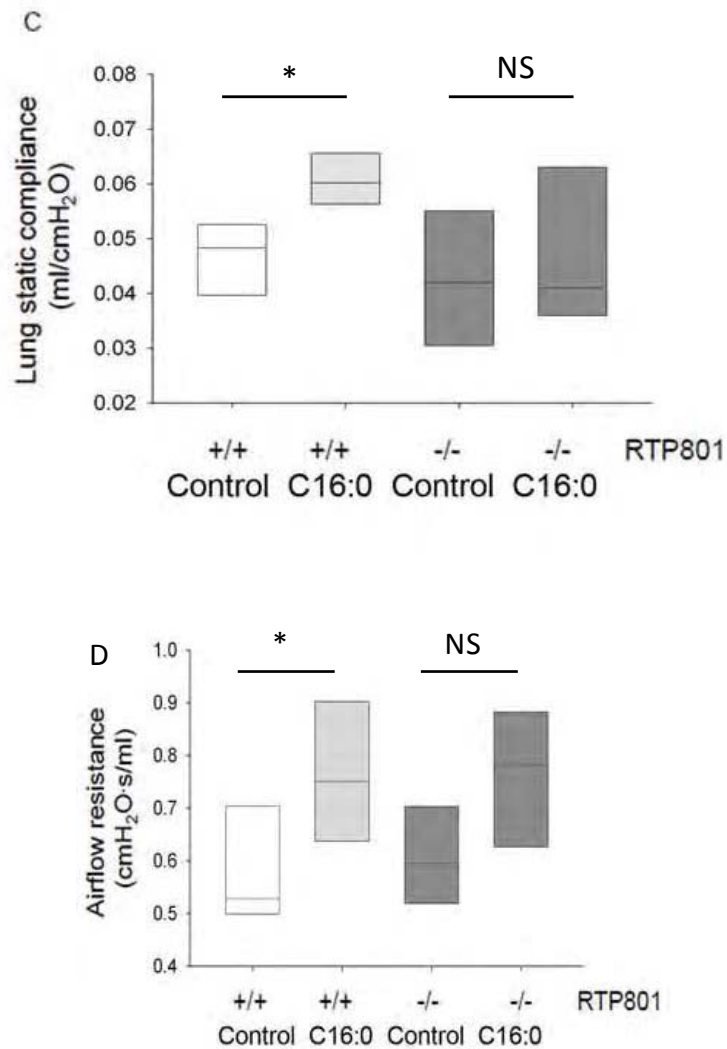
Figure 20. Requirement for RTP801 in ceramide-induced changes of lung

alveolar morphology and function. (A-D) Measurements in response to

exogenous ceramide 16:0 (5mg/kg; 48 h) or vehicle (control) intra-tracheal

instillation in wild type or *rtp*801-null mice. (A-B) Mean linear intercept (MLI); (A)

expressed as boxplot (box indicating the 25th and 75th percentile with the middle

line showing the median; the 5th and 95th percentiles indicated by whiskers; n=5;

8-10 lung fields/mouse) measured by automated morphometry of lung

parenchyma on paraffin embedded lung sections stained with hematoxyllin-eosin

(B). (C) Lung compliance measured with Flexivent in anesthetized mice; Box

plot; n=4 (wild type) or 5 (*rtp*801-null). Two-way ANOVA; *: $p < 0.05$ or NS (not

statistically significant). (D) Airflow resistance measured with Flexivent in

anesthetized mice. Two-way ANOVA: * $p < 0.05$ or NS (not statistically significant);

n=5/group.

REFERENCES

1. The definition of emphysema. Report of a National Heart, Lung, and Blood Institute, Division of Lung Diseases workshop. *Am Rev Respir Dis* 1985, 132(1):182-185.
2. Kohansal R, Martinez-Camblor P, Agusti A, Buist AS, Mannino DM, Soriano JB: The natural history of chronic airflow obstruction revisited: an analysis of the Framingham offspring cohort. *Am J Respir Crit Care Med* 2009, 180(1):3-10.
3. Salvi S, Barnes PJ: Is exposure to biomass smoke the biggest risk factor for COPD globally? *Chest* 2010, 138(1):3-6.
4. Kan H, Heiss G, Rose KM, Whitsel E, Lurmann F, London SJ: Traffic exposure and lung function in adults: the Atherosclerosis Risk in Communities study. *Thorax* 2007, 62(10):873-879.
5. Sandford AJ, Weir TD, Pare PD: Genetic risk factors for chronic obstructive pulmonary disease. *The European respiratory journal : official journal of the European Society for Clinical Respiratory Physiology* 1997, 10(6):1380-1391.
6. Tabak C, Feskens EJ, Heederik D, Kromhout D, Menotti A, Blackburn HW: Fruit and fish consumption: a possible explanation for population differences in COPD mortality (The Seven Countries Study). *European journal of clinical nutrition* 1998, 52(11):819-825.
7. Fischer BM, Pavlisko E, Voynow JA: Pathogenic triad in COPD: oxidative stress, protease-antiprotease imbalance, and inflammation. *International journal of chronic obstructive pulmonary disease* 2011, 6:413-421.
8. Tuder RM, Petrache I, Elias JA, Voelkel NF, Henson PM: Apoptosis and emphysema: the missing link. *Am J Respir Cell Mol Biol* 2003, 28(5):551-554.
9. Tuder RM, Yoshida T, Arap W, Pasqualini R, Petrache I: State of the art. Cellular and molecular mechanisms of alveolar destruction in emphysema: an evolutionary perspective. *Proc Am Thorac Soc* 2006, 3(6):503-510.
10. Tuder RM, Yoshida T, Fijalkowka I, Biswal S, Petrache I: Role of lung maintenance program in the heterogeneity of lung destruction in emphysema. *Proc Am Thorac Soc* 2006, 3(8):673-679.
11. Jemal A, Ward E, Hao Y, Thun M: Trends in the leading causes of death in the United States, 1970-2002. *JAMA : the journal of the American Medical Association* 2005, 294(10):1255-1259.
12. O'Donnell R, Breen D, Wilson S, Djukanovic R: Inflammatory cells in the airways in COPD. *Thorax* 2006, 61(5):448-454.
13. Cosio MG, Saetta M, Agusti A: Immunologic aspects of chronic obstructive pulmonary disease. *N Engl J Med* 2009, 360(23):2445-2454.
14. O'Shaughnessy TC, Ansari TW, Barnes NC, Jeffery PK: Inflammation in bronchial biopsies of subjects with chronic bronchitis: inverse relationship of CD8+ T lymphocytes with FEV1. *Am J Respir Crit Care Med* 1997, 155(3):852-857.

15.   Saetta M, Di Stefano A, Turato G, Facchini FM, Corbino L, Mapp CE, Maestrelli P, Ciaccia A, Fabbri LM: CD8+ T-lymphocytes in peripheral airways of smokers with chronic obstructive pulmonary disease. *Am J Respir Crit Care Med* 1998, 157(3 Pt 1):822-826.

16.   Presson RG, Jr., Brown MB, Fisher AJ, Sandoval RM, Dunn KW, Lorenz KS, Delp EJ, Salama P, Molitoris BA, Petrache I: Two-photon imaging within the murine thorax without respiratory and cardiac motion artifact. *Am J Pathol* 2011, 179(1):75-82.

17.   Pilewski JM, Albelda SM: Adhesion molecules in the lung. An overview. *Am Rev Respir Dis* 1993, 148(6 Pt 2):S31-37.

18.   Seth R, Raymond FD, Makgoba MW: Circulating ICAM-1 isoforms: diagnostic prospects for inflammatory and immune disorders. *Lancet* 1991, 338(8759):83-84.

19.   Fujishima S, Hoffman AR, Vu T, Kim KJ, Zheng H, Daniel D, Kim Y, Wallace EF, Larrick JW, Raffin TA: Regulation of neutrophil interleukin 8 gene expression and protein secretion by LPS, TNF-alpha, and IL-1 beta. *J Cell Physiol* 1993, 154(3):478-485.

20.   Garofalo R, Faden H, Sharma S, Ogra PL: Release of leukotriene B4 from human neutrophils after interaction with nontypeable Haemophilus influenzae. *Infect Immun* 1991, 59(11):4221-4226.

21.   Jeffery PK: Structural and inflammatory changes in COPD: a comparison with asthma. *Thorax* 1998, 53(2):129-136.

22.   Finkelstein R, Fraser RS, Ghezzo H, Cosio MG: Alveolar inflammation and its relation to emphysema in smokers. *Am J Respir Crit Care Med* 1995, 152(5 Pt 1):1666-1672.

23.   Tetley TD: Macrophages and the pathogenesis of COPD. *Chest* 2002, 121(5 Suppl):156S-159S.

24.   Pober JS: Activation and injury of endothelial cells by cytokines. *Pathol Biol (Paris)* 1998, 46(3):159-163.

25.   Davis CN, Tabarean I, Gaidarova S, Behrens MM, Bartfai T: IL-1beta induces a MyD88-dependent and ceramide-mediated activation of Src in anterior hypothalamic neurons. *Journal of neurochemistry* 2006, 98(5):1379-1389.

26.   Goggel R, Winoto-Morbach S, Vielhaber G, Imai Y, Lindner K, Brade L, Brade H, Ehlers S, Slutsky AS, Schutze S *et al*: PAF-mediated pulmonary edema: a new role for acid sphingomyelinase and ceramide. *Nature medicine* 2004, 10(2):155-160.

27.   Garcia-Ruiz C, Colell A, Mari M, Morales A, Calvo M, Enrich C, Fernandez-Checa JC: Defective TNF-alpha-mediated hepatocellular apoptosis and liver damage in acidic sphingomyelinase knockout mice. *The Journal of clinical investigation* 2003, 111(2):197-208.

28.   Clauss M: Functions of the VEGF receptor-1 (FLT-1) in the vasculature. *Trends Cardiovasc Med* 1998, 8(6):241-245.

29.   Clauss M: Molecular biology of the VEGF and the VEGF receptor family. *Semin Thromb Hemost* 2000, 26(5):561-569.

30. Kasahara Y, Tuder RM, Taraseviciene-Stewart L, Le Cras TD, Abman S, Hirth PK, Waltenberger J, Voelkel NF: Inhibition of VEGF receptors causes lung cell apoptosis and emphysema. *J Clin Invest* 2000, 106(11):1311-1319.
31. Tang K, Rossiter HB, Wagner PD, Breen EC: Lung-targeted VEGF inactivation leads to an emphysema phenotype in mice. *J Appl Physiol* 2004, 97(4):1559-1566.
32. Petrache I, Natarajan V, Zhen L, Medler TR, Richter AT, Cho C, Hubbard WC, Berdyshev EV, Tuder RM: Ceramide upregulation causes pulmonary cell apoptosis and emphysema-like disease in mice. *Nature medicine* 2005, 11(5):491-498.
33. Petrache I, Natarajan V, Zhen L, Medler TR, Richter A, Berdyshev EV, Tuder RM: Ceramide causes pulmonary cell apoptosis and emphysema: a role for sphingolipid homeostasis in the maintenance of alveolar cells. *Proc Am Thorac Soc* 2006, 3(6):510.
34. Snider GL, Stone PJ, Lucey EC, Breuer R, Calore JD, Seshadri T, Catanese A, Maschler R, Schnebli HP: Eglin-c, a polypeptide derived from the medicinal leech, prevents human neutrophil elastase-induced emphysema and bronchial secretory cell metaplasia in the hamster. *Am Rev Respir Dis* 1985, 132(6):1155-1161.
35. Kao RC, Wehner NG, Skubitz KM, Gray BH, Hoidal JR: Proteinase 3. A distinct human polymorphonuclear leukocyte proteinase that produces emphysema in hamsters. *J Clin Invest* 1988, 82(6):1963-1973.
36. Guenter CA, Coalson JJ, Jacques J: Emphysema associated with intravascular leukocyte sequestration. Comparison with papain-induced emphysema. *Am Rev Respir Dis* 1981, 123(1):79-84.
37. Sommerhoff CP, Nadel JA, Basbaum CB, Caughey GH: Neutrophil elastase and cathepsin G stimulate secretion from cultured bovine airway gland serous cells. *J Clin Invest* 1990, 85(3):682-689.
38. Finlay GA, O'Driscoll LR, Russell KJ, D'Arcy EM, Masterson JB, FitzGerald MX, O'Connor CM: Matrix metalloproteinase expression and production by alveolar macrophages in emphysema. *Am J Respir Crit Care Med* 1997, 156(1):240-247.
39. Campbell EJ, White RR, Senior RM, Rodriguez RJ, Kuhn C: Receptor-mediated binding and internalization of leukocyte elastase by alveolar macrophages in vitro. *The Journal of clinical investigation* 1979, 64(3):824-833.
40. Miravitlles M: Alpha-1-antitrypsin and other proteinase inhibitors. *Current opinion in pharmacology* 2012.
41. Turino GM, Seniorrm, Garg BD, Keller S, Levi MM, Mandl I: Serum elastase inhibitor deficiency and alpha 1-antitrypsin deficiency in patients with obstructive emphysema. *Science* 1969, 165(3894):709-711.
42. Campos M, Shmuels D, Walsh J: Detection of Alpha-1 Antitrypsin Deficiency in the US. *The American journal of medicine* 2012.

43.	Valko M, Leibfritz D, Moncol J, Cronin MT, Mazur M, Telser J: Free radicals and antioxidants in normal physiological functions and human disease. *Int J Biochem Cell Biol* 2007, 39(1):44-84.

44.	Halliwell B: Oxidative stress and cancer: have we moved forward? *Biochem J* 2007, 401(1):1-11.

45.	Ramond A, Godin-Ribuot D, Ribuot C, Totoson P, Koritchneva I, Cachot S, Levy P, Joyeux-Faure M: Oxidative stress mediates cardiac infarction aggravation induced by intermittent hypoxia. *Fundamental & clinical pharmacology* 2011.

46.	MacNee W: Oxidants/antioxidants and COPD. *Chest* 2000, 117(5 Suppl 1):303S-317S.

47.	Pryor WA, Stone K: Oxidants in cigarette smoke. Radicals, hydrogen peroxide, peroxynitrate, and peroxynitrite. *Ann N Y Acad Sci* 1993, 686:12-27; discussion 27-18.

48.	Church DF, Pryor WA: Free-radical chemistry of cigarette smoke and its toxicological implications. *Environmental health perspectives* 1985, 64:111-126.

49.	Rahman I, MacNee W: Role of oxidants/antioxidants in smoking-induced lung diseases. *Free radical biology & medicine* 1996, 21(5):669-681.

50.	Schweitzer KS, Hatoum H, Brown MB, Gupta M, Justice MJ, Beteck B, Van Demark M, Gu Y, Presson RG, Jr., Hubbard WC *et al*: Mechanisms of lung endothelial barrier disruption induced by cigarette smoke: role of oxidative stress and ceramides. *Am J Physiol Lung Cell Mol Physiol* 2011, 301(6):L836-846.

51.	Lavrentiadou SN, Chan C, Kawcak T, Ravid T, Tsaba A, van der Vliet A, Rasooly R, Goldkorn T: Ceramide-mediated apoptosis in lung epithelial cells is regulated by glutathione. *Am J Respir Cell Mol Biol* 2001, 25(6):676-684.

52.	Kolesnick R, Fuks Z: Radiation and ceramide-induced apoptosis. *Oncogene* 2003, 22(37):5897-5906.

53.	Hannun YA, Obeid LM: The Ceramide-centric universe of lipid-mediated cell regulation: stress encounters of the lipid kind. *J Biol Chem* 2002, 277(29):25847-25850.

54.	Hannun YA, Luberto C: Ceramide in the eukaryotic stress response. *Trends Cell Biol* 2000, 10(2):73-80.

55.	Tuder RM, McGrath S, Neptune E: The pathobiological mechanisms of emphysema models: what do they have in common? *Pulm Pharmacol Ther* 2003, 16(2):67-78.

56.	Hanada K: Serine palmitoyltransferase, a key enzyme of sphingolipid metabolism. *Biochim Biophys Acta* 2003, 1632(1-3):16-30.

57.	Pruett ST, Bushnev A, Hagedorn K, Adiga M, Haynes CA, Sullards MC, Liotta DC, Merrill AH, Jr.: Biodiversity of sphingoid bases ("sphingosines") and related amino alcohols. *J Lipid Res* 2008, 49(8):1621-1639.

58.	Merrill AH, Jr., Williams RD: Utilization of different fatty acyl-CoA thioesters by serine palmitoyltransferase from rat brain. *J Lipid Res* 1984, 25(2):185-188.

59. Zitomer NC, Mitchell T, Voss KA, Bondy GS, Pruett ST, Garnier-Amblard EC, Liebeskind LS, Park H, Wang E, Sullards MC *et al*: Ceramide synthase inhibition by fumonisin B1 causes accumulation of 1-deoxysphinganine: a novel category of bioactive 1-deoxysphingoid bases and 1-deoxydihydroceramides biosynthesized by mammalian cell lines and animals. *J Biol Chem* 2009, 284(8):4786-4795.

60. Hojjati MR, Li Z, Jiang XC: Serine palmitoyl-CoA transferase (SPT) deficiency and sphingolipid levels in mice. *Biochim Biophys Acta* 2005, 1737(1):44-51.

61. Batheja AD, Uhlinger DJ, Carton JM, Ho G, D'Andrea MR: Characterization of serine palmitoyltransferase in normal human tissues. *J Histochem Cytochem* 2003, 51(5):687-696.

62. Yasuda S, Nishijima M, Hanada K: Localization, topology, and function of the LCB1 subunit of serine palmitoyltransferase in mammalian cells. *J Biol Chem* 2003, 278(6):4176-4183.

63. Hornemann T, Penno A, Rutti MF, Ernst D, Kivrak-Pfiffner F, Rohrer L, von Eckardstein A: The SPTLC3 subunit of serine palmitoyltransferase generates short chain sphingoid bases. *J Biol Chem* 2009, 284(39):26322-26330.

64. Bayes M, Goldaracena B, Martinez-Mir A, Iragui-Madoz MI, Solans T, Chivelet P, Bussaglia E, Ramos-Arroyo MA, Baiget M, Vilageliu L *et al*: A new autosomal recessive retinitis pigmentosa locus maps on chromosome 2q31-q33. *Journal of medical genetics* 1998, 35(2):141-145.

65. Hjelmqvist L, Tuson M, Marfany G, Herrero E, Balcells S, Gonzalez-Duarte R: ORMDL proteins are a conserved new family of endoplasmic reticulum membrane proteins. *Genome biology* 2002, 3(6):RESEARCH0027.

66. Moffatt MF, Kabesch M, Liang L, Dixon AL, Strachan D, Heath S, Depner M, von Berg A, Bufe A, Rietschel E *et al*: Genetic variants regulating ORMDL3 expression contribute to the risk of childhood asthma. *Nature* 2007, 448(7152):470-473.

67. Tafesse FG, Holthuis JC: Cell biology: A brake on lipid synthesis. *Nature* 2010, 463(7284):1028-1029.

68. Roelants FM, Breslow DK, Muir A, Weissman JS, Thorner J: Protein kinase Ypk1 phosphorylates regulatory proteins Orm1 and Orm2 to control sphingolipid homeostasis in Saccharomyces cerevisiae. *Proc Natl Acad Sci U S A* 2011, 108(48):19222-19227.

69. Merrill AH, Jr.: De novo sphingolipid biosynthesis: a necessary, but dangerous, pathway. *J Biol Chem* 2002, 277(29):25843-25846.

70. Futerman AH, Riezman H: The ins and outs of sphingolipid synthesis. *Trends Cell Biol* 2005, 15(6):312-318.

71. Pewzner-Jung Y, Ben-Dor S, Futerman AH: When do Lasses (longevity assurance genes) become CerS (ceramide synthases)?: Insights into the regulation of ceramide synthesis. *J Biol Chem* 2006, 281(35):25001-25005.

72. Guillas I, Kirchman PA, Chuard R, Pfefferli M, Jiang JC, Jazwinski SM, Conzelmann A: C26-CoA-dependent ceramide synthesis of Saccharomyces cerevisiae is operated by Lag1p and Lac1p. *EMBO J* 2001, 20(11):2655-2665.

73. Schorling S, Vallee B, Barz WP, Riezman H, Oesterhelt D: Lag1p and Lac1p are essential for the Acyl-CoA-dependent ceramide synthase reaction in Saccharomyces cerevisae. *Mol Biol Cell* 2001, 12(11):3417-3427.

74. Winter E, Ponting CP: TRAM, LAG1 and CLN8: members of a novel family of lipid-sensing domains? *Trends in biochemical sciences* 2002, 27(8):381-383.

75. Guillas I, Jiang JC, Vionnet C, Roubaty C, Uldry D, Chuard R, Wang J, Jazwinski SM, Conzelmann A: Human homologues of LAG1 reconstitute Acyl-CoA-dependent ceramide synthesis in yeast. *J Biol Chem* 2003, 278(39):37083-37091.

76. Kageyama-Yahara N, Riezman H: Transmembrane topology of ceramide synthase in yeast. *Biochem J* 2006, 398(3):585-593.

77. Medler TR, Petrusca DN, Lee PJ, Hubbard WC, Berdyshev EV, Skirball J, Kamocki K, Schuchman E, Tuder RM, Petrache I: Apoptotic sphingolipid signaling by ceramides in lung endothelial cells. *Am J Respir Cell Mol Biol* 2008, 38(6):639-646.

78. Spassieva S, Seo JG, Jiang JC, Bielawski J, Alvarez-Vasquez F, Jazwinski SM, Hannun YA, Obeid LM: Necessary role for the Lag1p motif in (dihydro)ceramide synthase activity. *J Biol Chem* 2006, 281(45):33931-33938.

79. Mesika A, Ben-Dor S, Laviad EL, Futerman AH: A new functional motif in Hox domain-containing ceramide synthases: identification of a novel region flanking the Hox and TLC domains essential for activity. *J Biol Chem* 2007, 282(37):27366-27373.

80. Mandon EC, Ehses I, Rother J, van Echten G, Sandhoff K: Subcellular localization and membrane topology of serine palmitoyltransferase, 3-dehydrosphinganine reductase, and sphinganine N-acyltransferase in mouse liver. *J Biol Chem* 1992, 267(16):11144-11148.

81. Mizutani Y, Kihara A, Igarashi Y: Mammalian Lass6 and its related family members regulate synthesis of specific ceramides. *Biochem J* 2005, 390(Pt 1):263-271.

82. Venkataraman K, Futerman AH: Do longevity assurance genes containing Hox domains regulate cell development via ceramide synthesis? *FEBS Lett* 2002, 528(1-3):3-4.

83. Riebeling C, Allegood JC, Wang E, Merrill AH, Jr., Futerman AH: Two mammalian longevity assurance gene (LAG1) family members, trh1 and trh4, regulate dihydroceramide synthesis using different fatty acyl-CoA donors. *J Biol Chem* 2003, 278(44):43452-43459.

84. Lahiri S, Lee H, Mesicek J, Fuks Z, Haimovitz-Friedman A, Kolesnick RN, Futerman AH: Kinetic characterization of mammalian ceramide synthases: determination of K(m) values towards sphinganine. *FEBS Lett* 2007, 581(27):5289-5294.

85. Mizutani Y, Kihara A, Igarashi Y: LASS3 (longevity assurance homologue 3) is a mainly testis-specific (dihydro)ceramide synthase with relatively broad substrate specificity. *Biochem J* 2006, 398(3):531-538.

86. Becker I, Wang-Eckhardt L, Yaghootfam A, Gieselmann V, Eckhardt M: Differential expression of (dihydro)ceramide synthases in mouse brain: oligodendrocyte-specific expression of CerS2/Lass2. *Histochemistry and cell biology* 2008, 129(2):233-241.

87. Cai XF, Tao Z, Yan ZQ, Yang SL, Gong Y: Molecular cloning, characterisation and tissue-specific expression of human LAG3, a member of the novel Lag1 protein family. *DNA sequence : the journal of DNA sequencing and mapping* 2003, 14(2):79-86.

88. Laviad EL, Albee L, Pankova-Kholmyansky I, Epstein S, Park H, Merrill AH, Jr., Futerman AH: Characterization of ceramide synthase 2: tissue distribution, substrate specificity, and inhibition by sphingosine 1-phosphate. *J Biol Chem* 2008, 283(9):5677-5684.

89. Rabionet M, van der Spoel AC, Chuang CC, von Tumpling-Radosta B, Litjens M, Bouwmeester D, Hellbusch CC, Korner C, Wiegandt H, Gorgas K *et al*: Male germ cells require polyenoic sphingolipids with complex glycosylation for completion of meiosis: a link to ceramide synthase-3. *J Biol Chem* 2008, 283(19):13357-13369.

90. Mizutani Y, Kihara A, Chiba H, Tojo H, Igarashi Y: 2-Hydroxy-ceramide synthesis by ceramide synthase family: enzymatic basis for the preference of FA chain length. *J Lipid Res* 2008, 49(11):2356-2364.

91. Coderch L, Lopez O, de la Maza A, Parra JL: Ceramides and skin function. *American journal of clinical dermatology* 2003, 4(2):107-129.

92. Wang G, Silva J, Dasgupta S, Bieberich E: Long-chain ceramide is elevated in presenilin 1 (PS1M146V) mouse brain and induces apoptosis in PS1 astrocytes. *Glia* 2008, 56(4):449-456.

93. Xu Z, Zhou J, McCoy DM, Mallampalli RK: LASS5 is the predominant ceramide synthase isoform involved in de novo sphingolipid synthesis in lung epithelia. *J Lipid Res* 2005, 46(6):1229-1238.

94. Weinmann A, Galle PR, Teufel A: LASS6, an additional member of the longevity assurance gene family. *International journal of molecular medicine* 2005, 16(5):905-910.

95. Schiffmann S, Sandner J, Birod K, Wobst I, Angioni C, Ruckhaberle E, Kaufmann M, Ackermann H, Lotsch J, Schmidt H *et al*: Ceramide synthases and ceramide levels are increased in breast cancer tissue. *Carcinogenesis* 2009, 30(5):745-752.

96. Erez-Roman R, Pienik R, Futerman AH: Increased ceramide synthase 2 and 6 mRNA levels in breast cancer tissues and correlation with sphingosine kinase expression. *Biochem Biophys Res Commun* 2010, 391(1):219-223.

97. Laviad EL, Kelly S, Merrill AH, Jr., Futerman AH: Modulation of Ceramide Synthase Activity via Dimerization. *J Biol Chem* 2012, 287(25):21025-21033.

98. Michel C, van Echten-Deckert G, Rother J, Sandhoff K, Wang E, Merrill AH, Jr.: Characterization of ceramide synthesis. A dihydroceramide desaturase introduces the 4,5-trans-double bond of sphingosine at the level of dihydroceramide. *J Biol Chem* 1997, 272(36):22432-22437.

99. Geeraert L, Mannaerts GP, van Veldhoven PP: Conversion of dihydroceramide into ceramide: involvement of a desaturase. *Biochem J* 1997, 327 (Pt 1):125-132.

100. Mikami T, Kashiwagi M, Tsuchihashi K, Akino T, Gasa S: Substrate specificity and some other enzymatic properties of dihydroceramide desaturase (ceramide synthase) in fetal rat skin. *J Biochem* 1998, 123(5):906-911.

101. Idkowiak-Baldys J, Apraiz A, Li L, Rahmaniyan M, Clarke CJ, Kraveka JM, Asumendi A, Hannun YA: Dihydroceramide desaturase activity is modulated by oxidative stress. *Biochem J* 2010, 427(2):265-274.

102. Devlin CM, Lahm T, Hubbard WC, Van Demark M, Wang KC, Wu X, Bielawska A, Obeid LM, Ivan M, Petrache I: Dihydroceramide-based response to hypoxia. *J Biol Chem* 2011, 286(44):38069-38078.

103. Munoz-Olaya JM, Matabosch X, Bedia C, Egido-Gabas M, Casas J, Llebaria A, Delgado A, Fabrias G: Synthesis and biological activity of a novel inhibitor of dihydroceramide desaturase. *ChemMedChem* 2008, 3(6):946-953.

104. Kanfer JN, Young OM, Shapiro D, Brady RO: The metabolism of sphingomyelin. I. Purification and properties of a sphingomyelin-cleaving enzyme from rat liver tissue. *J Biol Chem* 1966, 241(5):1081-1084.

105. Goni FM, Alonso A: Sphingomyelinases: enzymology and membrane activity. *FEBS Lett* 2002, 531(1):38-46.

106. Duan RD: Alkaline sphingomyelinase: an old enzyme with novel implications. *Biochim Biophys Acta* 2006, 1761(3):281-291.

107. Marchesini N, Hannun YA: Acid and neutral sphingomyelinases: roles and mechanisms of regulation. *Biochemistry and cell biology = Biochimie et biologie cellulaire* 2004, 82(1):27-44.

108. Gatt S: Enzymic Hydrolysis and Synthesis of Ceramides. *J Biol Chem* 1963, 238:3131-3133.

109. Brady RO, Kanfer JN, Mock MB, Fredrickson DS: The metabolism of sphingomyelin. II. Evidence of an enzymatic deficiency in Niemann-Pick diseae. *Proc Natl Acad Sci U S A* 1966, 55(2):366-369.

110. Horinouchi K, Erlich S, Perl DP, Ferlinz K, Bisgaier CL, Sandhoff K, Desnick RJ, Stewart CL, Schuchman EH: Acid sphingomyelinase deficient mice: a model of types A and B Niemann-Pick disease. *Nat Genet* 1995, 10(3):288-293.

111. Schuchman EH, Levran O, Pereira LV, Desnick RJ: Structural organization and complete nucleotide sequence of the gene encoding human acid sphingomyelinase (SMPD1). *Genomics* 1992, 12(2):197-205.

112. Spence MW, Byers DM, Palmer FB, Cook HW: A new Zn2+-stimulated sphingomyelinase in fetal bovine serum. *J Biol Chem* 1989, 264(10):5358-5363.
113. Smith EL, Schuchman EH: The unexpected role of acid sphingomyelinase in cell death and the pathophysiology of common diseases. *FASEB J* 2008, 22(10):3419-3431.
114. Tabas I: Secretory sphingomyelinase. *Chem Phys Lipids* 1999, 102(1-2):123-130.
115. Krut O, Wiegmann K, Kashkar H, Yazdanpanah B, Kronke M: Novel tumor necrosis factor-responsive mammalian neutral sphingomyelinase-3 is a C-tail-anchored protein. *J Biol Chem* 2006, 281(19):13784-13793.
116. Tani M, Ito M, Igarashi Y: Ceramide/sphingosine/sphingosine 1-phosphate metabolism on the cell surface and in the extracellular space. *Cell Signal* 2007, 19(2):229-237.
117. Andrieu-Abadie N, Levade T: Sphingomyelin hydrolysis during apoptosis. *Biochim Biophys Acta* 2002, 1585(2-3):126-134.
118. Hofmann K, Tomiuk S, Wolff G, Stoffel W: Cloning and characterization of the mammalian brain-specific, Mg2+-dependent neutral sphingomyelinase. *Proc Natl Acad Sci U S A* 2000, 97(11):5895-5900.
119. Tomiuk S, Hofmann K, Nix M, Zumbansen M, Stoffel W: Cloned mammalian neutral sphingomyelinase: functions in sphingolipid signaling? *Proc Natl Acad Sci U S A* 1998, 95(7):3638-3643.
120. Clarke CJ, Snook CF, Tani M, Matmati N, Marchesini N, Hannun YA: The extended family of neutral sphingomyelinases. *Biochemistry* 2006, 45(38):11247-11256.
121. Zumbansen M, Stoffel W: Neutral sphingomyelinase 1 deficiency in the mouse causes no lipid storage disease. *Molecular and cellular biology* 2002, 22(11):3633-3638.
122. Stoffel W, Jenke B, Holz B, Binczek E, Gunter RH, Knifka J, Koebke J, Niehoff A: Neutral sphingomyelinase (SMPD3) deficiency causes a novel form of chondrodysplasia and dwarfism that is rescued by Col2A1-driven smpd3 transgene expression. *Am J Pathol* 2007, 171(1):153-161.
123. Levy M, Castillo SS, Goldkorn T: nSMase2 activation and trafficking are modulated by oxidative stress to induce apoptosis. *Biochem Biophys Res Commun* 2006, 344(3):900-905.
124. Levy M, Khan E, Careaga M, Goldkorn T: Neutral sphingomyelinase 2 is activated by cigarette smoke to augment ceramide-induced apoptosis in lung cell death. *Am J Physiol Lung Cell Mol Physiol* 2009, 297(1):L125-133.
125. Filosto S, Castillo S, Danielson A, Franzi L, Khan E, Kenyon N, Last J, Pinkerton K, Tuder R, Goldkorn T: Neutral sphingomyelinase 2: a novel target in cigarette smoke-induced apoptosis and lung injury. *Am J Respir Cell Mol Biol* 2011, 44(3):350-360.
126. Filosto S, Fry W, Knowlton AA, Goldkorn T: Neutral sphingomyelinase 2 (nSMase2) is a phosphoprotein regulated by calcineurin (PP2B). *J Biol Chem* 2010, 285(14):10213-10222.

127. Filosto S, Ashfaq M, Chung S, Fry W, Goldkorn T: Neutral sphingomyelinase 2 activity and protein stability are modulated by phosphorylation of five conserved serines. *J Biol Chem* 2012, 287(1):514-522.
128. Castillo SS, Levy M, Thaikoottathil JV, Goldkorn T: Reactive nitrogen and oxygen species activate different sphingomyelinases to induce apoptosis in airway epithelial cells. *Exp Cell Res* 2007, 313(12):2680-2686.
129. Valsecchi M, Mauri L, Casellato R, Prioni S, Loberto N, Prinetti A, Chigorno V, Sonnino S: Ceramide and sphingomyelin species of fibroblasts and neurons in culture. *J Lipid Res* 2007, 48(2):417-424.
130. Luberto C, Stonehouse MJ, Collins EA, Marchesini N, El-Bawab S, Vasil AI, Vasil ML, Hannun YA: Purification, characterization, and identification of a sphingomyelin synthase from Pseudomonas aeruginosa. PlcH is a multifunctional enzyme. *J Biol Chem* 2003, 278(35):32733-32743.
131. van Helvoort A, van't Hof W, Ritsema T, Sandra A, van Meer G: Conversion of diacylglycerol to phosphatidylcholine on the basolateral surface of epithelial (Madin-Darby canine kidney) cells. Evidence for the reverse action of a sphingomyelin synthase. *J Biol Chem* 1994, 269(3):1763-1769.
132. Yeang C, Varshney S, Wang R, Zhang Y, Ye D, Jiang XC: The domain responsible for sphingomyelin synthase (SMS) activity. *Biochim Biophys Acta* 2008, 1781(10):610-617.
133. Ternes P, Brouwers JF, van den Dikkenberg J, Holthuis JC: Sphingomyelin synthase SMS2 displays dual activity as ceramide phosphoethanolamine synthase. *J Lipid Res* 2009, 50(11):2270-2277.
134. Yeang C, Ding T, Chirico WJ, Jiang XC: Subcellular targeting domains of sphingomyelin synthase 1 and 2. *Nutrition & metabolism* 2011, 8:89.
135. Albi E, Magni MV: Sphingomyelin synthase in rat liver nuclear membrane and chromatin. *FEBS Lett* 1999, 460(2):369-372.
136. Yang Z, Khoury C, Jean-Baptiste G, Greenwood MT: Identification of mouse sphingomyelin synthase 1 as a suppressor of Bax-mediated cell death in yeast. *FEMS yeast research* 2006, 6(5):751-762.
137. Separovic D, Semaan L, Tarca AL, Awad Maitah MY, Hanada K, Bielawski J, Villani M, Luberto C: Suppression of sphingomyelin synthase 1 by small interference RNA is associated with enhanced ceramide production and apoptosis after photodamage. *Exp Cell Res* 2008, 314(8):1860-1868.
138. Yano M, Watanabe K, Yamamoto T, Ikeda K, Senokuchi T, Lu M, Kadomatsu T, Tsukano H, Ikawa M, Okabe M *et al*: Mitochondrial dysfunction and increased reactive oxygen species impair insulin secretion in sphingomyelin synthase 1-null mice. *The Journal of biological chemistry* 2011, 286(5):3992-4002.
139. Tafesse FG, Ternes P, Holthuis JC: The multigenic sphingomyelin synthase family. *J Biol Chem* 2006, 281(40):29421-29425.

140. Wang X, Dong J, Zhao Y, Li Y, Wu M: Adenovirus-mediated sphingomyelin synthase 2 increases atherosclerotic lesions in ApoE KO mice. *Lipids in health and disease* 2011, 10:7.

141. Hailemariam TK, Huan C, Liu J, Li Z, Roman C, Kalbfeisch M, Bui HH, Peake DA, Kuo MS, Cao G *et al*: Sphingomyelin synthase 2 deficiency attenuates NFkappaB activation. *Arteriosclerosis, thrombosis, and vascular biology* 2008, 28(8):1519-1526.

142. Liu J, Huan C, Chakraborty M, Zhang H, Lu D, Kuo MS, Cao G, Jiang XC: Macrophage sphingomyelin synthase 2 deficiency decreases atherosclerosis in mice. *Circulation research* 2009, 105(3):295-303.

143. Zhang Y, Dong J, Zhu X, Wang W, Yang Q: The effect of sphingomyelin synthase 2 (SMS2) deficiency on the expression of drug transporters in mouse brain. *Biochemical pharmacology* 2011, 82(3):287-294.

144. Vivekananda J, Smith D, King RJ: Sphingomyelin metabolites inhibit sphingomyelin synthase and CTP:phosphocholine cytidylyltransferase. *Am J Physiol Lung Cell Mol Physiol* 2001, 281(1):L98-L107.

145. Taguchi Y, Kondo T, Watanabe M, Miyaji M, Umehara H, Kozutsumi Y, Okazaki T: Interleukin-2-induced survival of natural killer (NK) cells involving phosphatidylinositol-3 kinase-dependent reduction of ceramide through acid sphingomyelinase, sphingomyelin synthase, and glucosylceramide synthase. *Blood* 2004, 104(10):3285-3293.

146. Wijesinghe DS, Massiello A, Subramanian P, Szulc Z, Bielawska A, Chalfant CE: Substrate specificity of human ceramide kinase. *J Lipid Res* 2005, 46(12):2706-2716.

147. Raas-Rothschild A, Pankova-Kholmyansky I, Kacher Y, Futerman AH: Glycosphingolipidoses: beyond the enzymatic defect. *Glycoconj J* 2004, 21(6):295-304.

148. Xu R, Jin J, Hu W, Sun W, Bielawski J, Szulc Z, Taha T, Obeid LM, Mao C: Golgi alkaline ceramidase regulates cell proliferation and survival by controlling levels of sphingosine and S1P. *FASEB J* 2006, 20(11):1813-1825.

149. Galadari S, Wu BX, Mao C, Roddy P, El Bawab S, Hannun YA: Identification of a novel amidase motif in neutral ceramidase. *Biochem J* 2006, 393(Pt 3):687-695.

150. Johnson KR, Johnson KY, Becker KP, Bielawski J, Mao C, Obeid LM: Role of human sphingosine-1-phosphate phosphatase 1 in the regulation of intra- and extracellular sphingosine-1-phosphate levels and cell viability. *J Biol Chem* 2003, 278(36):34541-34547.

151. Hait NC, Oskeritzian CA, Paugh SW, Milstien S, Spiegel S: Sphingosine kinases, sphingosine 1-phosphate, apoptosis and diseases. *Biochim Biophys Acta* 2006, 1758(12):2016-2026.

152. Bandhuvula P, Saba JD: Sphingosine-1-phosphate lyase in immunity and cancer: silencing the siren. *Trends in molecular medicine* 2007, 13(5):210-217.

153. Danial NN, Korsmeyer SJ: Cell death: critical control points. *Cell* 2004, 116(2):205-219.

154. Antonsson B: Mitochondria and the Bcl-2 family proteins in apoptosis signaling pathways. *Molecular and cellular biochemistry* 2004, 256-257(1-2):141-155.

155. Sharpe JC, Arnoult D, Youle RJ: Control of mitochondrial permeability by Bcl-2 family members. *Biochim Biophys Acta* 2004, 1644(2-3):107-113.

156. Green DR, Kroemer G: The pathophysiology of mitochondrial cell death. *Science* 2004, 305(5684):626-629.

157. Fadeel B, Orrenius S: Apoptosis: a basic biological phenomenon with wide-ranging implications in human disease. *Journal of internal medicine* 2005, 258(6):479-517.

158. Dejean LM, Martinez-Caballero S, Manon S, Kinnally KW: Regulation of the mitochondrial apoptosis-induced channel, MAC, by BCL-2 family proteins. *Biochim Biophys Acta* 2006, 1762(2):191-201.

159. Kerr JF, Wyllie AH, Currie AR: Apoptosis: a basic biological phenomenon with wide-ranging implications in tissue kinetics. *Br J Cancer* 1972, 26(4):239-257.

160. Hacker G: The morphology of apoptosis. *Cell and tissue research* 2000, 301(1):5-17.

161. Savill J, Fadok V: Corpse clearance defines the meaning of cell death. *Nature* 2000, 407(6805):784-788.

162. Kurosaka K, Takahashi M, Watanabe N, Kobayashi Y: Silent cleanup of very early apoptotic cells by macrophages. *J Immunol* 2003, 171(9):4672-4679.

163. Igney FH, Krammer PH: Death and anti-death: tumour resistance to apoptosis. *Nat Rev Cancer* 2002, 2(4):277-288.

164. Martinvalet D, Zhu P, Lieberman J: Granzyme A induces caspase-independent mitochondrial damage, a required first step for apoptosis. *Immunity* 2005, 22(3):355-370.

165. Hsu H, Xiong J, Goeddel DV: The TNF receptor 1-associated protein TRADD signals cell death and NF-kappa B activation. *Cell* 1995, 81(4):495-504.

166. Wajant H: The Fas signaling pathway: more than a paradigm. *Science* 2002, 296(5573):1635-1636.

167. Wajant H, Pfizenmaier K, Scheurich P: TNF-related apoptosis inducing ligand (TRAIL) and its receptors in tumor surveillance and cancer therapy. *Apoptosis* 2002, 7(5):449-459.

168. Kischkel FC, Hellbardt S, Behrmann I, Germer M, Pawlita M, Krammer PH, Peter ME: Cytotoxicity-dependent APO-1 (Fas/CD95)-associated proteins form a death-inducing signaling complex (DISC) with the receptor. *The EMBO journal* 1995, 14(22):5579-5588.

169. Elmore S: Apoptosis: a review of programmed cell death. *Toxicologic pathology* 2007, 35(4):495-516.

170. Chipuk JE, Moldoveanu T, Llambi F, Parsons MJ, Green DR: The BCL-2 family reunion. *Molecular cell* 2010, 37(3):299-310.

171.   Saelens X, Festjens N, Vande Walle L, van Gurp M, van Loo G, Vandenabeele P: Toxic proteins released from mitochondria in cell death. *Oncogene* 2004, 23(16):2861-2874.

172.   Du C, Fang M, Li Y, Li L, Wang X: Smac, a mitochondrial protein that promotes cytochrome c-dependent caspase activation by eliminating IAP inhibition. *Cell* 2000, 102(1):33-42.

173.   van Loo G, van Gurp M, Depuydt B, Srinivasula SM, Rodriguez I, Alnemri ES, Gevaert K, Vandekerckhove J, Declercq W, Vandenabeele P: The serine protease Omi/HtrA2 is released from mitochondria during apoptosis. Omi interacts with caspase-inhibitor XIAP and induces enhanced caspase activity. *Cell Death Differ* 2002, 9(1):20-26.

174.   Garrido C, Galluzzi L, Brunet M, Puig PE, Didelot C, Kroemer G: Mechanisms of cytochrome c release from mitochondria. *Cell Death Differ* 2006, 13(9):1423-1433.

175.   Chinnaiyan AM: The apoptosome: heart and soul of the cell death machine. *Neoplasia* 1999, 1(1):5-15.

176.   Schimmer AD, Welsh K, Pinilla C, Wang Z, Krajewska M, Bonneau MJ, Pedersen IM, Kitada S, Scott FL, Bailly-Maitre B *et al*: Small-molecule antagonists of apoptosis suppressor XIAP exhibit broad antitumor activity. *Cancer cell* 2004, 5(1):25-35.

177.   Joza N, Susin SA, Daugas E, Stanford WL, Cho SK, Li CY, Sasaki T, Elia AJ, Cheng HY, Ravagnan L *et al*: Essential role of the mitochondrial apoptosis-inducing factor in programmed cell death. *Nature* 2001, 410(6828):549-554.

178.   Li LY, Luo X, Wang X: Endonuclease G is an apoptotic DNase when released from mitochondria. *Nature* 2001, 412(6842):95-99.

179.   Susin SA, Daugas E, Ravagnan L, Samejima K, Zamzami N, Loeffler M, Costantini P, Ferri KF, Irinopoulou T, Prevost MC *et al*: Two distinct pathways leading to nuclear apoptosis. *J Exp Med* 2000, 192(4):571-580.

180.   Enari M, Sakahira H, Yokoyama H, Okawa K, Iwamatsu A, Nagata S: A caspase-activated DNase that degrades DNA during apoptosis, and its inhibitor ICAD. *Nature* 1998, 391(6662):43-50.

181.   Sakahira H, Enari M, Nagata S: Cleavage of CAD inhibitor in CAD activation and DNA degradation during apoptosis. *Nature* 1998, 391(6662):96-99.

182.   Kuwana T, Mackey MR, Perkins G, Ellisman MH, Latterich M, Schneiter R, Green DR, Newmeyer DD: Bid, Bax, and lipids cooperate to form supramolecular openings in the outer mitochondrial membrane. *Cell* 2002, 111(3):331-342.

183.   Lindsten T, Ross AJ, King A, Zong WX, Rathmell JC, Shiels HA, Ulrich E, Waymire KG, Mahar P, Frauwirth K *et al*: The combined functions of proapoptotic Bcl-2 family members bak and bax are essential for normal development of multiple tissues. *Molecular cell* 2000, 6(6):1389-1399.

184. Wei MC, Zong WX, Cheng EH, Lindsten T, Panoutsakopoulou V, Ross AJ, Roth KA, MacGregor GR, Thompson CB, Korsmeyer SJ: Proapoptotic BAX and BAK: a requisite gateway to mitochondrial dysfunction and death. *Science* 2001, 292(5517):727-730.

185. Green DR, Chipuk JE: Apoptosis: Stabbed in the BAX. *Nature* 2008, 455(7216):1047-1049.

186. Chipuk JE, Fisher JC, Dillon CP, Kriwacki RW, Kuwana T, Green DR: Mechanism of apoptosis induction by inhibition of the anti-apoptotic BCL-2 proteins. *Proc Natl Acad Sci U S A* 2008, 105(51):20327-20332.

187. Kuwana T, Bouchier-Hayes L, Chipuk JE, Bonzon C, Sullivan BA, Green DR, Newmeyer DD: BH3 domains of BH3-only proteins differentially regulate Bax-mediated mitochondrial membrane permeabilization both directly and indirectly. *Molecular cell* 2005, 17(4):525-535.

188. Letai A, Bassik MC, Walensky LD, Sorcinelli MD, Weiler S, Korsmeyer SJ: Distinct BH3 domains either sensitize or activate mitochondrial apoptosis, serving as prototype cancer therapeutics. *Cancer cell* 2002, 2(3):183-192.

189. Slee EA, Adrain C, Martin SJ: Executioner caspase-3, -6, and -7 perform distinct, non-redundant roles during the demolition phase of apoptosis. *J Biol Chem* 2001, 276(10):7320-7326.

190. Gulbins E: Regulation of death receptor signaling and apoptosis by ceramide. *Pharmacol Res* 2003, 47(5):393-399.

191. Ruvolo PP, Deng X, Ito T, Carr BK, May WS: Ceramide induces Bcl2 dephosphorylation via a mechanism involving mitochondrial PP2A. *J Biol Chem* 1999, 274(29):20296-20300.

192. Heinrich M, Wickel M, Winoto-Morbach S, Schneider-Brachert W, Weber T, Brunner J, Saftig P, Peters C, Kronke M, Schutze S: Ceramide as an activator lipid of cathepsin D. *Adv Exp Med Biol* 2000, 477:305-315.

193. Stromhaug PE, Klionsky DJ: Approaching the molecular mechanism of autophagy. *Traffic* 2001, 2(8):524-531.

194. Kundu M, Thompson CB: Autophagy: basic principles and relevance to disease. *Annual review of pathology* 2008, 3:427-455.

195. Petrusca DN, Gu Y, Adamowicz JJ, Rush NI, Hubbard WC, Smith PA, Berdyshev EV, Birukov KG, Lee CH, Tuder RM *et al*: Sphingolipid-mediated inhibition of apoptotic cell clearance by alveolar macrophages. *J Biol Chem* 2010, 285(51):40322-40332.

196. Monick MM, Carter AB, Robeff PK, Flaherty DM, Peterson MW, Hunninghake GW: Lipopolysaccharide activates Akt in human alveolar macrophages resulting in nuclear accumulation and transcriptional activity of beta-catenin. *J Immunol* 2001, 166(7):4713-4720.

197. Yvan-Charvet L, Pagler TA, Seimon TA, Thorp E, Welch CL, Witztum JL, Tabas I, Tall AR: ABCA1 and ABCG1 protect against oxidative stress-induced macrophage apoptosis during efferocytosis. *Circ Res* 2010, 106(12):1861-1869.

198. Siskind LJ: Mitochondrial ceramide and the induction of apoptosis. *J Bioenerg Biomembr* 2005, 37(3):143-153.

199. Li H, Junk P, Huwiler A, Burkhardt C, Wallerath T, Pfeilschifter J, Forstermann U: Dual effect of ceramide on human endothelial cells: induction of oxidative stress and transcriptional upregulation of endothelial nitric oxide synthase. *Circulation* 2002, 106(17):2250-2256.
200. Didion SP, Faraci FM: Ceramide-induced impairment of endothelial function is prevented by CuZn superoxide dismutase overexpression. *Arterioscler Thromb Vasc Biol* 2005, 25(1):90-95.
201. Petrache I, Medler TR, Richter AT, Kamocki K, Chukwueke U, Zhen L, Gu Y, Adamowicz J, Schweitzer KS, Hubbard WC *et al*: Superoxide dismutase protects against apoptosis and alveolar enlargement induced by ceramide. *Am J Physiol Lung Cell Mol Physiol* 2008, 295(1):L44-53.
202. Spyridopoulos I, Mayer P, Shook KS, Axel DI, Viebahn R, Karsch KR: Loss of cyclin A and G1-cell cycle arrest are a prerequisite of ceramide-induced toxicity in human arterial endothelial cells. *Cardiovasc Res* 2001, 50(1):97-107.
203. Smith EL, Schuchman EH: Acid sphingomyelinase overexpression enhances the antineoplastic effects of irradiation in vitro and in vivo. *Mol Ther* 2008, 16(9):1565-1571.
204. Gupta N, Nodzenski E, Khodarev NN, Yu J, Khorasani L, Beckett MA, Kufe DW, Weichselbaum RR: Angiostatin effects on endothelial cells mediated by ceramide and RhoA. *EMBO Rep* 2001, 2(6):536-540.
205. Venable ME, Yin X: Ceramide induces endothelial cell senescence. *Cell Biochem Funct* 2009, 27(8):547-551.
206. Haimovitz-Friedman A, Cordon-Cardo C, Bayoumy S, Garzotto M, McLoughlin M, Gallily R, Edwards CK, 3rd, Schuchman EH, Fuks Z, Kolesnick R: Lipopolysaccharide induces disseminated endothelial apoptosis requiring ceramide generation. *J Exp Med* 1997, 186(11):1831-1841.
207. Kuebler WM, Yang Y, Samapati R, Uhlig S: Vascular barrier regulation by PAF, ceramide, caveolae, and NO - an intricate signaling network with discrepant effects in the pulmonary and systemic vasculature. *Cell Physiol Biochem*, 26(1):29-40.
208. Lindner K, Uhlig U, Uhlig S: Ceramide alters endothelial cell permeability by a nonapoptotic mechanism. *Br J Pharmacol* 2005, 145(1):132-140.
209. Petrache I, Verin AD, Crow MT, Birukova A, Liu F, Garcia JG: Differential effect of MLC kinase in TNF-alpha-induced endothelial cell apoptosis and barrier dysfunction. *Am J Physiol Lung Cell Mol Physiol* 2001, 280(6):L1168-1178.
210. Diab KJ, Adamowicz JJ, Kamocki K, Rush NI, Garrison J, Gu Y, Schweitzer KS, Skobeleva A, Rajashekhar G, Hubbard WC *et al*: Stimulation of sphingosine 1-phosphate signaling as an alveolar cell survival strategy in emphysema. *Am J Respir Crit Care Med* 2010, 181(4):344-352.

211. Le A, Zielinski R, He C, Crow MT, Biswal S, Tuder RM, Becker PM: Pulmonary epithelial neuropilin-1 deletion enhances development of cigarette smoke-induced emphysema. *Am J Respir Crit Care Med* 2009, 180(5):396-406.
212. Cantin AM: Cellular response to cigarette smoke and oxidants: adapting to survive. *Proc Am Thorac Soc* 2010, 7(6):368-375.
213. Bodas M, Min T, Vij N: Critical role of CFTR dependent lipid-rafts in cigarette smoke induced lung epithelial injury. *Am J Physiol Lung Cell Mol Physiol*.
214. Filosto S, Castillo S, Danielson A, Franzi L, Khan E, Kenyon N, Last J, Pinkerton K, Tuder R, Goldkorn T: Neutral sphingomyelinase 2: a novel target in cigarette smoke-induced apoptosis and lung injury. *Am J Respir Cell Mol Biol*, 44(3):350-360.
215. Levy M, Khan E, Careaga M, Goldkorn T: Neutral sphingomyelinase 2 is activated by cigarette smoke to augment ceramide-induced apoptosis in lung cell death. *Am J Physiol Lung Cell Mol Physiol* 2009.
216. Bodas M, Min T, Mazur S, Vij N: Critical modifier role of membrane-cystic fibrosis transmembrane conductance regulator-dependent ceramide signaling in lung injury and emphysema. *J Immunol*, 186(1):602-613.
217. Noe J, Petrusca D, Rush N, Deng P, Vandemark M, Berdyshev E, Gu Y, Smith P, Schweitzer K, Pilewsky J *et al*: CFTR Regulation of Intracellular pH and Ceramides is Required for Lung Endothelial Cell Apoptosis. *Am J Respir Cell Mol Biol* 2009.
218. Gulbins E, Grassme H: Ceramide and cell death receptor clustering. *Biochim Biophys Acta* 2002, 1585(2-3):139-145.
219. Teichgraber V, Ulrich M, Endlich N, Riethmuller J, Wilker B, De Oliveira-Munding CC, van Heeckeren AM, Barr ML, von Kurthy G, Schmid KW *et al*: Ceramide accumulation mediates inflammation, cell death and infection susceptibility in cystic fibrosis. *Nature medicine* 2008, 14(4):382-391.
220. Petrusca DN, Gu Y, Adamowicz JJ, Rush NI, Hubbard WC, Smith PA, Berdyshev EV, Birukov KG, Lee CH, Tuder RM *et al*: Sphingolipid-mediated inhibition of apoptotic cell clearance by alveolar macrophages. *J Biol Chem*, 285(51):40322-40332.
221. Vandivier RW, Henson PM, Douglas IS: Burying the dead: the impact of failed apoptotic cell removal (efferocytosis) on chronic inflammatory lung disease. *Chest* 2006, 129(6):1673-1682.
222. Uhlig S, Gulbins E: Sphingolipids in the lungs. *Am J Respir Crit Care Med* 2008, 178(11):1100-1114.
223. Saba JD, Hla T: Point-counterpoint of sphingosine 1-phosphate metabolism. *Circ Res* 2004, 94(6):724-734.
224. Berdyshev EV, Gorshkova I, Usatyuk P, Kalari S, Zhao Y, Pyne NJ, Pyne S, Sabbadini RA, Garcia JG, Natarajan V: Intracellular S1P generation is essential for S1P-induced motility of human lung endothelial cells: role of sphingosine kinase 1 and S1P lyase. *PLoS One*, 6(1):e16571.

225. Singleton PA, Dudek SM, Chiang ET, Garcia JG: Regulation of sphingosine 1-phosphate-induced endothelial cytoskeletal rearrangement and barrier enhancement by S1P1 receptor, PI3 kinase, Tiam1/Rac1, and alpha-actinin. *FASEB J* 2005, 19(12):1646-1656.
226. Sanchez T, Skoura A, Wu MT, Casserly B, Harrington EO, Hla T: Induction of vascular permeability by the sphingosine-1-phosphate receptor-2 (S1P2R) and its downstream effectors ROCK and PTEN. *Arterioscler Thromb Vasc Biol* 2007, 27(6):1312-1318.
227. Komarova YA, Mehta D, Malik AB: Dual regulation of endothelial junctional permeability. *Sci STKE* 2007, 2007(412):re8.
228. Dudek SM, Camp SM, Chiang ET, Singleton PA, Usatyuk PV, Zhao Y, Natarajan V, Garcia JG: Pulmonary endothelial cell barrier enhancement by FTY720 does not require the S1P1 receptor. *Cell Signal* 2007, 19(8):1754-1764.
229. Gon Y, Wood MR, Kiosses WB, Jo E, Sanna MG, Chun J, Rosen H: S1P3 receptor-induced reorganization of epithelial tight junctions compromises lung barrier integrity and is potentiated by TNF. *Proc Natl Acad Sci U S A* 2005, 102(26):9270-9275.
230. Retamales I, Elliott WM, Meshi B, Coxson HO, Pare PD, Sciurba FC, Rogers RM, Hayashi S, Hogg JC: Amplification of inflammation in emphysema and its association with latent adenoviral infection. *Am J Respir Crit Care Med* 2001, 164(3):469-473.
231. Yoshida T, Mett I, Bhunia AK, Bowman J, Perez M, Zhang L, Gandjeva A, Zhen L, Chukwueke U, Mao T *et al*: Rtp801, a suppressor of mTOR signaling, is an essential mediator of cigarette smoke-induced pulmonary injury and emphysema. *Nat Med* 2010, 16(7):767-773.
232. Weiss DJ, Strandjord TP, Liggitt D, Clark JG: Perflubron enhances adenovirus-mediated gene expression in lungs of transgenic mice with chronic alveolar filling. *Hum Gene Ther* 1999, 10(14):2287-2293.
233. Schweitzer K, Johnstone BH, Garrison J, Rush N, Cooper S, Traktuev DO, Feng D, Adamowicz JJ, Van Demark M, Fisher AJ *et al*: Adipose Stem Cell Treatment in Mice Attenuates Lung and Systemic Injury Induced by Cigarette Smoking. *Am J Respir Crit Care Med* 2010.
234. Tuder RM, Zhen L, Cho CY, Taraseviciene-Stewart L, Kasahara Y, Salvemini D, Voelkel NF, Flores SC: Oxidative stress and apoptosis interact and cause emphysema due to vascular endothelial growth factor receptor blockade. *Am J Respir Cell Mol Biol* 2003, 29(1):88-97.
235. Berdyshev EV, Gorshkova IA, Usatyuk P, Zhao Y, Saatian B, Hubbard W, Natarajan V: De novo biosynthesis of dihydrosphingosine-1-phosphate by sphingosine kinase 1 in mammalian cells. *Cell Signal* 2006, 18(10):1779-1792.
236. Berdyshev EV, Gorshkova I, Skobeleva A, Bittman R, Lu X, Dudek SM, Mirzapoiazova T, Garcia JG, Natarajan V: FTY720 inhibits ceramide synthases and up-regulates dihydrosphingosine 1-phosphate formation in human lung endothelial cells. *J Biol Chem* 2009, 284(9):5467-5477.

237. Berdyshev EV, Gorshkova IA, Garcia JG, Natarajan V, Hubbard WC: Quantitative analysis of sphingoid base-1-phosphates as bisacetylated derivatives by liquid chromatography-tandem mass spectrometry. *Anal Biochem* 2005, 339(1):129-136.

238. Dobrowsky RT, Kolesnick RN: Analysis of sphingomyelin and ceramide levels and the enzymes regulating their metabolism in response to cell stress. *Methods Cell Biol* 2001, 66:135-165.

239. Samapati R, Yang Y, Yin J, Stoerger C, Arenz C, Dietrich A, Gudermann T, Adam D, Wu S, Freichel M *et al*: Lung endothelial Ca2+ and permeability response to platelet-activating factor is mediated by acid sphingomyelinase and transient receptor potential classical 6. *Am J Respir Crit Care Med* 2012, 185(2):160-170.

240. Shoshani T, Faerman A, Mett I, Zelin E, Tenne T, Gorodin S, Moshel Y, Elbaz S, Budanov A, Chajut A *et al*: Identification of a novel hypoxia-inducible factor 1-responsive gene, RTP801, involved in apoptosis. *Mol Cell Biol* 2002, 22(7):2283-2293.

241. Rangasamy T, Cho CY, Thimmulappa RK, Zhen L, Srisuma SS, Kensler TW, Yamamoto M, Petrache I, Tuder RM, Biswal S: Genetic ablation of Nrf2 enhances susceptibility to cigarette smoke-induced emphysema in mice. *J Clin Invest* 2004, 114(9):1248-1259.

242. Schweitzer KS, Hatoum H, Brown MB, Gupta M, Justice MJ, Beteck B, Van Demark M, Gu Y, Presson RG, Jr., Hubbard WC *et al*: Mechanisms of lung endothelial barrier disruption induced by cigarette smoke: role of oxidative stress and ceramides. *Am J Physiol Lung Cell Mol Physiol*, 301(6):L836-846.

243. Tuder RM, Wood K, Taraseviciene L, Flores SC, Voekel NF: Cigarette smoke extract decreases the expression of vascular endothelial growth factor by cultured cells and triggers apoptosis of pulmonary endothelial cells. *Chest* 2000, 117(5 Suppl 1):241S-242S.

CURRICULUM VITAE

KRZYSZTOF KAMOCKI

EDUCATION

10/1990-9/1996	M.D.	Medical University of Lodz, Poland
		Department of Medicine
10/1997-2/2000	D.D.S.	Medical University of Lodz, Poland
		Department of Dentistry
8/2007-11/2012	Ph.D.	Biochemistry and Molecular Biology
		Indiana University, Indianapolis, IN

EMPLOYMENT HISTORY

9/1989-5/1990   Nurse Assistant, Internal Diseases Division,

Public Hospital in Lodz, Poland

10/1996-9/1997   Resident Physician, Medical Internship Training

Public Hospitals in Lodz, Poland

3/2000-5/2001   Emergency Department and Outpatient Clinic

Staff Physician, Public Hospital in Lask, Poland

3/2000-5/2001   Resident Dentist, Dental Internship Training

Lodz-Polesie Health Care Unit, Poland

3/2001-9/2002   Staff Dentist

Dental Health Centers in Poland

9/2002-2/2003   Postgraduate Research

Chemistry and Biochemistry Department

Notre Dame University, USA

3/2003-5/2004	Staff Dentist
	Dental Health Centers in Poland
8/2004-1/2005	Volunteer Laboratory Assistant
	Department of Medical and Molecular Genetics, IUPUI
1/2005-7/2006	Part Time Laboratory Assistant
	Department of Medical and Molecular Genetics, IUPUI
7/2006-1/2008	Senior Laboratory Technician and Manager
	Pulmonary and Critical Care Medicine, IUPUI

TEACHING EXPERIENCE

| 10/2003-12/2003 | Tutoring for residents in Conservative Dentistry |
| | Lodz-Polesie Health Care Unit, Poland |

SOCIETY/PROFESSIONAL MEMBERSHIPS

| 1996-present | Polish Medical Chamber |
| 2008-present | AAAS |

ADDITIONAL EXPERIENCE

| 6/2005-7/2005 | Molecular Biology Workshop, G890 |
| | Department of Pathology, IUPUI |

PUBLICATIONS

1. **Kamocki K**, Van Demark M, Justice MJ, Hubbard W, Berdyshev EV, Petrache I. Role of ceramides in the development of emphysema. (In Preparation)

2. Petrache I, **Kamocki K**, Poirier C, Pewzner-Jung Y, Laviad LE, Schweitzer KS, Van Demark M, Justice MJ, Rezania S, Shilling RA, Hubbard WC and Futerman AH. Protective Role of Very Long Acyl Chain Ceramides against Cigarette Smoke-Induced Mouse Lung Injury,Journal of Biological Chemistry. (Submitted 2012 October)

3. **Kamocki K**, Van Demark M, Fisher A, Rush N, Presson RG, Hubbard W, Berdyshev EV, Adamsky S, Feinstein E, Gandjeva A, Tuder RM, Petrache I. RTP801 is required for ceramide-induced cell-specific death in the murine lung. American Journal of Respiratory Cell and Molecular Biology 2012 July.

4. Lockett AD, Van Demark M, Gu Y, Schweitzer KS, Sigua N, **Kamocki K**, Fijalkowska I, Garrison J, Fisher AJ, Serban K, Wise RA, Flotte TR, Mueller C, Presson RG, Petrache HI, Tuder RM, Petrache I. Effect of cigarette smoke exposure and structural modifications on the alpha-1 antitrypsin interaction with caspases. Mol Med. 2012 Jan 10. doi: 10.2119/molmed.2011.00207.

5. Petrache I, Petrusca DN, Russell PB, and **Kamocki K**. Involvement of Ceramide in Cell Death Responses in the Pulmonary Circulation**.** Proc Am Thorac Soc. 2011 Nov; 8(6):492-6. Review.

6. Schweitzer K, Johnstone BH, Garrison J, Rush N, Cooper S, Traktuev DO, Feng D, Adamowicz JJ, Van Demark M, Fisher AJ, **Kamocki K**, Brown MB, Presson Jr RG, Broxmeyer HE, March KL, Petrache I. Adipose Stem Cell Treatment in Mice Attenuates Lung and Systemic Injury Induced by Cigarette Smoking. Am J Respir Crit Care Med. 2010 Aug 13; 183(2):215-25.

7. Clauss M, Voswinckel R, Rajashekhar G, Sigua NL, Fehrenbach H, Rush NI, Schweitzer KS, Yildirim AO, **Kamocki K**, Fisher AJ. Gu Y, Safadi B, Nikam S, Hubbard WC, Tuder RM, Twigg HL 3rd, Presson RG, Sethi S, Petrache I. Lung endothelial monocyte-activating protein 2 is a mediator of cigarette smoke-induced emphysema in mice. J Clin Invest. 2011 Jun; 121(6):2470-9. doi: 10.1172/JCI43881.

8. Diab KJ, Adamowicz JJ, **Kamocki K**, Rush NI, Garrison J, Gu Y, Schweitzer KS, Skobeleva A, Rajashekhar G, Hubbard WC, Berdyshev EV, and Petrache I. Stimulation of sphingosine 1-phosphate signaling as an alveolar cell survival strategy in emphysema. Am J Respir Crit Care Med. 2010 Feb 15; 181(4):344-52.

9. Sohrab S, Petrusca DN, Lockett AD, Schweitzer KS, Rush NI, Gu Y, **Kamocki K**, Garrison J, and Petrache I. Mechanism of alfa-1 antitrypsin endocytosis by lung endothelium. FASEB J. 2009 May 7; 23(9):3149-58.

10. Petrache I, Medler TR, Richter AT, **Kamocki K**, Chukwueke U, Zhen L, Gu Y, Adamowicz J, Schweitzer KS, Hubbard WC, Berdyshev EV, Lungarella G, and Tuder RM. Superoxide dismutase protects against apoptosis and alveolar

enlargement induced by ceramide. Am J Physiol Lung Cell Mol Physiol. 2008 Jul; 295(1):L44-53.

11. Medler TR., Petrusca DN, Lee PJ, Hubbard WC, Berdyshev EV, Jarrett S, **Kamocki K**, Schuchman E, Tuder RM, and Petrache I. Apoptotic Sphingolipid Signaling by Ceramides in Lung Endothelial cells. Am J Respir Cell Mol Biol. 2008 Jun; 38(6):639-46.

ABSTRACTS

1. Petrache I, Medler TR, Richter AT, Chukwueke U, Zhen L, Hargreaves CA, **Kamocki K**, and Tuder RM. The role of oxidative stress in ceramide-induced apoptosis and emphysema-like alveolar enlargement in mice (ATS, 2007).

2. Sohrab S, Fijalkowska I, Smith PA, Gu Y, **Kamocki K**, Hargreaves C, and Petrache I. Effect of cigarette smoke on the non-canonical protective functions of human alpha 1-antitrypsin (A1AT) in emphysema (FAMRI, 2007).

3. Diab KJ, Gu Y, Adamowicz J, **Kamocki K**, Berdyshey EV, and Petrache I. S1P augmentation, an alveolar cell pro-survival therapeutic strategy in experimental emphysema (ATS, 2007).

4. Sohrab S, Smith PA, Gu Y,**Kamocki K**, and Petrache I. Alpha-1-antitrypsin (A1AT) polymerization and cigarette smoke exposure impair the uptake of human A1AT by primary lung endothelial cells. The Fourth Annual Respiratory Disease Young Investigators Forum (Pittsburgh, 2007).

5. Clauss M, Rajashekhar G, Sigua N, **Kamocki K**, Ahlbrecht K, Oender Yildirim A, Fehrenbach H, Voswinckel R, Petrache I. EMAP II overexpression induces endothelial apoptosis and emphysema in murine lungs (EB 2008).

6. **Kamocki K**, Fisher A, Presson R, Sidner R, and Petrache I. Evaluation of cell-specific apoptosis in murine lungs following ceramide-16 PEG intratracheal instillation. (Biochemistry Retreat Program Booklet, Indiana University School of Medicine, 2008).

7. Sohrab S, Petrusca DN, **Kamocki K**, Adamowicz J, Gu Y, Rush NI, Fisher A, Presson RG, Schweitzer KS and Petrache I. Clathrin-mediated alpha-1-antitrypsin internalization by primary lung endothelial cells (ATS, 2009).

8. Petrache I, Schweitzer K, Johnstone B, Traktuev D, Garrison J, Rush N, Adamowicz J, Van Demark M, Fisher A, Cook T, Feng D, Merfeld-Clauss S, **Kamocki K**, Presson R, Broxmeyer H, March K. Protective effects of adipose stem cells against cigarette-smoke induced lung injury. (7th Annual Meeting of the International Federation of Adipose Therapeutics and Science, Daegu, Korea. October, 2009).

9. Sigua N, Rajashekhar G, Fehrenbach H, **Kamocki K**, Adamowicz J, Garrison J, Rush NI, Voswinckel R, Twigg HL III, Sethi S, Clauss M, and Petrache I. EMAP II is a novel cigarette smoke-induced biomarker in emphysema (ATS, 2009).

10. **Kamocki K**, Diab K, Van Demark M, Adamowicz JJ, and Petrache I. Anti-apoptotic effects of sphingosine-1 phosphate (S1P) and its analogs on alveolar endothelial and epithelial cells and role in the treatment of emphysema. (SERLC 2009) **Oral Presentation**.

11. **Kamocki K**, Diab K, Van Demark M, Adamowicz JJ, and Petrache I. Anti-apoptotic effects of sphingosine-1 phosphate (S1P) and its analogs on alveolar endothelial and epithelial cells and role in the treatment of emphysema (Biochemistry Retreat Program Booklet, Indiana University School of Medicine, 2010).

12. Petrache I, Petrusca D, Chen Z, Ndishabandi D, Justice M, **Kamocki K**, Rush IN, Van Demark M, Adamowicz J, Hubbard W, Choi A. Involvement of ceramides and dihydroceramides in lung apoptosis and authophagy (ATS 2010).

13. Petrache I, Goya J, Rush NI, Van Demark M, **Kamocki K**, Petrusca DN, Twigg III HL, Garcia JGN, S Ma, Natarajan V, Shen C, Berdyshev E. Ceramide and sphingosine-1-phosphate (S1P) levels in patients with COPD (ATS, 2010).

14. Schweitzer KS, Johnstone B, Cook T, Feng D, Albrecht M, Gao Y**, Kamocki K**, Cooper S, Broxmeyer H, March K, and Petrache I. Protection of human adipose-derived stem cells against cigarette-smoke induced lung injury NOD/SCID-IL2 null mice: the role of paracrine factors (ATS 2011).

15. **Kamocki K**, Van Demark M, Fisher A, Rush NI, Presson RG, Adamsky S, Feinstein E, Tuder RM, and Irina Petrache. Novel mechanistic integration of two cigarette smoke-induced stress responses: ceramide and Rtp-801 (Biochemistry Retreat Program Booklet, Indiana University School of Medicine, 2012).

16. Schweitzer KS, Justice M, Albrecht M, Van Demark M, Gu, Gao Y, **Kamocki K**, Bittman, R, and Petrache I. Therapeutic potential of FTY720-analogs in cigarette-smoke induced lung injury that is dependent upon sphingosine-1 phosphate receptor-1, S1PR1 (ATS, 2012).

RESEARCH SUPPORT